INHIBITION OF METABOLISM AND INDUCTION OF APOPTOSIS IN TRIPLE NEGATIVE BREAST CANCER CELLS BY *LIPPIA ORIGANOIDES* PLANT EXTRACTS.

by

Vishak Raman

A Dissertation

Submitted to the Faculty of Purdue University

In Partial Fulfillment of the Requirements for the degree of

Doctor of Philosophy

Department of Biological Sciences

West Lafayette, Indiana

May 2019

THE PURDUE UNIVERSITY GRADUATE SCHOOL
STATEMENT OF COMMITTEE APPROVAL

Dr. Ignacio G. Camarillo, Chair
Department of Biological Sciences, Purdue University, Indiana, USA
Dr. Claudio Aguilar
Department of Biological Sciences, Purdue University, Indiana, USA
Dr. Jorge Luis Fuentes Lorenzo
Escuela de Biología, Universidad Industrial de Santander, Bucaramanga, Colombia
Dr. Morris Levy
Department of Biological Sciences, Purdue University, Indiana, USA

Approved by:

Dr. Stephen Konieczny
Head of the Graduate Program, Biological Sciences

To Mum, Dad, Guha, Lavy, and Anika.

ACKNOWLEDGMENTS

As I look back at the journey I've taken to arrive here, I realize it quite simply would not have been possible without some very special people pushing me along throughout the way.

To begin with, I would like to thank my wonderful parents, who've taught me infinitely more than any academic institution could. I am the person I am today because of their love, support, and guidance. Knowing that they were there for me allowed me to keep my head up and remain motivated throughout my time in grad school.

Learning to live in a new country is never easy, and is made even harder when pursuing a PhD during that time. Having my brother, Guha, living in Indiana made my move here much easier to handle. During my time at Purdue, he met and married my (now) sister-in-law, Lavy, and they've even had a beautiful daughter (A lot has happened in five years!). With them around, I was never too far from family, and all the time spent with them has made Indiana feel like a second home.

I'd like to give a shout out to my best friends, Ish and Manoj, for the unconditional support they've given me, and for the incredibly fun times we've shared traveling around the United States. I want to thank the amazing friends I've made here at Purdue, especially Alix and Swetha. The weekly coffee-breaks with them – where we discussed everything from failed experiments to career ambitions – kept me cheerful and relaxed, and ready to take on the next research challenge.

I've had the amazing experience of working alongside and mentoring some astonishingly talented and motivated graduate and undergraduate students. With this in mind, I'd like to thank Lakshya and Rodrigo. Their hard work has pushed the lab's science in new directions and taken it to another level. Mentoring them has been a massive privilege.

I express my sincerest thanks and gratitude to my committee members, Dr. Aguilar, Dr. Levy, and Dr. Fuentes, and collaborating professors, Dr. Uma Aryal and Dr. Raji Sundararajan, whose useful feedback and advice throughout my PhD has added so much

to my research experience and to the content of my publications. I also want to extend a special thank-you to Dr. Fuentes, Dr. Morry Levy, and Maria (Mechas) Levy for entrusting me with this research project, which is part of an important on-going collaboration between Purdue and the Universidad Industrial de Santander, Bucaramanga; and I also thank them for their unlimited kindness and hospitality over the years.

Last but not the least, I want to thank my mentor, Dr. Ignacio Camarillo. Words cannot fully express the gratitude I feel for everything he has done for me. His positive influence has shaped me in a professional capacity, by improving and motivating me as a researcher, and on a personal level, by making me a more-rounded person. His guidance and support has given me the confidence to think and work independently, to foster collaborations with other labs and core facilities, and to mentor new students. His trust in my research and writing skills have given me the belief to pursue my own research questions, and have made me a better grant- and manuscript-writer. Outside of the lab, I will always remember the memorable concerts we attended, the long conversations over a couple of beers at the local pubs, and the Thanksgiving lunches at his home with his wife and children. Finally, I can never forget how supportive he was during my job hunt, and now in preparing me for my defense. I hope to emulate his work ethic and principles as I move on to the next phase of my life.

TABLE OF CONTENTS

LIST OF TABLES

LIST OF FIGURES

LIST OF ABBREVIATIONS

ABBREVIATION	TERM
7-AAD	7-Aminoactinomycin D
AAT	Aspartate aminotransferase
ABC	Ammonium bicarbonate
ACAT1	Acetyl CoA acetyltransferase
ACN	Acetonitrile
AE	Adverse effect
α-KG	α-ketoglutarate
α-KGHDC	α-ketoglutarate dehydrogenase complex
Akt/AKT	Protein kinase B
ALCAM	Activated Leukocyte Cell Adhesion Molecule
ALDHA1	Aldehyde dehydrogenase 1 family, member A1
ALK	Anaplastic lymphoma kinase
AML	Acute myeloid leukemia
AMPK	AMP-activated protein kinase
ANOVA	Analysis of Variance
AOA	Amino oxyacetate
AP1	Activating protein-1
APC	Adenomatous polyposis coli (protein)
APOD	Apolipoprotein D
AR	Androgen receptor
ATM	Ataxia-telangiectasia mutated (ser/thr kinase)
ATP	Adenosine triphosphate
AURKA	Aurora kinase A
AURKB	Aurora kinase B
BAC	Bioactive component
BAR	Bright, Alert, Responsive
BARD1	BRCA1-associated RING domain protein 1
BCA	Bicinchoninic acid
BCAA	Branched chain amino acid
BCL2	B-cell lymphoma 2
Bcl-xL	B-cell lymphoma-extra large
BMI	Body Mass Index
BMP2	Bone morphogenetic protein 2
BRCA1	Breast cancer type 1 susceptibility protein
BRCA2	Breast cancer type 2 susceptibility protein
BRIP1	BRCA1 Interacting Protein C-Terminal Helicase 1
BSA	Bovine Serum Albumin
BW	Body weight

CBR1	Carbonyl reductase 1
CD24	Cluster of differentiation 24 (cell surface protein)
CD44	Cluster of differentiation 44 (cell surface protein)
CF1α	Cleavage factor 1α
cFLIP	Cellular FLICE-inhibitory protein
CHEK1	Checkpoint kinase 1
CI	Confidence interval
CIAP1	Cellular inhibitor of apoptosis 1
CIAP2	Cellular inhibitor of apoptosis 2
CMF	Cyclophosphamide, methotrexate, 5-fluorouracil
CML	Chronic myeloid leukemia
c-Myc	Cellular myelocytomatosis
CNS	Central nervous system
COX	Cyclooxygenase
CPT	Camptothecin
c-Rel	Proto-oncogene REL
CSC	Cancer stem cell
CSL	CBF1, Suppressor of Hairless, Lag-1
CTRL	Control
CV	Coefficient of variation
DFS	Disease-free survival
DLD	Dihydrolipoamide dehydrogenase
DLST	Dihydrolipoamide S-succinyltransferase
DMEM	Dulbecco's modified essential medium
DMSO	Dimethyl sulfoxide
DRFS	Distant-recurrence free survival
DTT	Dithiothreitol
ECM	Extracellular matrix
EDTA	Ethylenediaminetetraacetic acid
EGFR	Epidermal growth factor receptor
ELISA	Enzyme-linked immunosorbent assay
EMT	Epithelial-mesenchymal transition
ER	Estrogen receptor
ETC	Electron transport chain
EZH2	Enhancer Of Zeste 2 Polycomb Repressive Complex 2 Subunit
FA	Formic acid
FAS	Fatty acid synthase
Fas	First apoptosis signal
FBS	Fetal bovine serum
FDR	False discovery rate
FEC	5'-fluorouracil, epirubicin and cyclophosphamide

FEC-P	5’-fluorouracil, epirubicin and cyclophosphamide-paclitaxel
Fz	Frazzled
GC/MS	Gas chromatography/Mass spectrometry
GDH	Glutamate dehydrogenase
GDP	Guanosine diphosphate
GLI	Glioma-associated oncogene
GLS	Glutaminase
GLUL	Glutamine synthetase
GLUT1/SLC2A1	Glucose transporter 1
GO	Gene ontology
GPCR	G-protein coupled receptor
GSK3	Glycogen synthase kinase 3
H&E	Hematoxylin eosin
HDAC	Histone deacetylase
HER2/neu/erbb2	Human epidermal growth factor receptor 2
Hh	Hedgehog
HIF-1α	Hypoxia-inducible factor 1α
HOX	Homeobox
HOXA10	Homeobox protein A10
HOXA5	Homeobox protein A5
HPLC-ESI-MS/MS	High performance liquid chromatography-electrospray ionization-tandem mass spectrometry
HR	Hazard ratio
IκB	NF-κB inhibitor
IKK	Inhibitor of κB kinase
IL-6	Interleukin-6
JAK	Janus kinase
L42	*Lippia origanoides* extract from chemotype 42, COL 560267
LFQ	Label-free quantitation
LKB1	Liver kinase B1
LOE	*Lippia origanoides* extract from chemotype 08, COL 560259
LTA4H	Leukotriene-A4 hydrolase
MAPK	Mitogen-activated protein kinase
ME	Malic enzyme
MMP	Matrix metalloprotease
MpBC	Metaplastic breast cancer
MTD	Maximum Tolerated Dose
mTOR	Mammalian target of rapamycin
mTORC1	Mammalian target of rapamycin, complex 1

MTT	3-(4,5-dimethylthiazol-2-yl)-2,5-diphenyltetrazolium bromide
NACT	Neoadjuvant chemotherapy
NADH	Nicotinamide adenine dinucleotide, reduced
NADPH	Nicotinamide adenine dinucleotide phosphate, reduced
NCI	National Cancer Institute
NF-κB	Nuclear factor κB
NGFR	Neuronal growth factor receptor
NICD	Notch receptor intracellular domain
NIH	National Institutes of Health
NQO2	NAD(P)H dehydrogenase, quinone 2
NT	Non-treated/untreated
OC	Oral contraceptive
OCR	Oxygen consumption rate
OGDH	Oxoglutarate dehydrogenase
OR	Odds ratio
ORR	Objective response rate
OS	Overall survival
OXPHOS	Oxidative phosphorylation
p50/p105	NFKB1 - Nuclear factor NF-kappa-B p105 subunit
p52/p100/NFKB2	NFKB2 - Nuclear factor NF-kappa-B p100 subunit
p65/RELA	Nuclear factor NF-kappa-B p65 subunit
PALB2	Partner and localizer of BRCA2
PARP	Poly-ADP ribose polymerase
PBS	Phosphate buffered saline
pCR	Pathological complete response
PCR	Polymerase chain reaction
PDGF	Platelet-derived growth factor
PDX	Patient-derived xenograft
PFS	Progression-free survival
PI	Propidium iodide
PI3K	Phosphatidylinositol-3-kinase
PIK3CA	Phosphatidylinositol 3-kinase, catalytic, alpha
PIP	Phosphatidylinositol phosphate
PKCα	Protein kinase C alpha
PKD1	Polycystin 1
PMN	Polymorphonuclear neutrophil
Polα	DNA polymerase alpha
PP2A	Protein phosphatase 2
PR	Progesterone receptor
PTCH1	Patched 1
PTEN	Phosphatase and tensin homolog
PVDF	Polyvinyl difluoride

RAD51C	RAD51 homolog C
RAD51D	RAD51 homolog D
RIP1	Receptor-interacting protein 1
RIPA	Radioimunnoprecipitation assay
ROS	Reactive oxygen species
RPMI	Rosewell Park Memorial Institute
RTI	Research Triangle Institute
SCID	Severe combined immunodeficient
SDS-PAGE	Sodium dodecyl sulfate-polyacrylamide gel electrophoresis
SHH	Sonic hedgehog
SLC1A5/ASCT2	Solute carrier family 1 member 5
SMO	Smoothened
SNAI2	Snail Family Transcriptional Repressor 1
SP1	Specificity protein 1
SPE	Solid-phase extraction
STAT3	Signal transducer and activator of transcription 3
TCA	Tricarboxylic acid
TCF/LEF	Transcription factor/Lymphoid enhancer-binding factor 1
TDLU	Terminal duct lobular units
TGF-β	Transforming growth factor-β
THY1	Thy-1 Cell Surface Antigen
TMOD1	Tropomodulin 1
TMRE	Tetramethylrhodamine, Ethyl Ester, Perchlorate
TNF	Tumor necrosis factor
TNFR1	Tumor necrosis factor receptor 1
TP53	Tumor protein 53
TRAIL	TNF-related apoptosis-inducing ligand
TRAILR2	TNF-related apoptosis-inducing ligand receptor 2
TWIST1	Twist Family BHLH Transcription Factor 1
VCAM1	Vascular cell adhesion molecule 1
VCR	Vincristine
VEGF-A	Vascular endothelial growth factor-A
VEGFR2	Vascular endothelial growth factor receptor 2
VEH	Vehicle (methanol)
VLB	Vinblastine
VM-26	Teniposide
VP-16	Etoposide
WHR	Waist-to-hip ratio
Wnt	Wingless
ZEB1	Zinc Finger E-Box Binding Homeobox 1

ABSTRACT

Author: Raman, Vishak. PhD
Institution: Purdue University
Degree Received: May 2019
Title: Inhibition of Metabolism and Induction of Apoptosis in Triple Negative Breast Cancer Cells by *Lippia origanoides* Plant Extracts
Committee Chair: Ignacio G. Camarillo

According to the Global Cancer Incidence, Mortality, and Prevention (GLOBOCAN) study for 2018, 2,089,000 women will have been diagnosed with breast cancer worldwide, with 627,000 breast cancer-related mortalities. It is estimated that between 15 – 20 % of breast cancer diagnoses are of the triple-negative subtype. Triple-negative breast cancers (TNBCs) do not express the receptors for estrogen, progesterone, and human epidermal growth factor 2, and hence cannot be treated using hormone receptor-targeted therapy.

TNBCs are commonly of the basal-like phenotype, with high expression levels of proteins involved in epithelial-mesenchymal transition, extracellular-matrix (ECM) remodeling, cell cycle progression, survival and drug resistance, invasion, and metastasis. 5-year survival rates are significantly lower for TNBC patients, and the disease is characterized by poorer grade at the time of diagnosis as well as higher 5-year distant relapse rates, with a greater chance of lung and CNS metastases. Current treatments for TNBC take the form of aggressive cytotoxic chemotherapy regimens with multiple adverse side-effects. An important goal of on-going studies is to identify new compounds with significant TNBC-specificity, in order to improve patient survival outcomes while preserving a high quality of life during treatment.

For several decades, compounds originally isolated from bioactive natural extracts, such as the taxanes and vinca alkaloids, have been at the forefront of chemotherapy. However, due to their non -specific mechanisms of action, treatment with these compounds eventually leads to significant toxicity to normal cells and tissues. Modern transcriptomics, metabolomics, and proteomics tools have greatly improved our understanding of the mechanisms governing cancer initiation and progression, and

revealed the considerable heterogeneity of tumor cells. This has allowed for the identification of potential vulnerabilities in multiple cancers, including TNBCs. By leveraging these new technologies and insights with the tremendous diversity of bioactive compounds from organisms that remain unstudied, new classes of onco-drugs targeting pathways specific to TNBC cells could be identified in the near future.

Here, we describe the cytotoxic effects of extracts from *Lippia origanoides* – a species of medicinal shrub native to Central and South America – on TNBC cells. We report that these extracts induce rapid, sustained, and irreversible apoptosis in TNBC cells *in vitro*, with significantly reduced cytotoxicity against normal mammary epithelial cells. The *L. origanoides* extracts LOE and L42 exploited two TNBC-specific characteristics to induce apoptosis in these cells: i) inhibiting the constitutively active survival and inflammatory NF-κB signaling pathway, and ii) significantly dysregulating the expression levels of mitochondrial enzymes required to maintain the TCA cycle and oxidative phosphorylation; metabolic pathways that are required for the maintenance of TNBC cell growth and proliferation.

Finally, to lay the foundations for future studies on the abilities of these extracts to prevent tumor initiation and inhibit tumor growth *in vivo*, we also show that the *L. origanoides* extract, L42, is non-toxic to immunocompetent C57BL/6 mice, and have developed an *in vivo* model of human TNBC in athymic *nu/nu* mice.

Collectively, our studies are the first to identify the anti-TNBC-specific properties of bioactive extracts from the *Lippia* species, and reveal that targeting NF-κB signaling and mitochondrial metabolism are potential avenues to new therapeutics against this subtype of breast cancer. Future work in our lab will focus on identifying the bioactive components (BACs) of the extract mediating its apoptotic effects, and shedding light on their protein binding partners within the cell.

CHAPTER 1. INTRODUCTION

1.1 Breast Cancer Overview

Breast cancer is a major health concern worldwide - and a leading cause of cancer-related deaths among women in the United States where over 245,000 new cases are diagnosed and 45,000 deaths occur each year [1]. In about 80 % of cases, this disease presents as hormone-sensitive breast cancer with over-expression of Estrogen Receptor (ER), Progesterone Receptor (PR) and/or Human Epidermal Growth Factor Receptor 2 (HER2/neu). These cancers typically depend on hormone-receptor signaling for tumor growth and progression. Consequently, conventional hormone therapy against the majority of breast cancers targets these receptors (e.g. tamoxifen, a selective Estrogen Receptor modulator and herceptin, an antibody that inhibits HER2 activity) or attempts to inhibit enzymes involved in estrogen synthesis (e.g. aromatase inhibitors such as letrozole) [2-4]. In these scenarios, therapies targeting hormone receptors or hormone production have provided clinical benefit.

In contrast, the deadliest subtype of this disease – known clinically as triple-negative breast cancer (TNBC) and which constitutes approximately 15% of invasive breast cancers – is not dependent on hormonal signaling for progression and consequently does not respond to conventional hormone therapy [5]. TNBC treatment options often take the form of cytotoxic chemotherapy, which is unable to fully distinguish tumor cells from normal cells, thereby leading to serious side-effects such as severe nausea and vomiting, peripheral neuropathy, anemia, myelosuppression, extreme fatigue, and kidney toxicity. Hence, a critical need of the hour is the identification of TNBC-specific molecular markers, and small molecule inhibitors to target them.

1.1.1 Breast Cancer Epidemiology

For 2018, the Global Cancer Incidence, Mortality, and Prevention (GLOBOCAN) study estimates approximately 2,000,000 women will be diagnosed with breast cancer worldwide [6]. The American Cancer Society predicts 266,120 new female breast cancer diagnoses in the United States alone, along with 40,920 deaths [7]. The disease remains

the leading cancer-type diagnosed in women (30% of cancer-related diagnoses), and is the second-leading cause of cancer-related death in women (14% of cancer-related mortalities, second only to lung cancer at 25%) [7]. Lifestyle factors including high-fat and high-sugar diets, reduced physical activity, increased alcohol intake, and smoking have all been shown to contribute to heightened breast cancer risk [8-11]. In Western countries in particular, high-calorie diets and lack of exercise leading to higher rates of obesity is held to be a major preventable cause of the growing number of breast cancer cases [12].

Additional factors influencing breast cancer incidence, subtype, and mortality are age at menarche, parity, breastfeeding, genetics, race, and environmental factors such as exposure to pollution and second-hand smoke [13-19]. Specifically, a lower age at menarche and higher age at menopause increased the risk of breast cancer incidence, while a greater number of birth (>3 births) was associated with increased breast cancer-specific mortality [13, 14]. Race has been found to influence the subtype of breast cancer, with a study of over 40,000 women from the state of California, diagnosed with breast cancer between 2006-2007, finding that African-American women more likely to be diagnosed with TNBC compared to white or Hispanic women, while Hispanic women were at greatest risk of developing luminal breast cancer [17].

Multiple studies have confirmed the link between passive smoking and breast cancer risk, while evidence linking active smoking with breast cancer risk is more contentious. For example, a 2011 study by Luo et al. of ~ 80,000 women aged 50-79 enrolled in the Women's Health Initiative Observational Study between 1993-1998, found that breast cancer risk was significantly elevated among former and current smokers, with the highest risk among women who had smoked for ≥ 50 y. [hazard ratio 1.45 (1.06 to 1.98) compared with lifetime non-smokers with no exposure to passive smoking]. In addition, women with extensive exposure to passive smoking had a 32 % increased risk of breast cancer compared to women who had never been exposed to passive smoking [11]. In contrast, a meta-analysis of 51 studies (3 cohort and 48 case-control studies) looking at the association between smoking and breast cancer in Chinese women found that passive smoking, but not active smoking, was significantly associated

with breast cancer incidence [odds ratio (OR): 1.62; 95% confidence interval (CI): 1.39-1.85, $P < 0.001$; $n = 26$] [18].

Overall, while a number of breast cancer cases could be prevented by improving lifestyle choices; race, genetics, and hormonal changes influence a significant portion of incidences, and will therefore require novel treatment options to improve survival outcomes.

1.1.2 Mammary Histology and Origins of Breast Cancer Subtypes

Histopathological analysis of the mammary gland has shown it is a branching ductal network embedded in a stromal environment rich with adipose. Ductal structures are primarily composed of two types of epithelial cells – an inner luminal layer for milk production and transport, and an outer myoepithelial basal layer for milk ejection [20]. At the end of each duct are lobular units known as terminal duct lobular units (TDLUs), which have been identified as the locational origin for most breast tumors [21]. This is perhaps unsurprising, given that TDLUs are the products of branching morphogenesis in the breasts; a complex process involving rapid cell growth, proliferation, and differentiation throughout the female reproductive period [22]. Based on current understanding of the differentiation process in the mammary gland, it is commonly acknowledged that most primitive mammary stem and progenitor cells are ER-negative and localize to the basal layer [23]. These differentiate into ER-positive and ER-negative oligo- and bi-potent progenitor cells predominantly localized to the luminal compartment, which can then eventually give rise to differentiated luminal and myoepithelial cells (Figure 1.1). This model was supported by Gudjonsson et al, who identified progenitor cells in the luminal epithelial compartment and showed they were capable of differentiating into either cell type *in vitro*, and into entire TDLU-like structures in 3D culture [24].

Stem and progenitor cells are commonly distinguished by their expression levels of the cell surface adhesion receptors CD44 and CD24. Specifically, mammary stem/progenitor cells are characterized by high levels of CD44 and low levels of CD24 ($CD44^{high}/CD24^{lo}$), a characteristic shared by breast cancer stem cells (CSCs) [23]. CSCs are a subpopulation of tumor cells capable of self-renewal and differentiation into non-

tumorigenic progeny that contribute to overall tumor growth. Genetic alterations in mammary stem and progenitor cells could produce CSCs expressing hormone receptor-, stemness-, and lineage-specific markers that reflect their cell-of-origin [25]. However, as the CSCs continue to proliferate and differentiate, they form highly heterogeneous tumors comprised of cells characterized by distinct phenotypes and gene expression profiles [26]. These resulting differing phenotypes within a single tumor contribute to the substantial complexity of developing effective treatment options for breast cancer.

Breast cancer is therefore an extremely heterogeneous disease, currently classified on the basis of molecular stratification using gene signatures into “intrinsic” molecular subtypes (Luminal A, Luminal B, HER-2 enriched, basal-like, and normal-like), and also through histopathological features and patient clinical information. The intrinsic molecular subtype classification was developed through pioneering studies by Sørlie and Perou in the early 2000s [27]. The expression levels of 496 ‘intrinsic’ genes (genes with significantly higher variability in expression across different tumors than between paired samples from the same tumors) were compared across 65 tumor tissues, and used to order the samples into subtypes. Five subtypes emerged from their analysis: Luminal-A and Luminal-B, basal-like, ERBB2-overexpressing, and normal-like. These subtypes were found to correlate strongly with hormone receptor status, i.e. with the expression levels of receptors for estrogen (ER), progesterone (PR), and human epidermal growth factor (HER2). The identification of intrinsic subtypes of patient tumors has both prognostic and diagnostic value, and is currently utilized extensively in the clinical setting (*See Table 1.1*).

Table 1.1 Classification of breast tumors into intrinsic molecular subtypes. *Source: Dai, X., Li, T., Bai, Z., Yang, Y., Liu, X., Zhan, J., & Shi, B. (2015). American Journal of Cancer Research, 5(10), 2929–2943. [Ref. 216]*

Intrinsic subtype	IHC status	Grade	Outcome	Prevalence
Luminal A	[ER+ PR+] HER2- Ki67-	1|2	Good	23.7 %
Luminal B	[ER+ PR+] HER2- Ki67+	2|3	Intermediate	38.8 %
	[ER+ PR+] HER2+ Ki67+	2|3	Poor	14 %
HER2 over-expressing	[ER- PR-] HER2+	2|3	Poor	11.2 %
Basal	[ER- PR-] HER2- Basal markers+	3	Poor	12.3 %
Normal-like	[ER+ PR+] HER2- Ki67-	1|2|3	Intermediate	7.8 %

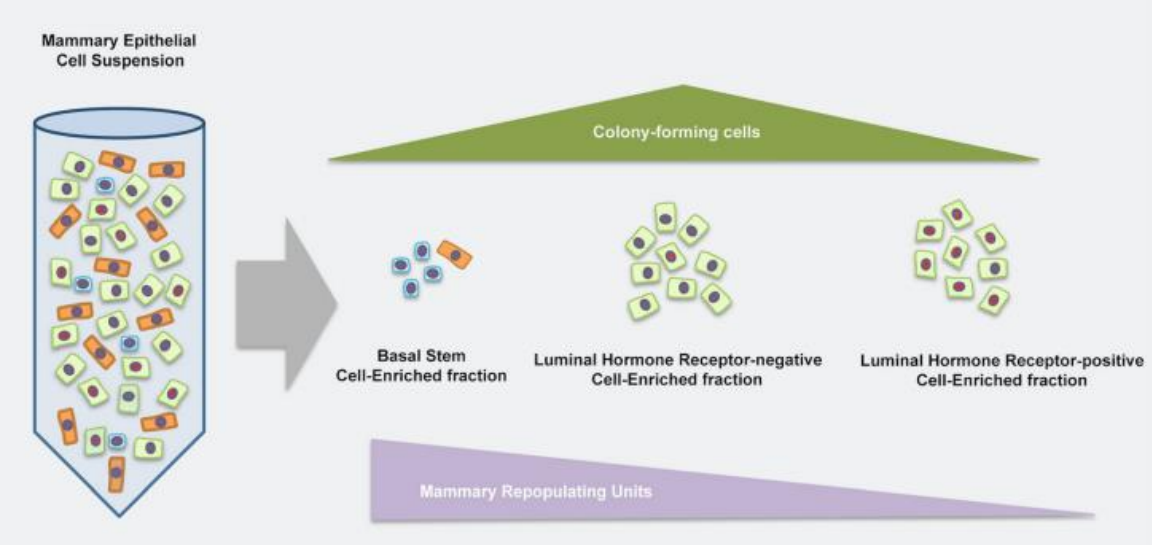

Figure 1.1 Hormone receptor status correlates with luminal phenotype and degree of differentiation. Fluorescence-assisted cell sorting (FACS) of mammary epithelial cells based on surface markers including Estrogen Receptor (ER) and luminal and basal markers allows for fractionation into distinct populations. Fractions enriched for ER+ cells contain a low frequency of stem-like cells and progenitors capable of mammary repopulation upon transplantation, and colony formation *in vitro.* Conversely, fractions enriched for ER- and basal-like cells exhibit enhanced colony-formation and mammary repopulation abilities, and are thus considered to have a greater population of stem and progenitor cells.

Source: Tornillo, G., & Smalley, M. J. (2015). Journal of Mammary Gland Biology and Neoplasia, 20(1-2), 63–73. [Ref. 23]

1.2 Triple-Negative Breast Cancer Overview

A particularly aggressive form of breast cancer is triple-negative breast cancer (TNBC), identified as having < 1% of tumors cells expressing the three hormone receptors commonly utilized for subtyping [28]. Pathologically, TNBC tumors are associated with higher grade at diagnosis, the presence of unfavorable mitotic features such as higher mitotic index, marked nuclear pleomorphisms, pushing borders of invasion, geographic tumor necrosis, and poor overall differentiation [29]. 71 % of TNBCs are found to be basal-like, and 77 % of basal-like breast cancers are triple-negative [30]. Basal-like breast cancer are characterized by high expression levels of basal epithelial markers including keratin 5 and 17, laminin, and fatty acid binding protein 7, and low levels of luminal markers [31, 32]. Patients diagnosed with TNBC have lower overall median survival rates compared to those diagnosed with hormone receptor-positive (HR+)/HER2- tumors [overall survival: adjusted hazard ratio, 2.72; 95% confidence interval, 2.39-3.10; P < .0001], with a dramatically increased risk of death within the first 2 years of diagnosis [overall survival for 0-2 years: OR, 6.10; 95% confidence interval, 4.81-7.74] [33].

1.2.1 Epidemiology and Behavioral/Genetic Risk Factors for TNBC

Triple-negative/basal-like cancers make up 10-20 % of invasive breast cancers diagnoses. Between 2010-2014, the incidence rate of TNBC was observed to be twice as high in African American women (24/100,000) as in non-Hispanic white women (12/100,000), and thrice as high compared to Asian/Pacific Islander women (8/100,000) [34]. A genetic explanation for this difference has not been identified, but a 2010 study by Stark et al. showed African ancestry strongly correlated with younger age of cancer diagnoses (48.0 y.o. for Ghanaian women, as opposed to 60.8 y.o. for African Americans, and 62.4 y.o. for white Americans.), and higher proportion of TNBC (82.2 % for Ghanaians, 26.4 % for African Americans, and 16 % for white Americans) [35].

Several reproductive factors have been shown to influence risk of TNBC incidence. In a 2010 study looking at 1197 breast cancer cases and 2015 controls, Ma et al. determined that women aged 45-64 y.o. who had a history of oral contraceptive (OC) usage before age 18 had a 2.9-fold increased risk of TNBC [36]. In a follow-up 2017 study, Ma et al. performed a pooled analysis of 2658 white and African American

patients with breast cancer (of which 554 were diagnosed with TNBC) along with 2448 controls, with all patients aged between 20-64 years, and found that TNBC risk in parous women who breast fed for at least 1 year was 31 % lower than in parous women who never breast fed [37]. Remarkably, parous African American women between 20-44 y.o. who breast fed for ≥ 6 months had an 82 % lowered risk of TNBC than those that did not breast feed.

In addition to early OC use and non-breast feeding, TNBC risk has been linked to premenopausal status as women under 40 y.o. are disproportionately diagnosed with ER- breast cancers (33.8 %) compared to older women (21.9 %) [38]. A 2006 analysis of 496 samples from the Carolina Breast Cancer Study found that premenopausal African American women had a higher prevalence of TNBC (39 %) compared to postmenopausal African American women (14 %) [39].

In 2014, 40. 4 % of American women were defined as obese (BMI ≥ 30 kg/m^2), with 9.9 % considered severely obese (BMI ≥ 40 kg/m^2) [40]. A 2008 study by Millikan et al., using the Carolina Breast Cancer Study samples, showed that TNBC risk was increased significantly for women with higher waist-to-hip ratio (WHR) [OR = 2.3; 95% CI, 1.4–3.6], with a similar effect described for premenopausal ER-/PR- breast cancer in the Women's Circle of Health Study in 2009 [41, 42]. Mechanisms by which obesity may support TNBC initiation, progression, and metastasis include i) influencing the Akt/mTOR pathway and glycolysis through insulin signaling, ii) secretion of obesity-related inflammatory cytokines such as leptin, as well as promotion of a general inflammatory state characterized by heightened circulating levels of pro-inflammatory cytokines which can in-turn stimulate STAT3, NFκB, and Wnt/EZH2 signaling, and iii) promote breast tumor aggressiveness and progression through the influence of the adipose tissue microenvironment, including elevation of estrogen levels and promotion of infiltration of immune cells [43-45].

Finally, specific genetic risk factors are known to be major contributors to TNBC such as *BRCA1* and *BRCA2* mutations. BRCA1 and BRCA2 are proteins involved in the error-free repair of double-strand DNA breaks, with germline *BRCA* mutations commonly associated with risk of development of breast cancer. The Consortium of

Investigators of Modifiers of BRCA1/2 (CIMBA) utilized data from 4,325 *BRCA1* and 2,568 *BRCA2* mutation carriers, and found that the proportion of TNBCs decreased with age at diagnosis for *BRCA1* mutation carriers and increased with age at diagnosis for *BRCA2* mutation carriers [46]. In addition, 69 % of breast cancers in women with *BRCA1* mutations were triple-negative. Also, 20 % of TNBCs carry *BRCA1* mutations [47]. In a 2018 study, multigene panel testing methods utilized two TNBC patient cohorts – one in which 21 breast cancer predisposition genes in 8753 patients were tested in Ambry Genetics clinical laboratory, and another in which 17 genes from 2148 patients were tested by a Triple-Negative Breast Cancer Consortium (TNBCC) – and found that *BARD1, BRCA1, BRCA2, PALB2,* and *RAD51D* germline variants correlated with high risk (OR > 5.0) of TNBC, while pathogenic variants for *BRIP1, RAD51C,* and *TP53* were associated with moderate risk (OR = 2.0 - 5.0) in Caucasian women [48].

1.2.2 Clinical Outcomes and Treatment Options for TNBC

Cancer ‘staging’ often utilizes the TNM system, where ‘T’ refers to the size of the tumor, ‘N’ to the node status, i.e. if the cancer has invaded regional lymph nodes, and ‘M’ to the degree of metastasis. In comparison to other subtypes of breast cancer, TNBCs have a worse prognosis, a more aggressive trajectory, and are more commonly diagnosed in younger and obese women, with an average age of disease onset at 53 years. The poor prognosis of TNBC is likely correlated with later stage at diagnosis, as most TNBCs are T2 and T3 at the time of diagnosis (i.e. present with larger tumors), and are more likely to be positive for lymphovascular invasion [49]. TNBCs also display preferential metastasis to the brain and lungs, with a lower incidence of metastasis to the bone [50]. Lin et al. conducted a study of 15,204 women who presented at the National Comprehensive Cancer Network centers with Stage I-III breast cancer [33]. The study, which included 2,569 TNBCs, 2,602 HER2+, and 10,033 HR+/HER2- diagnoses, reported decreased overall survival (OS) for TNBC compared to other HR+/HER2- cancers (HR 2.72 [2.39-3.10], p <0.0001). Notably, the TNBC group had a dramatically increased risk of death within the first 2 years of diagnosis (HR for OS for 0 - 2 y 6.10 [95% CI 4.81, 7.74]), with the risk declining markedly over time [33].

Curiously, early-stage TNBCs have a better response rate than HR+/HER2- tumors to anthracycline-based neoadjuvant chemotherapy (NACT) (85 % vs 47 %) [51]. The chemosensitivity of early stage TNBCs to NACT also leads to higher rates of pathologic complete response (pCR), which is an important marker for improved survival across all breast cancer subtypes. Unfortunately, patients with TNBCs also have the highest 3-year relapse rates, with an increased risk of visceral relapse (i.e. metastatic tumor relapse sites at lungs, pleura, liver, brain, or other thoracoabdominal organs). The lower OS for TNBC patients is due to extremely limited treatment options post-recurrence. Following recurrence, survival for TNBC patients rarely extends past 12 months, with British Columbia Cancer Agency data showing that median duration of survival for distant metastatic basal-like breast cancer is just 0.5 years [52].

Presently, NACT protocols for TNBC advise anthracycline (such as epirubicin and doxorubicin)- and taxane (such as paclitaxel and docetaxel)-based chemotherapy [53]. Anthracyclines work by intercalating between DNA and RNA strands, preventing replication and inhibiting cell division of rapidly proliferating cells such as those found in tumors [54]. Similarly, taxanes also inhibit cell division, but do so by disrupting microtubule formation through stabilizing GDP-bound tubulin molecules, preventing microtubule depolymerization [55]. Unfortunately, anthracyline and taxane treatments are non-specific, and are accompanied by major adverse side-effects which can themselves drive fatality.

Both anthracyclines as well as taxanes were first discovered from natural sources, with the anthracyline doxorubicin isolated from *Streptomyces*, and paclitaxel from the *Taxus brevifolia* (Pacific Yew) conifer tree. Aside from the standard NACT regimen, drugs with indications for TNBC include 5'-fluorouracil (currently hypothesized to be a thymidylate synthase inhibitor preventing DNA formation) and bevacizumab (a monoclonal antibody to VEGF-A, acting as an angiogenesis inhibitor) [53, 56, 57]. Meta-analysis results from several clinical trials have supported the use of platinum (carboplatin or cisplatin)-based chemotherapy regimens to improve pathological complete response rates (pCR, i.e. the percentage of patients with lack of all signs of cancer in tissue biopsies post-therapy), and objective response rates (ORR, i.e. percentage

of patients with tumors that shrink or disappear upon therapy), at the cost of greater adverse events (AEs) due to toxicity [58]. However, there is currently no evidence that platinum-based chemotherapy can increase overall survival (OS) or progression-free survival (PFS), and its clinical use remains controversial.

The current adjuvant chemotherapy regimens for TNBC commonly utilizes anthracycline and taxane-based combination treatments, which have been shown to marginally improve 3-year disease-free survival (DFS) rates from 68 % to 73.5 % (HR = 0.50; 95% CI, 0.29 to 1.00; P = .051) [59]. In addition, sequential anthracycline-based and taxane-based treatment regimens such as FEC (5'-fluorouracil, epirubicin and cyclophosphamide) followed by paclitaxel/docetaxel (a sequential regimen known as FEC-P) are commonly used for medium-to-high risk TNBCs, and show significantly better DFS rates compared to FEC alone [60]. Another treatment option is the combination of cyclophosphamide, methotrexate, and 5'-flurouracil (CMF) which causes lower toxicity but requires a longer treatment duration. Patients with TNBC were shown to have a significantly lower cumulative relapse rate with CMF treatment versus no chemotherapy (21 % *v* 36 %), as well as longer time to relapse (HR: 0.46; 95% CI, 0.29 to 0.73; P = .009 relative to endocrine receptor–present subtype) [61].

Current areas of clinical research for TNBC treatment include poly-ADP ribose (PARP)-inhibitors such as veliparib which interfere with base excision repair mechanisms and are thought to be particularly lethal to BRCA1-mutated tumors; often associated with TNBC [62]. Also, VEGF-inhibitors such as the monoclonal antibody bevacizumab were evaluated at the level of phase III trials but unfortunately, did not improve major patient outcomes in the adjuvant setting [63].

Taken together, TNBCs respond well to pre-operative (neoadjuvant) chemotherapy compared to other subtypes, but conversely, have a much worse response to post-operative (adjuvant) chemotherapy following relapse. Unfortunately, due to their higher 3-year relapse rates, greater propensity for CNS-directed metastasis, and poor chemo-sensitivity in the adjuvant setting, metastatic TNBCs have the worst median survival time (< 6 months) among breast cancer subtypes [52], and highlights the pressing need to

identify novel TNBC-specific signaling pathways and vulnerabilities that can be targeted for therapy.

1.3 Molecular Heterogeneity of TNBC

Several studies have attempted to provide a mechanistic basis for the poor differentiation status, aggressiveness, and drug resistance of TNBC tumors. In 2011, Lehmann et. al provided a seminal description of the considerable heterogeneity of TNBCs through expression profiling of 13,060 unique genes from 587 TNBC samples [64]. Clustering analysis of these genes identified the 6 TNBC subtypes described below (Basal-like 1, BL1; Immunomodulatory, IM; Mesenchymal, M; Mesenchymal stem-like, MSL; and Luminal Androgen Receptor, LAR) classified on the basis of expression of gene clusters from specific cellular pathways:

The *Basal-like 1 (BL1)* TNBC subtype is characterized by overexpression of genes involved in proliferation (e.g. *AURKA* and *AURKB*) and DNA damage response (e.g. *CHEK1* and *RAD51*), while the *Basal-like 2 (BL2)* subtype overexpresses genes regulating growth factor signaling, glycolysis and gluconeogenesis. Unsurprisingly, basal-like (BL1 and BL2) TNBC has been found to be significantly more susceptible to taxane-based therapies targeting cell division compared to the mesenchymal-like and Luminal Androgen Receptor (LAR) subtypes (63 % pathological complete response (PCR) for BL-TNBC, vs. 31% and 14 % for M-TNBC and LAR-TNBC respectively, $P = 0.042$).

The *Immunomodulatory (IM)* subtype is characterized by enrichment of immune cell process gene ontologies (GOs). Several genes regulating events specific to immune cells such as T cell receptor, B cell receptor, and NK cell signaling were shown to be overexpressed, and immune signaling genes regulating NFκB, TNF, and JAK/STAT pathways are also enriched in the IM subtype.

Both the *Mesenchymal (M)* and *Mesenchymal Stem-like (MSL)* subtypes share enrichment for GOs involving cell motility (Rho pathway), differentiation and growth (Wnt, ALK, and TGF-β pathways). Both subtypes are enriched for epithelial-

mesenchymal transition (EMT) genes (e.g. *MMP2*, *TWIST1*, *ZEB1*, and *SNAI2*), and often have high rates of aberrations in the PI3K/AKT/mTOR pathway. However, the MSL subtype also includes overexpression of genes functioning in growth factor signaling such as EGFR, calcium signaling, and PDGF, and interestingly, has lower expression of proliferation genes and a greater enrichment for stem-like genes, HOX genes, and mesenchymal markers (e.g. *BCL2*, *BMP2*, *ALDHA1*, *THY1*, *HOXA5*, *HOXA10*, *NGFR*, and *VCAM1*).

Further, using the GSE-10890 and ETABM-157 breast cancer cell line data sets, the authors identified 30 non-overlapping TNBC cell lines, and correlated their gene expression profiles to the 6 identified TNBC subtypes (Figure 1.2) [64]. Of note, the MDA-MB-231 cell line, utilized as the primary model of aggressive TNBC in this dissertation, was found to correlate with the mesenchymal stem-like (MSL) subtype.

Approximately 10 – 30 % of mesenchymal TNBCs have been morphologically determined to fall within a class of rare, malignant form of drug-resistant breast cancer known as metaplastic breast cancer (MpBC) [217, 218]. In addition, both mesenchymal and metaplastic breast cancers contain aberrations in the mTOR pathway, and a phase I trial of combination chemotherapy using doxorubicin, bavcizumab, and the mTOR inhibitors temsirolimus or everolimus to treat MpBC patients (n = 52), showed an overall response rate (ORR) of 21 % and a clinical benefit rate of 40 % [219].

The *Luminal Androgen Receptor (LAR)*-type, while also ER-, is characterized by enrichment for hormone regulated pathways including steroid synthesis and androgen/estrogen metabolism. Driving these pathways in this subtype is an overabundance of androgen receptor (AR), expressed at 9-fold greater levels than other subtypes, with downstream AR targets and coactivators also expressed (e.g. *ALCAM*, *PIP*, and *APOD*). IHC staining also showed a significant, >10-fold increase in AR protein expression in this TNBC subtype over others, making AR signaling an exciting potential target against LAR-subtype TNBC tumors. The LAR subtype makes up roughly 11 % of all TNBCs [64], and respond poorly to sequential taxane- and anthracycline-based cytotoxic neoadjuvant chemotherapy, with patients diagnosed with LAR-TNBC showing only 10 % pathological complete response (PCR) compared to 52 % for those with BL1-

TNBC [220]. However, treatment of advanced AR-positive TNBC with the antiandrogen enzalutamide in a phase II trial showed a clinical benefit rate (CBR) of 29 % at 24 weeks of treatment, and a median progression-free survival (PFS) of 14 weeks.

In summary, expression profiling of TNBC tumors and cell lines has helped distinguish subtypes of clinical importance, and has provided a molecular basis for tumor behavior and response to therapy, while also identifying potentially targetable vulnerabilities.

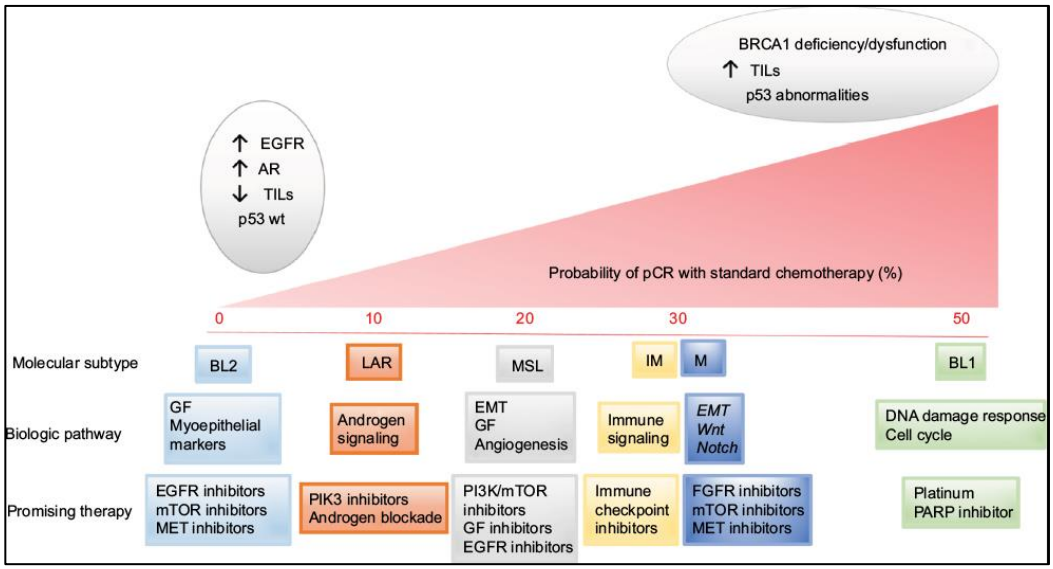

Figure 1.2 TNBC subtypes. Classification of TNBCs on the basis of gene expression and signaling pathways involved. The subclasses show varying rates of pathological complete response (pCR) to standard chemotherapy, with promising targeted therapies suggested for each subclass.

Source: Reproduced with permission from Omarini, C., et al (2017). Cancer Management and Research, 10; 91-103 [Ref 222].

1.3.1 Overview of Major Signaling Pathways in TNBC

Several molecular pathways, including those involved in development (Wnt/β-catenin, Notch, and Hedgehog), survival (PI3K/Akt) and inflammation (NF-κB signaling), have been implicated in the oncogenesis, growth, invasion, metastasis, and development of drug-resistance of triple-negative breast cancers. The evidence supporting the involvement of these molecular pathways in TNBC are highlighted in this section below, with an extended overview of the influence of NF-κB signaling on TNBC covered in section 1.3.2.

Wnt Signaling: Aberrations in Wnt signaling, a highly conserved developmental pathway, have been shown to promote proliferation and survival [65], and epithelial-mesenchymal transition [66] in cancer cells. Normally, β-catenin, a dual function cell-cell adhesion and transcriptional co-activator protein, is routinely cleared from the cytoplasm by a destruction complex composed of APC, PP2A, GSK3, and CF1α. However, ligand-binding of Wnt to the G-protein coupled receptor (GPCR), Frazzled (Fz), induces recruitment of the destruction complex to the cell membrane and subsequent de-activation, leading to an accumulation of β-catenin within the cytoplasm. β-catenin eventually translocates to the nucleus, where it binds to and co-activates TCF/LEF-family transcription factors, thereby inducing transcription of genes involved in proliferation, EMT, and migration, such as Cyclin D1 and *c-myc*.

The importance of Wnt signaling in promoting tumor growth in TNBC was revealed by Xu et al. [67], who demonstrated that siRNA-mediated knockdown of β-catenin expression in TNBC cells implanted in mammary fat pads significantly reduced the size and growth rate of tumors in mice. In addition, analysis of expression of Wnt signaling genes in multiple patient tumor cohorts showed that an increase in Wnt/β-catenin signaling correlated with higher grade, poorer prognosis, and increase in lung and brain metastasis in triple-negative breast cancer [68].

Notch Signaling: The highly conserved Notch developmental pathway is also linked to breast cancer, with elevated Notch-1 and its ligand, Jagged-1, strongly correlating with low overall survival in patients [69]. Notch signaling involves binding of

transmembrane Notch ligands (named Delta-like and Jagged-like in mammalian cells) to Notch receptors which are usually expressed on neighboring cells. Ligand binding leads to cleavage of the Notch receptor intracellular domain NICD, which translocates to the nucleus and regulates gene expression by activating the transcription factor CSL. Notch signaling heavily influences the determination of cell fate, for example, in hematopoiesis and mammary gland development, and is also involved in angiogenesis, and in neuronal function and development.

In 2006, Hu et al. showed that constitutive overexpression of Notch-1 (N1IC) and Notch-4 (N4IC) could form spontaneous mammary tumors in a murine model [70]. Later studies revealed TNBC cells have increased nuclear localization of Notch-4, and SCID mice injected with MDA-MB-231 cells silenced for Notch-4 had reduced tumorigenesis as well as tumor volume [71].

Hedgehog Signaling: The Hedgehog (Hh) developmental pathway begins with the binding of a secreted ligand protein, Sonic hedgehog (SHH), to the Patched-1 receptor (PTCH1), which usually inhibits the activity of a transmembrane GPCR known as Smoothened (SMO). However, SHH-binding to PTCH1 inactivates it, thereby leading to SMO activation. SMO subsequently activates the GLI transcription factors, which are responsible for regulating the expression of genes involved in proliferation and differentiation.

Studies have shown Hedgehog signaling can promote self-renewal in breast cancer stem cells [72], and chemotherapy-resistant tumor growth [73, 74]. In the latter two studies, inhibiting Hh signaling was shown to reduce tumor growth and prevent clonogenic expansion of resistant cell lines respectively, providing a mechanistic explanation for the development of resistance in breast cancer cells. The GLI family of transcription factors, which include Gli1, Gli2, and Gli3, are the primary effectors of Hh signaling, and Gli1 overexpression and nuclear localization have been demonstrated as poor prognostic markers in women diagnosed with TNBC [75]. Gli1 overexpression can promote migration, invasion and metastasis in MDA-MB-231 TNBC cells by up-regulating matrix mettaloproteinase 11 (MMP-11), and inhibiting Gli1 can reduce the number of pulmonary metastases in mice injected with Gli1-silenced MDA-MB-231 cells

via tail vein [76]. Also of note is that Hh signaling is implicated in promoting angiogenesis in TNBC cells; Gli1 levels correlate strongly with vasoendothelial growth factor receptor 2 (VEGFR2) expression in tumor microarray studies, and silencing of Gli1 decreased protein levels of VEGFR2 in MDA-MB-468 TNBC cells [77].

PI3K/AKT/mTOR Signaling: PI3K signaling plays an important role in promoting cell survival, and anomalies in the PI3K/AKT/mTOR pathway are commonly found across breast cancer subtypes [78]. In TNBCs, aberrant PI3K signaling occurs primarily due to overexpression of epidermal growth factor receptor (EGFR), an upstream PI3K regulator, or due to activating mutations in PI3K catalytic subunit α (PIK3CA), or loss of function/expression mutations in downstream regulators such as phosphatase and tensin homolog (PTEN) and proline-rich inositol phosphate [79-81]. The inhibition of PI3K/Akt/mTOR in cisplatin-resistant HCC38 and MDA-MB-231 TNBC cells using the dual inhibitor NVP-BEZ235 was shown to re-sensitize the cells to cisplatin, and synergism between NVP-BEZ235 and carboplatin treatment has also been shown in TNBCs [82, 83].

1.3.2 NF-κB Signaling in TNBC

The NF-κB family of transcription factors includes five genes: p65 (RelA), RelB, c-Rel, p50/p105 (NF-κB1), and p52/p100 (NF-κB2). Most commonly, the heterodimer p50/RelA is sequestered to the perinuclear cytoplasm by IκB proteins. Canonical NF-κB signaling begins with TNF-α binding to its membrane receptor TNFR1, followed by TNFR1 trimerization [84, 85]. TNFR1 then recruits Complex I, which eventually leads to translocation of p50/RelA to the nucleus, where it acts as a transcription factor for several pro-survival genes [86-89]. If Complex I or downstream canonical signaling is inhibited, TNFR1 stimulation leads instead to recruitment of Complex II which recruits and activates caspase-8, leading to apoptosis [87]. Caspase-8 also cleaves RIP1, a key kinase of Complex I, thereby halting pro-survival canonical signaling [90]. Conversely, signaling through Complex I leads to increased expression of the Complex II inhibitor, cFLIP [89]. Thus, the activation states of Complex I and Complex II can determine cell fate in response to TNFR1 stimulation (Figure 1.3).

Over the last three decades, a mounting body of evidence has implicated aberrant NF-κB signaling in promoting TNBC progression. In 1997, Nakshatri et al. showed that NF-κB was constitutively activated during the advancement of RM22-F5 rat mammary carcinoma cells from a hormone-dependent, non-malignant phenotype to hormone-independent, malignant growth [91]. Constitutive activation of NF-κB has also been associated with human TNBC models such as MDA-MB-231 cells [91, 92].

Studies have indicated that targeting the NF-kB pathway can be useful for suppressing TNBC. For example, the chemical compound Bay-11-7082 ((E)-3-(4-Methylphenylsulfonyl)-2-propenenitrile) can prevent IκB phosphorylation by IKK, thereby preventing NF-κB translocation to the nucleus. Smith et al. showed that inhibition of NF-κB signaling by Bay-11-7082 induced CD44 repression and inhibition of proliferation and invasiveness of MDA-MB-231 and SUM159 TNBC cells [93]. Inhibiting NF-κB signaling directly or preventing the positive feedback mechanism via *TNF-α* knockout has also been shown to induce apoptosis in both ER- breast cancer cells as well as other cancer cell lines [94-98].

NF-κB signaling maintains an autocrine loop of pro-inflammatory cytokines like IL-6 and TNF-a, promotes expression of pro-survival factors such as Bcl-xL, cIAP1 and cIAP2 and proteins involved in cell cycle progression, for example Cyclin D1, as well as invasion and metastasis markers such as MMP-9 and Vimentin [84, 99-104]. Tropomodulin-1 (TMOD1) is a protein that inhibits elongation and depolymerization of actin filaments, and shows elevated expression in TNBC cells constitutively expressing NF-κB. TMOD1 was shown to be an NF-κB target gene capable of enhancing *in vivo* tumor growth of MDA-MB-231 cells in a mouse xenograft model [105].

Finally, the gene expression of several NF-κB-family members including RELA, RELB, and NFKB2 are controlled by SP1 and STAT3 transcription factors, with increased expression of RELA and SP1 correlating with lower 5-year distant recurrence-free survival (DRFS) in TNBC patients treated with adjuvant doxorubicin chemotherapy [106].

Overall, constitutive activation of NF-κB in cancer contributes to poor differentiation, aggressiveness and ability to survive and maintain hormone-independent

growth. Finding new NF-κB inhibitors is therefore an exciting avenue to therapeutics against TNBCs.

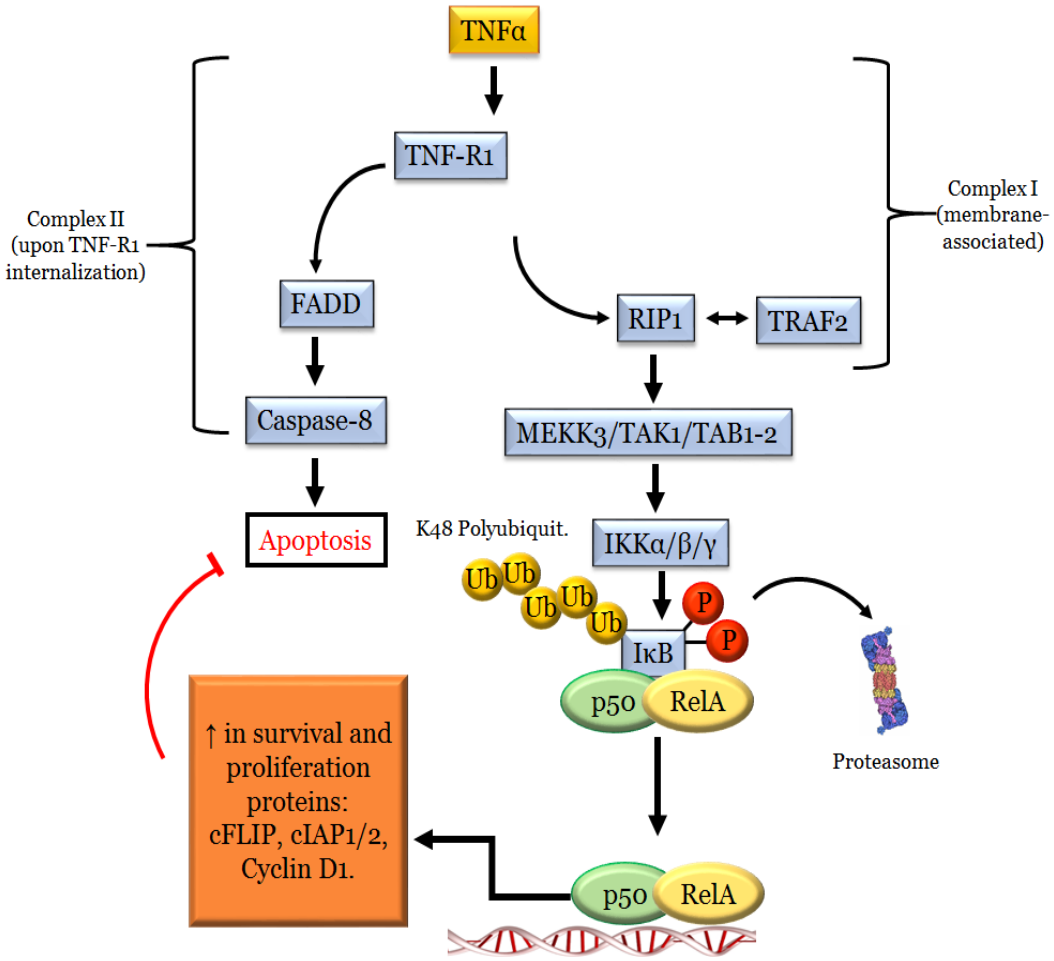

Figure 1.3 NF-κB signaling: Interplay between Complex I and Complex II determines cell fate upon TNF-R1 activation.

1.4 Metabolism in Triple-Negative Breast Cancer

As part of their sequel paper to their seminal review “The Hallmarks of Cancer”, Hanahan and Weinburg described metabolic reprogramming as one of the fundamental traits of cancer cells required to sustain their continuous growth and division [107]. In brief, cancer cells have been observed to shift their utilization of glucose towards ‘aerobic’ glycolysis (i.e. glycolysis in the presence of oxygen), and away from mitochondrial metabolism, a phenomenon known as the ‘Warburg effect’, in honor of Otto Warburg who first described this effect in the 1920’s - 50’s through a series of investigations into tumor metabolism [108, 109]. Subsequent studies highlighted below reveal TNBCs in particular are characterized by extensive metabolic reprogramming; with the identification of druggable targets from these pathways becoming a major focus of current research.

In TNBCs, EGFR signaling has been shown to elevate aerobic glycolysis, leading to the build-up of intermediates which can promote tumor growth, and local immune suppression of cytotoxic T-cells [110]. The transport of glucose into the cell is facilitated by the GLUT family of transporters, and in a study of 55 patient tumors of TNBC, GLUT1 (SLC2A1) was expressed in 42 (76.4 %) cases [111]. Metformin, a mitochondrial Complex I inhibitor commonly used as an anti-diabetic, has been shown to down-regulate the expression of several GLUT-family transporters, and can suppress proliferation and reduce the cancer stem cell population in TNBCs [112-114]. Indeed, a meta-analysis of 11 studies of over 5000 breast cancer patients found that the use of metformin among diabetic breast cancer patients has been associated with a 47 % decreased risk of death from all causes (HR: 0.53; 95% CI: 0.39-0.71) and significantly improved cancer-specific survival times (HR: 0.89; 95% CI: 0.79-1.00) [221].

Recent studies have described the complexity of metabolic reprogramming in TNBC cells as extending far beyond aerobic glycolysis. TNBCs are now understood to have a fundamentally altered metabolic profile with higher oxidative stress through increased reactive oxygen species (ROS) levels partially attributed to lower glutathione biosynthesis [115], and elevated uptake and utilization of glucose [116], glutamine [117-

119], and TCA cycle intermediates [120], as well as increased fatty acid β-oxidation [121].

1.4.1 Amino Acid Metabolism in TNBC

Amino acids serve as important precursors for TCA cycle entry in TNBC cells. In a comprehensive metabolomics study comparing the metabolite profiles of 15 TNBC vs 15 ER+ breast cancer tissue samples from African-American patients, Kanaan et al. found that 8 of 20 amino acids detected (aspartate, asparagine, glutamate, phenylalanine, methionine, and the branched-chain amino acids (BCAAs) leucine, isoleucine and valine) were significantly elevated in TNBC samples [120]. Transport of amino acids into cells is hypothesized to occur via a catalytic reaction with glutathione that converts them to γ-glutamyl amino acids, which can then traverse the plasma membrane. Following a reverse catalytic reaction that regenerates glutathione via a 5-oxoproline intermediate, the original amino acids are released into the intracellular space [122]. 6 of 7 γ-glutamyl amino acids identified in the study were significantly increased in TNBC samples, implying increased amino acid transportation in TNBC cells [120].

All 20 amino acids enter the TCA cycle via conversion to intermediates. Methionine and the BCAAs valine and isoleucine are first converted to Succinyl CoA which is rapidly converted to succinate and subsequently fumarate, while phenylalanine and aspartate are converted directly to fumarate [122]. TNBCs were shown to have elevated levels of the TCA intermediates fumarate, succinate, and malate, further supporting that TNBCs amplify the utilization of amino acid metabolism to meet their energy requirements [120].

The increase in amino acid metabolites in TNBCs has been validated in subsequent studies as well, with glutamine metabolism emerging as a therapeutic target [123]. “Glutamine addiction” is a term used to describe the dependence of many cancers, including TNBCs, on glutamine as a carbon and nitrogen source, and their inability to survive upon glutamine deprivation. Glutamine is shuttled into the cell through several transporters including alanine, serine, cysteine-preferring transporter 2 (SLC1A5/ASCT2), and subsequently converted to glutamate via glutaminase (GLS1),

before conversion to α-ketoglutarate by glutamate dehydrogenase (GDH) which marks the entry into the TCA cycle (Figure 1.4).

A 2016 study by van Geldermalsen et al. revealed mRNA expression of glutamine-metabolism genes SLC1A5, GLS, and GLUL (glutamine synthetase, which catalyzes *de novo* glutamine synthesis) were uniformly elevated across a cohort of 90 TNBC patient tumor samples [119]. The authors also showed pharmaceutical inhibition of SLC1A5 inhibited mTORC1 signaling, growth and progression of TNBC cells specifically *in vitro*, and SLC1A5 knockdown repressed TNBC mammary tumor growth, and improved survival in an *in vivo* mouse xenograft model. Suppression of GLS by both shRNA-mediated knockdown as well as pharmacological inhibition led to TNBC cell growth inhibition *in vitro* and *in vivo* [117, 124]. GLS inhibition by the chemical agent CB-839 was also associated with reduction in glutamine consumption and glutamate production, as well as decreases in oxygen consumption, glutathione levels, and TCA cycle intermediates including fumarate, malate, and citrate [124]. Finally, in a 2018 study, Mauro-Lizcano and Lopez-Rivas revealed that glutamine deprivation sensitized TNBC cells to tumor necrosis factor-related apoptosis-inducing ligand (TRAIL)-induced apoptosis through upregulation of TRAIL Receptor 2 (TRAILR2) [125]. Collectively, these studies highlight the importance of glutamine metabolism in maintaining energy homeostasis in TNBC cells, and supports investigations into targeting glutamine transporters and GLS as an avenue to TNBC therapy.

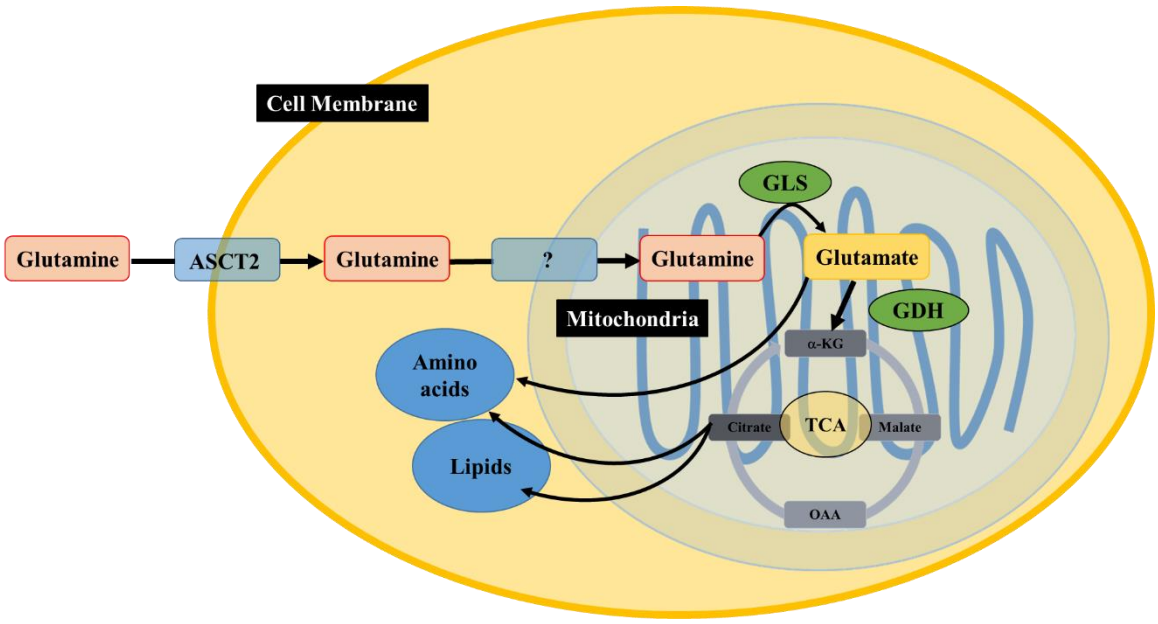

Figure 1.4 Glutamine transport and metabolism. Extracellular glutamine is transported into the cell through transporters such as alanine, serine, cysteine-preferring transporter 2 (SLC1A5/ASCT2). Transport into the mitochondria is carried out through a currently unknown mechanism but is theorized to occur based on the mitochondrial localization of glutaminase (GLS), and glutamate dehydrogenase (GDH). The end product of GDH action on glutamate results in the TCA Cycle intermediate, α-ketoglutarate (α-KG). Glutamate and the TCA Cycle intermediate citrate can also be further utilized in amino acid and lipid synthesis.

1.4.2 Mitochondrial metabolism in TNBC

Until recently, it was widely accepted that the 'Warburg effect', or increased aerobic glycolysis, was accompanied by a suppression of mitochondrial biogenesis in neoplastic cells. Beginning in the early 2000s however, a number of studies have shown that mitochondria are not only functionally active in many different cancer types, but that oncogenic activation of mitochondrial function is associated with increased malignancy and a dependence on oxidative phosphorylation (OXPHOS) for energy production, with breast cancer cells producing ~ 80 % of their ATP through mitochondrial metabolism [126-128].

In order to explain these two observations seemingly at odds with one another, in 2011, Smolkova et al. advanced the hypothesis that multiple "waves of gene expression" promote metabolic adaptations to the transforming tumor microenvironment and changing metabolic requirements [129]. The initial waves promote rapid proliferation by upregulating glycolysis at the expense of mitochondrial OXPHOS, leading to aglycemia and nutrient shortages. To compensate for this, and to promote tumor cell survival and clonal selection, subsequent waves re-establish glutaminolysis-driven TCA cycle and OXPHOS through oncogenic activation of c-Myc, and upregulation of PI3K-Akt-mTOR and LKB1-AMPK-p53 pathways [130-132]. As mentioned previously, glutamine uptake and utilization is upregulated in many cancers, including TNBC. Mazurek et al. revealed that when OXPHOS proceeds unencumbered, glutamine can fully compensate for a lack of glucose in cancer cells [133]. A summary of these findings are portrayed in Figure 1.5.

The oncogene c-Myc drives cell cycle progression, metabolic pathways, and survival under oxidative stress in cancer cells, with 54 % of chemotherapy-resistant TNBCs harboring c-Myc amplifications [134]. Indeed, cancer stem cells (CSCs) derived from TNBC cell lines have elevated c-Myc levels that correlate with increased ROS production and mitochondrial OXPHOS activity [135]. Treatment of SUM159PT and MDA-MB-436 TNBC cells (which express elevated levels of c-Myc) with oligomycin A (an ATP synthase inhibitor), or metformin (a Complex I inhibitor) can reduce the oxygen consumption rate (OCR) and mammosphere formation in these cell lines [135]. In another study, c-Myc was shown to inhibit mitochondrial glutaminase (GLS) repression

in P-493B lymphoma PC3 prostate cancer cells, thereby upregulating glutamine catabolism for ATP production through TCA cycle activity [136]. The siRNA-mediated silencing of GLS inhibited cell proliferation, and addition of the TCA intermediate oxaloacetate could partially rescue proliferation, further underlining the importance of mitochondrial metabolism in the growth and proliferation of cancer cells [136].

The advantages of glutamine metabolism to cancer cells was highlighted in a 2009 review by Weinberg and Chandel [137]. By serving as a substrate for the TCA cycle, glutamine drives ATP production via OXPHOS and also satisfies the proliferating cell's demand for lipid, nucleotide, and protein synthesis. Citrate produced in the TCA cycle, for example, is transported to the cytosol and converted to Acetyl-CoA required in lipid biosynthesis, while malate, another TCA intermediate, is instead converted to oxaloacetate in the cytosol, and then to aspartate via aspartate aminotransferase (AAT); this is required for synthesis of pyrimidines that make up DNA. Malate can also be decarboxylated in the cytosol by malic enzyme (ME) to produce pyruvate and NADPH, the latter of which is shuttled toward lipid biosynthesis and regeneration of reduced glutathione. Thus, targeting enzymes utilizing TCA intermediates for cellular biosynthesis may prove useful against aggressive cancers with elevated mitochondrial metabolism. Indeed, inhibiting AAT activity in MDA-MB-231 TNBC cells using amino oxyacetate (AOA) or siRNA-mediated silencing inhibited proliferation and oxygen consumption *in vitro*, and reduced tumor xenograft growth *in vivo*.

Taken together, studies on cancer metabolism report that there are shifts in preference for glycolysis-driven or mitochondrial-driven ATP production that are dependent on tumor stage, cancer type and subtype, nutrient availability, and tumor microenvironment. Mounting evidence supports a dependence of aggressive, late-stage cancers on TCA cycle intermediates that drive glucose-independent ATP production via OXPHOS while also giving rise to biosynthetic precursor metabolites. Targeting the TCA cycle and OXPHOS in such cancers – including triple-negative breast cancer – may be a highly viable avenue to novel therapeutics.

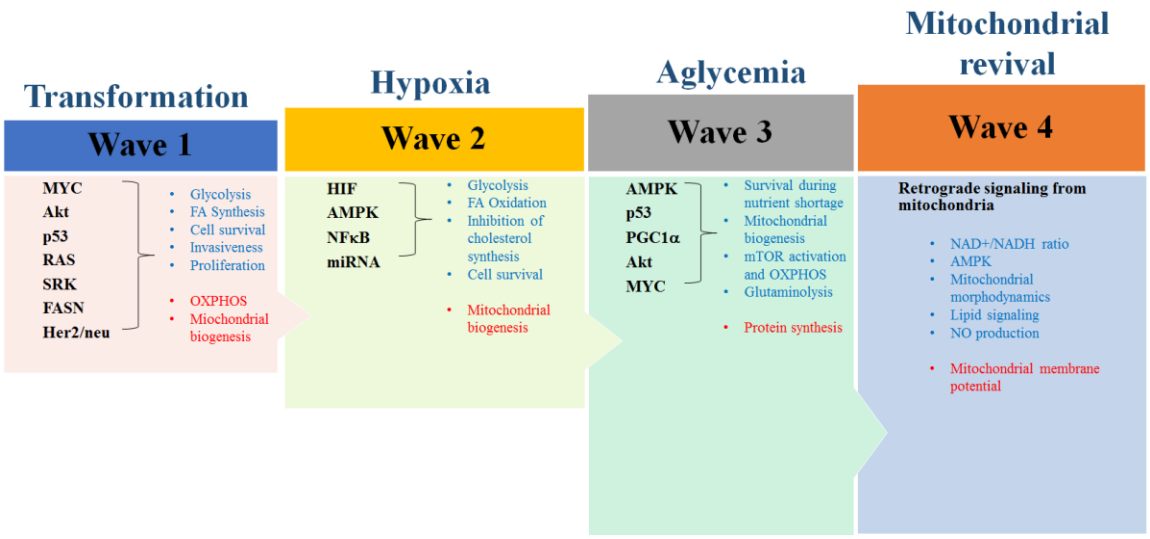

Figure 1.5 Waves of metabolic reprogramming during carcinogenesis. Wave 1: Oncogenic transformation leads to enhanced glycolytic activity at the expense of OXPHOS and mitochondrial biogenesis, leading to rapid proliferation. Wave 2: Promotion of cell survival through HIF and NFκB signaling, with sustained glycolytic activity and inhibition of mitochondrial biogenesis. Wave 3: Activation of AMPK and Akt signaling leads to inhibition of protein synthesis. PGC1α activation leads to mitochondrial biogenesis followed by OXPHOS initiation, while MYC activation increases glutaminolysis. Wave 4: Mitochondrial biogenesis and activity leads to mitochondrial signaling activation through multiple effectors including NAD+/NADH ratio, AMPK, Ca^{2+} and lipid signaling, and NO production. In addition, changes in mitochondrial inner membrane potential and morphology may lead to downstream signaling activation/inhibition.

Source: Modified from Smolkova et al. (2011). The International Journal of Biochemistry & Cell Biology, 43(7), 950–968.

1.5 An Important Role for Plant-derived Metabolites in Cancer Therapy

The use of plants in medicine has a deep history, widely recorded in multiple cultures across the globe. The study of such plant-based traditional remedies has had a lasting impact on onco-drug discovery; with vinca alkaloids, camptothecins, epipodophyllotoxins, and taxanes currently in clinical use against a range of cancers including leukemia, lymphomas, neuroblastomas, small cell lung cancer, ovarian, colon, stomach, prostate, head and neck, and breast cancer. Given the rich diversity of plant life and the identification of several phytochemicals with anticancer properties, research into plant-derived bioactive compounds remains an important source of novel therapeutics against cancer.

1.5.1 Cancer Drug Discovery from Plant Sources: A Historical Perspective

Discovery of the topoisomerase II-inhibitor, etoposide: One of the first intensively researched plants to yield a cancer therapeutic was from the genus *Podophyllum.* This genus includes two species: American *Podophyllum (Podophyllum peltatum),* and Indian *Podophyllum (Podophyllum hexandrum)* [138]. Native Americans had been known to use extracts of *P. peltatum* for several purposes. *P. peltatum* root extracts were used as cathartics, antihelminthics, and purgatives [139], with the first recorded use of *Podophyllum* to treat ‘cancer’ by the Penobscot Indians of Maine [140]. It was soon found that the medicinal properties of *Podophyllum* could be attributed to their rhizomes, which were rich in resin. In 1844, Dr. John King published the first report on the alcohol extraction of *Podophyllum* resin, which he named podophyllin [141-143], and finally, in 1881, Podwyssotzki isolated and crystalized the major bioactive component of *Podophyllum* extracts, which he named podophyllotoxin [144].

Beginning with Kaplan in 1942 [145], several studies on podophyllin and podophyllotoxin uncovered its antimitotic effects *in vitro*, and in 1947, Hartwell and Shear demonstrated its ability to kill cancer cells *in vivo* [146]. Investigations into the mechanism of action of podophyllotoxin revealed that it could bind strongly to tubulin, thereby inhibiting the formation of mitotic spindle and inducing cell cycle arrest. However, the acute gastrointestinal toxicity of podophyllotoxin led investigators to synthesize derivatives with less severe side-effects. In the mid-50s, Stähelin and Von

Wartburg painstakingly tested hundreds of hemisynthetic β-D-glycosidic derivatives of podophyllotoxin, culminating in the identification of VP-16 (etoposide) and VM-26 (teniposide), which were selected on the basis of their *in vivo* efficacy in increasing survival time in mice inoculated with the L-1210 leukemia cell line [147]. It was later found that VP-16 induced cell arrest by inhibiting topoisomerase II activity, thereby introducing double strand breaks in DNA that activated apoptotic signaling cascades in rapidly dividing cancer cells [148]. Etoposide is currently FDA-approved for the treatment of small cell lung cancer and refractory testicular cancer.

Discovery of the microtubule polymerization inhibitors, vinca indole alkolids: The vinca alkaloids were first isolated from the leaves of the plant *Catharanathus roseus (aka. Vinca rosea)*. The plant was originally brought to the attention of the medical community in the mid-1950s when it was noted that the native peoples of Jamaica used *C. roseus* leaves to make an herbal tea believed to benefit diabetics [149].

Investigations by Dr. J. B. Collip and Dr. Robert L. Noble at the University of Western Ontario found that aqueous extracts of the leaves had little to no effect on blood sugar levels, but when injected in rats, led instead to a transient, rapid decrease in white blood cell (WBC) count due to bone marrow destruction. This exciting discovery motivated Collip and Noble, in association with Dr. Charles T. Beer and Dr. Henry Cutts, to isolate the bioactive component of the extract by bioassay-driven fractionation. After a year of intense research, the team isolated vincaleukoblastine (VLB, later shortened to vinblastine), and another team at Eli Lilly Company isolated vincristine (VCR); with the two later shown to be dimeric indole alkaloids [150].

X-ray crystallographic studies of VLB and VCR by Moncrief and Lipscomb in 1965 revealed that the two molecules differed by a single functional group, with VCR possessing an aldehyde (CHO) group where VLB has a methyl (CH_3) group [151]. This small difference accounted for the difference in clinical responses to these drugs; VLB is primarily used against lymphomas and causes acute toxicity to the bone marrow, while VCR is mostly used to treat acute leukemia and displays peripheral nervous system toxicity.

Clinical trials showcasing the efficacy of vinblastine and vincristine have led to FDA approval for single-drug use in Hodgkin's lymphoma, acute leukemia, melanoma, testicular, bladder, and prostate cancer, as well as in combination chemotherapy for Hodgkin's lymphoma, Non-Hodgkin's malignant lymphomas, rhabdomyosarcoma, neuroblastoma, and Wilm's Tumor.

In conclusion, the serendipitous discovery of such anticancer drugs through studies of traditional folk remedies in the 1950s lead the National Institutes of Health (NIH) to begin large-scale screening of natural extracts on cancer models to isolate and identify their bioactive anticancer compounds [152]. This work was carried out by the National Cancer Institute (NCI) through its Cancer Chemotherapy National Service Center (CCNSC). These experiments led directly to the discovery of the life-saving chemotherapeutics camptothecin and taxane by Monroe Wall, Mansukh Wani, and others at the Natural Products Laboratory, Research Triangle Institute (RTI), in North Carolina. The mechanism of action of these and other plant-derived compounds leading to cancer cell death are discussed in the following section.

1.5.2 Mechanisms of Anticancer Action of Plant-derived Compounds

1.5.2.1 Interference with microtubule assembly

Taxanes are a class of diterpenes originally derived from the bark of the Pacific Yew tree (*Taxus brevifolia*). Both taxanes as well as vinca alkaloids are 'spindle poisons' that target microtubule assembly to inhibit cell division. Taxanes stabilize GDP-bound tubulin to prevent microtubule *depolymerization* [153], while vinca alkaloids bind to the ends of assembled microtubules to prevent addition of new tubulin dimers, thereby inhibiting the *polymerization* process [154]. Consequently, these compounds are specifically potent to rapidly proliferating cells such as cancer cells, with the unfortunate side-effect of attacking frequently dividing cells in the bone marrow, intestinal lining, and hair follicles, leading to myelo/immuno-suppression, mucositis, and alopecia respectively.

1.5.2.2 Inhibition of DNA topoisomerases

Camptothecin (CPT), a cyclical compound derived from the bark of the *Camptotheca acuminata* tree, was first discovered in 1966 by Wall et al. at the Research Triangle

Institute [155]. In contrast to taxanes and vinca alkaloids, camptothecins are topoisomerase inhibitors. Topoisomerases are proteins involved in the winding or unwinding of DNA; functions critical for transcription and DNA replication. In 1983, Hsiang and Liu were the first to show CPT binds to mammalian DNA topoisomerase I to form ternary complexes that stabilize binding and result in DNA strand breaks, leading to apoptosis [156]. CPT analogues include topotecan and irinotecan, which have higher solubility and bioavailability than CPT and are currently in clinical use for colon, pancreatic, ovarian, cervical, and lung cancers.

In general, epipodophyllotoxins, derived from the root of the American Mayapple (*Podophyllum peltatum*), act through multiple mechanisms including inhibition of microtubule assembly [157]; however, etoposide (VP-16) and teniposide (VM-26), the most commonly utilized semisynthetic derivatives of the base compound podophyllotoxin, act predominantly through topoisomerase inhibition. As with CPT, multiple studies in the late 1980s showed that VP-16 and VM-26 can stabilize the interaction between topoisomerase II and DNA, interfering with the scissor-reunion reaction of the enzyme [158, 159], as well as its 'strand-passing' activity which allows it to disentangle topologically confined DNA [159, 160]. This leads to a halt in DNA replication and mitosis, eventually causing cell death.

1.5.2.3 Interference with multiple proliferative and survival pathways

In addition to impeding cell division mechanics, plant compounds can also bind and/or inhibit multiple protein targets, thereby regulating several cellular pathways that promote growth, proliferation, and survival in cancer cells. For example, resveratrol (5-((E)-2-(4-hydroxyphenyl) vinyl)-1,3-benzenediol), a compound found abundantly in grape skins, peanuts, and berries, has recently entered human clinical trials after a number of studies highlighted its ability to induce apoptosis, autophagy, and senescence in multiple cancer cell lines *in vitro*, and prevent tumor initiation, angiogenesis, and metastasis *in vivo* [161-167]. The variety of cancer cell death mechanisms triggered upon treatment with resveratrol can be explained by the observation that it directly targets over 20 different proteins, including those involved in metabolism (FAS, CBR1, NQO2), inflammation (COX1/2, LTA_4H), cell cycle arrest (Polα/β, ATM, AKT1), post-translational

modification (pan-HDAC inhibition, and inhibition of the kinases PKCα, AKT1, PKD1), and cell signaling (COX1/2, Phosphodiesterases) [168].

A review of cell death mechanisms induced by anti-cancer plant polyphenols, flavonoids, and terpenoids by Gali-Muhtasib in 2015 revealed that – while several pathways regulated by these compounds are unique – the majority of these compounds are capable of inhibiting the Akt/mTOR pathways, generating reactive oxygen species (ROS), or disrupting mitochondrial membrane potential [169]. For example, curcumin, the major bioactive polyphenol present in the turmeric rhizome (*Curcuma longa*), inhibited phosphorylation of Akt and induced autophagy in U87-MG and U373-MG human malignant glioma cells *in vitro* and significantly inhibited growth of malignant glioma tumors in nude mice upon intratumoral injection at 100 mg/kg body weight [170]. Similarly, the isoflavone genistein, originally isolated in 1899 from *Genista tinctoria* and found abundantly in soybean, also reduced P-Akt levels and significantly inhibited glucose uptake in ovarian cancer cells, again leading to autophagy [171].

Naturally-occurring and semi-synthetic analogues of the alkaloids noscapine and colchicine, initially isolated from *Lachryma papaveris* (opium) and *Colchicum autumnale* (meadow saffron), respectively, have been shown to induce autophagic cell death in prostate, leukemia, pancreatic and lung cancer cells via ROS generation [172-174].

Another example of a multifunctional anti-cancer plant compound is the terpenoid, parthenolide, from *Tanacetum parthenium*, which induced autophagy in MDA-MB-231 TNBC cells by generating ROS as well as by inhibiting NF-κB signaling, and is capable of inducing necrotic cell death in these cells by disrupting the mitochondrial membrane potential [175].

In addition, several of these and other polyphenols, alkaloids, and terpenoids have been observed to inhibit telomerases [176, 177], induce DNA damage [178, 179], reduce Cyclin D1 expression, [180] and activate AMPK-mediated cell death [181]. The variety of signaling pathways targeted by plant-derived compounds to induce cancer cell death is a reflection of their enormous diversity in structure and chemistry, and highlights the

need to develop technologies and processes to better exploit their potential in the development of novel cancer therapies.

1.5.3 *Lippia* species as a source of anti-cancer compounds

The genus *Lippia* comprises over 200 species of tropical flowering shrubs from the family Verbenaceae. The essential oils from these plants are usually aromatic and fragrant, and have been well documented as possessing anti-fungal [182, 183], anti-bacterial [183, 184], anti-mutagenic [185, 186], anti-inflammatory [187-189], and analgesic [188, 190-192] qualities. More recently, *L. sidoides*, *L. salviifolia*, and *L. rotundifolia* showed cytotoxicity against CT26 colon cancer cells [193], while *L. alba* induced G_0/G_1 cell cycle arrest and apoptosis against both lung (A549) and liver (HepG2) cell lines [194].

Lippia origanoides is a medicinal tropical plant native to South and Central America, and its extracts have previously been shown to possess anti-inflammatory and anti-nociceptive analgesic activities in mice [195]. Individual components of the extract have shown pro-apoptotic and anti-proliferative effects on several cancer cell lines [196-202]. Carvacrol and thymol, two of the major components of *L. origanoides*, also inhibited NF-κB signaling in models of hepatotoxicity and LPS-stimulation [203, 204]. As previously noted, NF-κB signaling is a pro-survival inflammatory pathway often constitutively activated in TNBC cells [90, 91]. Thus, a major goal of this research project was to describe the effect of *L. origanoides* extracts on NF-κB signaling in TNBC. However, keeping in mind the multi-component nature of these extracts, a further goal was to map the proteome-wide changes regulated by the extract to identify additional and possibly synergistic mechanisms of action.

1.6 Quantitative LC-MS-based Proteomics for Cancer Drug Discovery

Drug discovery from bioactive natural extracts has commonly been achieved through bioassay-driven fractionation schemes, which are both time-consuming and expensive [205, 206]. In addition, attempting to identify the mechanisms of drug action through standard molecular biology techniques such as Western Blotting, PCR, and ELISA does

not provide information on off-target, detrimental side-effects that only come to light *in vivo* or during clinical trials. Hence, there is a need to study cells and tissues at the systems level to better capture the effects of chemotherapy. Transcriptomics approaches using cDNA-microarrays and RNA-Seq technologies have provided a more holistic picture of cellular responses to treatments [207]. Changes at the RNA level, however, have often been shown not to translate to proportional changes in protein expression [208-210]. For this reason, when screening natural extracts and drugs, it is critical that new technologies be developed and employed to describe their effects on the entire **proteome**.

Quantitative proteomics using LC-MS-based instrumentation along with accompanying data analysis software tools has quickly established itself as the method of choice to study cell- and tissue-wide changes in protein levels. The label-free quantitative (LFQ) approach utilized in this study compares the chromatograms of peptide precursor ions belonging to a particular protein between treatment groups. Specialized software assigns an 'intensity value' for each peptide, calculated by integrating all the MS peaks over the peptide's chromatographic time scale. This value is then compared to the corresponding intensity value from the same peptide in the other experimental group(s) [211]. Aside from easier sample preparation and lower cost, the LFQ approach offers 3 main advantages over stable-isotope or chemical labelling-based proteomics methods, i.e. i) there is no limit to the number of experimental groups, ii) there is no increase in spectral complexity, and iii) LFQ provides a wider dynamic range.

Quantitative LC-MS-based proteomics has already seen wide-scale application in the field of cancer biomarker discovery. For example, by comparing the proteomes of cancer vs. normal cell lines, both Gronborg et al. and Everly et al. were able to identify unique protein signatures in pancreatic cancer and prostate cancer respectively [212, 213].

Proteomic has also been applied to studying the mechanisms of drug action. As mentioned previously, Her2 inhibition is a standard treatment strategy against breast cancers overexpressing Her2. In order to characterize the phosphoproteome signaling mechanisms mediated by Her2, Bose et al. utilized LC-MS based proteomics to quantify

changes in phosphoproteins in NIH 3T3 cells overexpressing Her2 and treated with PD168393, a selective Her2 tyrosine kinase inhibitor [214].

As the field of LC-MS-based proteomics grows, several large-scale studies have been conducted to provide deeper insights into cancer heterogeneity. In a massive LFQ study comparing the proteomes of 16 TNBC, 3 receptor-positive breast cancer, and one non-tumorigenic mammary cell line, along with 4 primary TNBC tumors, Lawrence et al. were able cluster TNBC cells into distinct phenotypic subtypes based on protein abundance (previously only performed on the basis of RNA *transcriptome* abundances) [215]. The authors were able to use their TNBC proteome database to identify TNBC biomarkers, highlight differences between the TNBC transcriptome and proteome, and describe pathways mediating drug sensitivity in different TNBC subtypes [215].

Studies such as these underline the advantages of quickly adopting powerful new proteomics technologies to tackle two of the major problems facing cancer researchers; namely, the lack of targetable biomarkers for several forms of cancer, and the lack of knowledge on off-target drug mechanisms leading to issues with sensitivity, safety, and drug resistance.

1.7 Research Questions

Despite significant advancements in targeted treatment options and survival outcomes for patients diagnosed with hormone receptor-positive breast cancer, targetable biomarkers for TNBC remain unidentified, and treatment regimens continue to depend on cytotoxic chemotherapy, causing severe side-effects and often rendered ineffective by the development of drug resistance. Plant-derived compounds offer a virtually unlimited and unexploited diversity of compounds which could provide the next generation of TNBC-specific chemo-drugs. The *Lippia origanoides* species, while revealed as capable of providing anti-inflammatory and analgesic effects, has not yet been studied as a source of anti-cancer compounds. Several compounds present in *L. origanoides* extracts have been shown to inhibit NF-κB signaling, a key inflammatory pathway promoting survival and drug resistance in cancer cells, and commonly activated in TNBC.

Here, the capacity of *L. origanoides* extract (LOE) to inhibit cell viability was investigated across multiple TNBC cell lines (MDA-MB-231, CRL-2321, MCF10AH), and compared to its effects on the normal mammary cell line MCF10A using the MTT viability assay [Chapter 2]. The effects of LOE on the cell cycle and mechanism of induction of cell death in MDA-MB-231 cells was also studied via flow cytometry, and further characterized by Western Blotting for common markers of proliferation and apoptosis including Cyclin D1 and caspase-8 respectively [Chapter 2]. Finally, based on the known anti-inflammatory effects of *Lippia* extracts, we examined the effect of LOE on the NF-κB signaling pathway in MDA-MB-231 cells, an inflammatory and commonly activated pathways in TNBC, to reveal a possible mechanism of action behind the apoptotic effects of LOE in these cells.

During the course of our research into *Lippia* extracts we studied L42, an extract prepared from the same species (*L. organoides*) as LOE, but from a different chemotype (grown under non-identical conditions). L42 was identified as having even higher potency against TNBC cells than LOE while retaining the reduced inhibitory effect against normal cells, and was used in subsequent mechanistic studies [Chapter 3]. It was recognized that the large number of compounds present in L42 could regulate multiple cellular pathways, and it was therefore necessary to utilize a proteomics-based approach to fully understand its inhibitory effects on TNBC cells. Chapter 3 describes our label-free quantitative LC-MS-based proteomics approach to investigate the molecular mechanism behind L42-induced apoptosis in MDA-MB-231 cells. Our study reveals that developing therapeutics to target mitochondrial metabolism may be a potent method of destroying aggressive breast cancers.

In summary, the studies presented here provide support for a more comprehensive program investigating the anti-cancer potential of naturally-sourced compounds. Our investigations highlight the advantages of using proteomics-based approaches to fully understand the multiple pathways regulated by single compounds and complex mixtures such as plant-derived extracts. Finally, we present the *L. origanoides* species as a source of cytotoxic compounds with significant potency against TNBC cells.

1.8 References

1. Siegel, R. L., Miller, K. D., & Jemal, A. (2018). Cancer statistics, 2018. CA, A Cancer Journal for Clinicians, 68(1), 7-30.
2. Jordan, V. C. (1992). The role of tamoxifen in the treatment and prevention of breast cancer. Current Problems in Cancer, 16(3), 134-176.
3. Buzdar, A., & Howell, A. (2001). Advances in aromatase inhibition, clinical efficacy and tolerability in the treatment of breast cancer. Clinical Cancer Research, 7(9),2620-35.
4. Romond, E. H., Perez, E. A., Bryant, J., Suman, V. J., Geyer, C. E., Davidson, N. E., et al. (2005). Trastuzumab plus Adjuvant Chemotherapy for Operable HER2-Positive Breast Cancer. New England Journal of Medicine, 353(16), 1673–1684.
5. Dent, R., Hanna, W. M., Trudeau, M., Rawlinson, E., Sun, P., & Narod, S. A. (2008). Pattern of metastatic spread in triple-negative breast cancer. Breast Cancer Research and Treatment, 115(2), 423–428.
6. Bray, F., Ferlay, J., Soerjomataram, I., Siegel, R. L., Torre, L. A. & Jemal, A. (2018). Global cancer statistics 2018, GLOBOCAN estimates of incidence and mortality worldwide for 36 cancers in 185 countries. CA, A Cancer Journal for Clinicians, 68, 394-424.
7. American Cancer Society. (2018). Cancer Facts & Figures 2018. Retrieved from https,//www.cancer.org/content/dam/cancer-org/research/cancer-facts-and-statistics/annual-cancer-facts-and-figures/2018/cancer-facts-and-figures-2018.pdf.
8. Sieri, S., Chiodini, P., Agnoli, C., Pala, V., Berrino, F., Trichopoulou, A., et al. (2014). Dietary Fat Intake and Development of Specific Breast Cancer Subtypes. JNCI, Journal of the National Cancer Institute, 106(5).
9. Lynch, B. M., Neilson, H. K., & Friedenreich, C. M. (2010). Physical Activity and Breast Cancer Prevention. Physical Activity and Cancer, 186, 13–42.
10. Terry, M., Zhang, F., Kabat, G., Britton, J., Teitelbaum, S., Neugut, A., & Gammon, M. (2006). Lifetime Alcohol Intake and Breast Cancer Risk. Annals of Epidemiology, 16(3), 230–240.

11. Luo, J., Margolis, K. L., Wactawski-Wende, J., Horn, K., Messina, C., Stefanick, M. L., et al. (2011). Association of active and passive smoking with risk of breast cancer among postmenopausal women, a prospective cohort study. BMJ, 342, d1016.
12. Shapira, N. (2017). The potential contribution of dietary factors to breast cancer prevention. European Journal of Cancer Prevention, 26(5), 385–395.
13. Collaborative Group on Hormonal Factors in Breast Cancer. (2012). Menarche, menopause, and breast cancer risk, individual participant meta-analysis, including 118 964 women with breast cancer from 117 epidemiological studies. The Lancet Oncology, 13(11), 1141–1151.
14. Sun, X., Nichols, H. B., Tse, C., Bell, M. B., Robinson, W. R., Sherman, M. E., et al. (2015). Association of Parity and Time since Last Birth with Breast Cancer Prognosis by Intrinsic Subtype. Cancer Epidemiology Biomarkers & Prevention, 25(1), 60–67.
15. Zhou, Y., Chen, J., Li, Q., Huang, W., Lan, H., & Jiang, H. (2015). Association Between Breastfeeding and Breast Cancer Risk, Evidence from a Meta-analysis. Breastfeeding Medicine, 10(3), 175–182.
16. Skol, A. D., Sasaki, M. M., & Onel, K. (2016). The genetics of breast cancer risk in the post-genome era, thoughts on study design to move past BRCA and towards clinical relevance. Breast Cancer Research, 18(1), 99.
17. Kurian, A. W., Fish, K., Shema, S. J., & Clarke, C. A. (2010). Lifetime risks of specific breast cancer subtypes among women in four racial/ethnic groups. Breast Cancer Research, 12(6).
18. Chen, C., Huang, Y., Liu, X., Gao, Y., Dai, H., Song, F., et al. (2014). Active and passive smoking with breast cancer risk for Chinese females, a systematic review and meta-analysis. Chinese Journal of Cancer, 33(6), 306–316.
19. White, A. J., O'Brien, K. M., Niehoff, N. M., Carroll, R., & Sandler, D. P. (2019). Metallic Air Pollutants and Breast Cancer Risk in a Nationwide Cohort Study. Epidemiology, 30(1), 20–28.
20. Inman, J. L., Robertson, C., Mott, J. D., & Bissell, M. J. (2015). Mammary gland development, cell fate specification, stem cells and the microenvironment. Development, 142(6), 1028–1042.

21. Wellings, S. (1980). A Hypothesis of the Origin of Human Breast Cancer from the Terminal Ductal Lobular Unit. Pathology - Research and Practice, 166(4), 515–535.
22. Lteif, A., & Javed, A. (2013). Development of the Human Breast. Seminars in Plastic Surgery, 27(01), 005–012.
23. Tornillo, G., & Smalley, M. J. (2015). ERrrr…Where are the Progenitors? Hormone Receptors and Mammary Cell Heterogeneity. Journal of Mammary Gland Biology and Neoplasia, 20(1-2), 63–73.
24. Gudjonsson, T. (2002). Isolation, immortalization, and characterization of a human breast epithelial cell line with stem cell properties. Genes & Development, 16(6), 693–706.
25. Liu, X., Feng, D., Liu, D., Wang, S., Yu, X., Dai, E., et al. (2016). Dissecting the Origin of Breast Cancer Subtype Stem Cell and the Potential Mechanism of Malignant Transformation. PLOS ONE, 11(10), e0165001.
26. Prasetyanti, P. R., & Medema, J. P. (2017). Intra-tumor heterogeneity from a cancer stem cell perspective. Molecular Cancer, 16(1), 41.
27. Perou, C. M., Sørlie, T., Eisen, M. B., Van de Rijn, M., Jeffrey, S. S., Rees, C. A., et al. (2000). Molecular portraits of human breast tumours. Nature, 406(6797), 747–752.
28. Gnant, M., Thomssen, C., & Harbeck, N. (2015). St. Gallen/Vienna 2015, A Brief Summary of the Consensus Discussion. Breast Care, 10(2), 124–130.
29. Cakir, A., Gonul, I., & Uluoglu, O. (2012). A comprehensive morphological study for basal-like breast carcinomas with comparison to nonbasal-like carcinomas. Diagnostic Pathology, 7(1), 145.
30. Bertucci, F., Finetti, P., Cervera, N., Esterni, B., Hermitte, F., Viens, P., & Birnbaum, D. (2008). How basal are triple-negative breast cancers? International Journal of Cancer, 123(1), 236–240.
31. Rakha, E. A., El-Sayed, M. E., Green, A. R., Paish, E. C., Lee, A. H. S., & Ellis, I. O. (2007). Breast carcinoma with basal differentiation, a proposal for pathology definition based on basal cytokeratin expression. Histopathology, 50(4), 434–438.
32. Alluri, P., & Newman, L. A. (2014). Basal-like and triple-negative breast cancers, searching for positives among many negatives. Surgical oncology clinics of North America, 23(3), 567-77.

33. Lin, N. U., Vanderplas, A., Hughes, M. E., Theriault, R. L., Edge, S. B., Wong, Y.-N., et al. (2012). Clinicopathologic features, patterns of recurrence, and survival among women with triple-negative breast cancer in the National Comprehensive Cancer Network. Cancer, 118(22), 5463–5472.
34. American Cancer Society. (2017). Breast Cancer Facts & Figures 2017-2018. Atlanta, American Cancer Society, Inc.
35. Stark, A., Kleer, C. G., Martin, I., Awuah, B., Nsiah-Asare, A., Takyi, V., Braman, M., Quayson, S. E., Zarbo, R., Wicha, M., et al. (2010). African ancestry and higher prevalence of triple-negative breast cancer, findings from an international study. Cancer, 116(21), 4926-32.
36. Ma, H., Wang, Y., Sullivan-Halley, J., Weiss, L., Marchbanks, P. A., Spirtas, R., et al. (2010). Use of Four Biomarkers to Evaluate the Risk of Breast Cancer Subtypes in the Women's Contraceptive and Reproductive Experiences Study. Cancer Research, 70(2), 575–587.
37. Ma, H., Ursin, G., Xu, X., Lee, E., Togawa, K., Duan, L., et al. (2017). Reproductive factors and the risk of triple-negative breast cancer in white women and African-American women, a pooled analysis. Breast Cancer Research, 19(1).
38. Hartley, M.C., McKinley, B.P., Rogers, E.A., Kalbaugh, C.A., Messich, H.S., Blackhurst, D.W., et al. (2006). Differential expression of prognostic factors and effect on survival in young (< or =40) breast cancer patients, a case-control study. The American Surgeon, 72(12), 1189-94.
39. Carey, L. A., Perou, C. M., Livasy, C. A., Dressler, L. G., Cowan, D., Conway, K., et al. (2006). Race, Breast Cancer Subtypes, and Survival in the Carolina Breast Cancer Study. JAMA, 295(21), 2492.
40. Flegal, K. M., Kruszon-Moran, D., Carroll, M. D., Fryar, C. D., & Ogden, C. L. (2016). Trends in Obesity Among Adults in the United States, 2005 to 2014. JAMA, 315(21), 2284.
41. Millikan, R. C., Newman, B., Tse, C., Moorman, P. G., Conway, K., Smith, L. V., et al. (2008). Epidemiology of basal-like breast cancer. Breast Cancer Research and Treatment, 109(1), 123–139.

42. Ambrosone, C. B., Ciupak, G. L., Bandera, E. V., Jandorf, L., Bovbjerg, D. H., Zirpoli, G., et al. (2009). Conducting Molecular Epidemiological Research in the Age of HIPAA, A Multi-Institutional Case-Control Study of Breast Cancer in African-American and European-American Women. Journal of Oncology, 2009, 1–15.
43. Dietze, E. C., Chavez, T. A., & Seewaldt, V. L. (2018). Obesity and Triple-Negative Breast Cancer. The American Journal of Pathology, 188(2), 280–290.
44. Massihnia, D., Galvano, A., Fanale, D., Perez, A., Castiglia, M., Incorvaia, L., et al. (2016). Triple negative breast cancer, shedding light onto the role of pi3k/akt/mtor pathway. Oncotarget, 7(37), 60712–60722.
45. Hartman, Z.C., Poage, G.M., den Hollander, P., Tsimelzon, A., Hill, J., Panupinthu, N., et al. (2013) Growth of triple-negative breast cancer cells relies upon coordinate autocrine expression of the proinflammatory cytokines IL-6 and IL-8. Cancer Research, 73(11), 3470–3480.
46. Mavaddat, N., Barrowdale, D., Andrulis, I. L., Domchek, S. M., Eccles, D., Nevanlinna, H., et al. (2011). Pathology of Breast and Ovarian Cancers among BRCA1 and BRCA2 Mutation Carriers, Results from the Consortium of Investigators of Modifiers of BRCA1/2 (CIMBA). Cancer Epidemiology Biomarkers & Prevention, 21(1), 134–147.
47. Greenup, R., Buchanan, A., Lorizio, W., Rhoads, K., Chan, S., Leedom, T., . . . Shelley Hwang, E. (2013). Prevalence of BRCA Mutations Among Women with Triple-Negative Breast Cancer (TNBC) in a Genetic Counseling Cohort. Annals of Surgical Oncology, 20(10), 3254–3258.
48. Shimelis, H., LaDuca, H., Hu, C., Hart, S. N., Na, J., Thomas, A., et al. (2018). Triple-Negative Breast Cancer Risk Genes Identified by Multigene Hereditary Cancer Panel Testing. JNCI, Journal of the National Cancer Institute, 110(8), 855–862.
49. Urru, S. A. M., Gallus, S., Bosetti, C., Moi, T., Medda, R., Sollai, E., et al. (2018). Clinical and pathological factors influencing survival in a large cohort of triple-negative breast cancer patients. BMC Cancer, 18(1).
50. Pogoda, K., Niwińska, A., Murawska, M., & Pieńkowski, T. (2013). Analysis of pattern, time and risk factors influencing recurrence in triple-negative breast cancer patients. Medical Oncology, 30(1).

51. Carey, L. A., Dees, E. C., Sawyer, L., Gatti, L., Moore, D. T., Collichio, F., et al. (2007). The Triple Negative Paradox, Primary Tumor Chemosensitivity of Breast Cancer Subtypes. Clinical Cancer Research, 13(8), 2329–2334.
52. Kennecke, H., Yerushalmi, R., Woods, R., Cheang, M. C. U., Voduc, D., Speers, C. H., et al. (2010). Metastatic Behavior of Breast Cancer Subtypes. Journal of Clinical Oncology, 28(20), 3271–3277.
53. McAndrew, N., & DeMichele, A. (2018). Neoadjuvant Chemotherapy Considerations in Triple-Negative Breast Cancer. The Journal of Targeted Therapies in Cancer, 7(1), 52-69.
54. Beretta, G. L., & Zunino, F. (2007). Molecular Mechanisms of Anthracycline Activity. Topics in Current Chemistry, 283, 1–19.
55. Schiff, P. B., & Horwitz, S. B. (1980). Taxol stabilizes microtubules in mouse fibroblast cells. Proceedings of the National Academy of Sciences, 77(3), 1561–1565.
56. Wang, J., Peng, L., Zhang, R., Zheng, Z., Chen, C., Cheung, K. L., et al. (2016). 5-Fluorouracil targets thymidylate synthase in the selective suppression of TH17 cell differentiation. Oncotarget, 7(15), 19312-26.
57. Ferrara, N., Hillan, K. J., & Novotny, W. (2005). Bevacizumab (Avastin), a humanized anti-VEGF monoclonal antibody for cancer therapy. Biochemical and Biophysical Research Communications, 333(2), 328–335.
58. Poggio, F., Bruzzone, M., Ceppi, M., Pondé, N. F., La Valle, G., Del Mastro, L., et al. (2018). Platinum-based neoadjuvant chemotherapy in triple-negative breast cancer, a systematic review and meta-analysis. Annals of Oncology, 29(7), 1497-1508.
59. Hugh, J., Hanson, J., Cheang, M. C. U., Nielsen, T. O., Perou, C. M., Dumontet, C., et al. (2009). Breast Cancer Subtypes and Response to Docetaxel in Node-Positive Breast Cancer, Use of an Immunohistochemical Definition in the BCIRG 001 Trial. Journal of Clinical Oncology, 27(8), 1168–1176.
60. Martin, M., Rodriguez-Lescure, A., Ruiz, A., Alba, E., Calvo, L., Ruiz-Borrego, M., et al. (2008). Randomized Phase 3 Trial of Fluorouracil, Epirubicin, and Cyclophosphamide Alone or Followed by Paclitaxel for Early Breast Cancer. JNCI Journal of the National Cancer Institute, 100(11), 805–814.

61. Colleoni, M., Cole, B. F., Viale, G., Regan, M. M., Price, K. N., Maiorano, E., et al. (2010). Classical cyclophosphamide, methotrexate, and fluorouracil chemotherapy is more effective in triple-negative, node-negative breast cancer, results from two randomized trials of adjuvant chemoendocrine therapy for node-negative breast cancer. Journal of Clinical Oncology, 28(18), 2966-73.
62. Han, H. S., Diéras, V., Robson, M., Palácová, M., Marcom, P. K., Jager, A., et al. (2017). Veliparib with temozolomide or carboplatin/paclitaxel versus placebo with carboplatin/paclitaxel in patients with BRCA1/2 locally recurrent/metastatic breast cancer, randomized phase II study. Annals of Oncology, 29(1), 154-161.
63. Bell, R., Brown, J., Parmar, M., Toi, M., Suter, T., Steger, G., et al. (2016). Final efficacy and updated safety results of the randomized phase III BEATRICE trial evaluating adjuvant bevacizumab-containing therapy in triple-negative early breast cancer. Annals of Oncology, 28(4), 754–760.
64. Lehmann, B. D., Bauer, J. A., Chen, X., Sanders, M. E., Chakravarthy, A. B., Shyr, Y., & Pietenpol, J. A. (2011). Identification of human triple-negative breast cancer subtypes and preclinical models for selection of targeted therapies. Journal of Clinical Investigation, 121(7), 2750–2767.
65. Zeng, G., Apte, U., Cieply, B., Singh, S., & Monga, S. P. (2007). siRNA-mediated beta-catenin knockdown in human hepatoma cells results in decreased growth and survival. Neoplasia, 9(11), 951-9.
66. Sanchez-Tillo, E., De Barrios, O., Siles, L., Cuatrecasas, M., Castells, A., & Postigo, A. (2011). β-catenin/TCF4 complex induces the epithelial-to-mesenchymal transition (EMT)-activator ZEB1 to regulate tumor invasiveness. Proceedings of the National Academy of Sciences, 108(48), 19204–19209.
67. Xu, J., Prosperi, J. R., Choudhury, N., Olopade, O. I., & Goss, K. H. (2015). β-Catenin Is Required for the Tumorigenic Behavior of Triple-Negative Breast Cancer Cells. PLOS ONE, 10(2), e0117097.

68. Dey, N., Barwick, B. G., Moreno, C. S., Ordanic-Kodani, M., Chen, Z., Oprea-Ilies, G., et al. (2013). Wnt signaling in triple negative breast cancer is associated with metastasis. BMC Cancer, 13(1), 537.

69. Reedijk, M., Odorcic, S., Chang, L., Zhang, H., Miller, N., McCready, D. R., et al. (2005). High-level Coexpression of JAG1 and NOTCH1 Is Observed in Human Breast Cancer and Is Associated with Poor Overall Survival. Cancer Research, 65(18), 8530–8537.

70. Hu, C., Diévart, A., Lupien, M., Calvo, E., Tremblay, G., & Jolicoeur, P. (2006). Overexpression of activated murine Notch1 and Notch3 in transgenic mice blocks mammary gland development and induces mammary tumors. The American Journal of Pathology, 168(3), 973-90.

71. Nagamatsu, I., Onishi, H., Matsushita, S., Kubo, M., Kai, M., Imaizumi, A., et al. (2014). NOTCH4 is a potential therapeutic target for triple-negative breast cancer. Anticancer Research, 34(1), 69-80.

72. Liu, S., Dontu, G., Mantle, I. D., Patel, S., Ahn, N., Jackson, K. W., et al. (2006). Hedgehog Signaling and Bmi-1 Regulate Self-renewal of Normal and Malignant Human Mammary Stem Cells. Cancer Research, 66(12), 6063–6071.

73. Heller, E., Hurchla, M. A., Xiang, J., Su, X., Chen, S., Schneider, J., et al. (2011). Hedgehog Signaling Inhibition Blocks Growth of Resistant Tumors through Effects on Tumor Microenvironment. Cancer Research, 72(4), 897–907.

74. Sims-Mourtada, J., Opdenaker, L. M., Davis, J., Arnold, K. M., & Flynn, D. (2014). Taxane-induced hedgehog signaling is linked to expansion of breast cancer stem-like populations after chemotherapy. Molecular Carcinogenesis, 54(11), 1480–1493.

75. Arnold, K., Pohlig, R., & Sims‐Mourtada, J. (2017). Co‐activation of Hedgehog and Wnt signaling pathways is associated with poor outcomes in triple negative breast cancer. Oncology Letters, 14(5), 5285–5292.

76. Kwon, Y., Hurst, D. R., Steg, A. D., Yuan, K., Vaidya, K. S., Welch, D. R., & Frost, A. R. (2011). Gli1 enhances migration and invasion via up-regulation of MMP-11 and promotes metastasis in ERα negative breast cancer cell lines. Clinical & Experimental Metastasis, 28(5), 437–449.

77. Di Mauro, C., Rosa, R., D'Amato, V., Ciciola, P., Servetto, A., Marciano, R., et al. (2017). Hedgehog signalling pathway orchestrates angiogenesis in triple-negative breast cancers. British Journal of Cancer, 116(11), 1425–1435.
78. Costa, R. L. B., Han, H. S., & Gradishar, W. J. (2018b). Targeting the PI3K/AKT/mTOR pathway in triple-negative breast cancer, a review. Breast Cancer Research and Treatment, 169(3), 397–406.
79. Davis, N. M., Sokolosky, M., Stadelman, K., Abrams, S. L., Libra, M., Candido, et al. (2014). Deregulation of the EGFR/PI3K/PTEN/Akt/mTORC1 pathway in breast cancer, possibilities for therapeutic intervention. Oncotarget, 5(13), 4603-50.
80. Cossu-Rocca, P., Orrù, S., Muroni, M. R., Sanges, F., Sotgiu, G., Ena, S., et al. (2015). Analysis of PIK3CA Mutations and Activation Pathways in Triple Negative Breast Cancer. PLOS ONE, 10(11), e0141763.
81. Ooms, L., Binge, L., Davies, E., Rahman, P., Conway, J., Gurung, R., et al. (2015). The Inositol Polyphosphate 5-Phosphatase PIPP Regulates AKT1-Dependent Breast Cancer Growth and Metastasis. Cancer Cell, 28(2), 155–169.
82. Gohr, K., Hamacher, A., Engelke, L. H., & Kassack, M. U. (2017). Inhibition of PI3K/Akt/mTOR overcomes cisplatin resistance in the triple negative breast cancer cell line HCC38. BMC Cancer, 17(1).
83. Montero, J. C., Esparís-Ogando, A., Re-Louhau, M. F., Seoane, S., Abad, M., Calero, R., et al. (2012). Active kinase profiling, genetic and pharmacological data define mTOR as an important common target in triple-negative breast cancer. Oncogene, 33(2), 148–156.

84. Khoshnan, A., Tindell, C., Laux, I., Bae, D., Bennett, B., & Nel, A. E. (2000). The NF- B Cascade Is Important in Bcl-xL Expression and for the Anti-Apoptotic Effects of the CD28 Receptor in Primary Human CD4+ Lymphocytes. The Journal of Immunology, 165(4), 1743–1754.
85. Banner, D.W., D'Arcy, A., Janes, W., Gentz, R., Schoenfeld, H.J., Broger, C., et al. (1993). Crystal structure of the soluble human 55 kd TNF receptor-human TNF beta complex: implications for TNF receptor activation. Cell, 73(3):431-45.

86. Chan, F. K. (2000). The pre-ligand binding assembly domain: a potential target of inhibition of tumor necrosis factor receptor function. Annals of the Rheumatic Diseases, 59(90001), i50–i53.
87. Micheau, O., & Tschopp, J. (2003). Induction of TNF receptor I-mediated apoptosis via two sequential signaling complexes. Cell, 114(2), 181–190.
88. Wirth, T., & Baltimore, D. (1988). Nuclear factor NF-kappa B can interact functionally with its cognate binding site to provide lymphoid-specific promoter function. The EMBO Journal, 7(10), 3109–3113.
89. Micheau, O., Lens, S., Gaide, O., Alevizopoulos, K., & Tschopp, J. (2001). NF-kappaB signals induce the expression of c-FLIP. Molecular and Cellular Biology, 21(16), 5299–5305.
90. Lin, Y., Devin, A., Rodriguez, Y., & Liu, Z. G. (1999). Cleavage of the death domain kinase RIP by caspase-8 prompts TNF-induced apoptosis. Genes & Development, 13(19), 2514–2526.
91. Nakshatri, H., Bhat-Nakshatri, P., Martin, D. A., Goulet, R. J., & Sledge, G. W. (1997). Constitutive activation of NF-kappaB during progression of breast cancer to hormone-independent growth. Molecular and Cellular Biology, 17(7), 3629–3639.
92. Sero, J. E., Sailem, H. Z., Ardy, R. C., Almuttaqi, H., Zhang, T., & Bakal, C. (2015). Cell shape and the microenvironment regulate nuclear translocation of NF-κB in breast epithelial and tumor cells. Molecular Systems Biology, 11(3), 790.
93. Smith, S. M., Lyu, Y. L., & Cai, L. (2014). NF-κB Affects Proliferation and Invasiveness of Breast Cancer Cells by Regulating CD44 Expression. PLoS ONE, 9(9).
94. Ciucci, A., Gianferretti, P., Piva, R., Guyot, T., Snape, T., Roberts, S. M., & Santoro, M. G. (2006). Induction of Apoptosis in Estrogen-Receptor Negative Breast Cancer Cells by Natural and Synthetic Cyclopentenones: Role of the IKK/NF-κB Pathway. Molecular Pharmacology.
95. Horie, R., Watanabe, T., & Umezawa, K. (2006). Blocking NF-kappaB as a potential strategy to treat adult T-cell leukemia/lymphoma. Drug News & Perspectives, 19(4), 201–209.

96. Patel, N. M., Nozaki, S., Shortle, N. H., Bhat-Nakshatri, P., Newton, T. R., Rice, S., et al. (2000). Paclitaxel sensitivity of breast cancer cells with constitutively active NF-kappaB is enhanced by IkappaBalpha super-repressor and parthenolide. Oncogene, 19(36), 4159–4169.
97. Pileczki, V., Braicu, C., Gherman, C. D., & Berindan-Neagoe, I. (2012). TNF-α gene knockout in triple negative breast cancer cell line induces apoptosis. International Journal of Molecular Sciences, 14(1), 411–420.
98. Rahman, K. W., Ali, S., Aboukameel, A., Sarkar, S. H., Wang, Z., Philip, P. A., et al. (2007). Inactivation of NF-κB by 3,3′-diindolylmethane contributes to increased apoptosis induced by chemotherapeutic agent in breast cancer cells. Molecular Cancer Therapeutics, 6(10), 2757–2765.
99. Hartman, Z. C., Poage, G. M., den Hollander, P., Tsimelzon, A., Hill, J., Panupinthu, N., et al. (2013). Growth of triple-negative breast cancer cells relies upon coordinate autocrine expression of the proinflammatory cytokines IL-6 and IL-8. Cancer Research, 73(11), 3470–3480.
100. Hinz, M., Krappmann, D., Eichten, A., Heder, A., Scheidereit, C., & Strauss, M. (1999). NF-kappaB function in growth control: regulation of cyclin D1 expression and G0/G1-to-S-phase transition. Molecular and Cellular Biology, 19(4), 2690–2698.
101. Huber, M. A., Azoitei, N., Baumann, B., Grünert, S., Sommer, A., Pehamberger, H., et al. (2004). NF-kappaB is essential for epithelial-mesenchymal transition and metastasis in a model of breast cancer progression. The Journal of Clinical Investigation, 114(4), 569–581.
102. Kagoya, Y., Yoshimi, A., Kataoka, K., Nakagawa, M., Kumano, K., Arai, S., et al. (2014). Positive feedback between NF-κB and TNF-α promotes leukemia-initiating cell capacity. The Journal of Clinical Investigation, 124(2), 528–542.
103. Wang, C. Y., Mayo, M. W., Korneluk, R. G., Goeddel, D. V., & Baldwin, A. S. (1998). NF-kappaB antiapoptosis: induction of TRAF1 and TRAF2 and c-IAP1 and c-IAP2 to suppress caspase-8 activation. Science (New York, N.Y.), 281(5383), 1680–1683.

104. Yousef, E. M., Tahir, M. R., St-Pierre, Y., & Gaboury, L. A. (2014). MMP-9 expression varies according to molecular subtypes of breast cancer. BMC Cancer, 14(1), 609.
105. Ito-Kureha, T., Koshikawa, N., Yamamoto, M., Semba, K., Yamaguchi, N., Yamamoto, T., et al. (2015). Tropomodulin 1 expression driven by NF-κB enhances breast cancer growth. Cancer Research, 75(1), 62–72.
106. Kim, J.-Y., Jung, H. H., Ahn, S., Bae, S., Lee, S. K., Kim, S. W., et al. (2016). The relationship between nuclear factor (NF)-κB family gene expression and prognosis in triple-negative breast cancer (TNBC) patients receiving adjuvant doxorubicin treatment. Scientific Reports, 6: 31804.
107. Hanahan, D., & Weinberg, R. A. (2011). Hallmarks of cancer: the next generation. Cell, 144(5), 646–674.
108. Warburg, O. (1956). Origin of Cancer Cells. Science, 123, 309-314.
109. Koppenol, W. H., Bounds, P. L., & Dang, C. V. (2011). Otto Warburg's contributions to current concepts of cancer metabolism. Nature Reviews Cancer, 11(5), 325–337.
110. Lim, S. O., Li, C. W., Xia, W., Lee, H. H., Chang, S. S., Shen, J., et al. (2016). EGFR signaling enhances aerobic glycolysis in triple-negative breast cancer cells to promote tumor growth and immune escape. Cancer Research, 76(5), 1284-96.
111. Hussein, Y. R., Bandyopadhyay, S., Semaan, A., Ahmed, Q., Albashiti, B., Jazaerly, T., Nahleh, Z., et al. (2011). Glut-1 expression correlates with basal-like breast cancer. translational oncology, 4(6), 321-7.
112. Wahdan-Alaswad, R. S., Edgerton, S. M., Salem, H. S., & Thor, A. D. (2018). Metformin targets glucose metabolism in triple negative breast cancer. Journal of oncology translational research, 4(1), 129.
113. Alimova, I. N., Liu, B., Fan, Z., Edgerton, S. M., Dillon, T., Lind, S. E., & Thor, A. D. (2009). Metformin inhibits breast cancer cell growth, colony formation and induces cell cycle arrest *in vitro*. Cell Cycle, 8(6), 909–915.
114. Shi, P., Liu, W., Tala, Wang, H., Li, F., Zhang, H., et al. (2017). Metformin suppresses triple-negative breast cancer stem cells by targeting KLF5 for degradation. Cell Discovery, 3, 17010.

115. Beatty, A., Fink, L. S., Singh, T., Strigun, A., Peter, E., Ferrer, C. M., … Peterson, J. R. (2018). Metabolite Profiling Reveals the Glutathione Biosynthetic Pathway as a Therapeutic Target in Triple-Negative Breast Cancer. Molecular Cancer Therapeutics, 17(1), 264–275.
116. Lim, S.O., Li, C.W., Xia, W.Y., Lee, H.H., Chang, S.S., Shen, J. et al. (2016). EGFR Signaling Enhances Aerobic Glycolysis in Triple-Negative Breast Cancer Cells to Promote Tumor Growth and Immune Escape, Cancer Research, 76, 1284-1296.
117. Lampa, M., Arlt, H., He, T., Ospina, B., Reeves, J., Zhang, B.L. et al. (2017). Glutaminase Is Essential for the Growth of Triple-Negative Breast Cancer Cells with a Deregulated Glutamine Metabolism Pathway and Its Suppression Synergizes with Mtor Inhibition. PLoS One, 12, e0185092.
118. Goode, G., Gunda, V., Chaika, N.V., Purohit, V., Yu, F., Singh, P.K. (2017). Muc1 Facilitates Metabolomic Reprogramming in Triple-Negative Breast Cancer. PLoS One, 12, e0176820.
119. Van Geldermalsen, M., Wang, Q., Nagarajah, R., Marshall, A.D., Thoeng, A., Gao, D. et al. (2016). ASCT2/SLC1A5 Controls Glutamine Uptake and Tumor Growth in Triple-Negative Basal-Like Breast Cancer. Oncogene, 35, 3201-3208.
120. Kanaan, Y.M., Sampey, B.P., Beyene, D., Esnakula, A.K., Naab, T.J., Ricks-Santi, L.J. et al. (2014). Metabolic Profile of Triple-Negative Breast Cancer in African-American Women Reveals Potential Biomarkers of Aggressive Disease. Cancer Genomics and Proteomics, 11, 279-294.
121. Wright, H.J., Hou, J., Xu, B., Cortez, M., Potma, E.O., Tromberg, B.J., & Razorenova, O.V. (2017). CDCP1 regulates lipid metabolism in TNBC. Proceedings of the National Academy of Sciences U.S.A., 8, 114 (32).
122. Berg, J. M., Tymoczko, J. L., & Stryer, L. (2002). Carbon Atoms of Degraded Amino Acids Emerge as Major Metabolic Intermediates. Biochemistry. 5th Edition.
123. Kung, H.-N., Marks, J. R., & Chi, J.-T. (2011). Glutamine Synthetase Is a Genetic Determinant of Cell Type–Specific Glutamine Independence in Breast Epithelia. PLOS Genetics, 7(8), e1002229.

124. Gross, M. I., Demo, S. D., Dennison, J. B., Chen, L., Chernov-Rogan, T., Goyal, B., et al. (2014). Antitumor activity of the glutaminase inhibitor CB-839 in triple-negative breast cancer. Molecular Cancer Therapeutics, 13(4), 890–901.
125. Mauro-Lizcano, M., & López-Rivas, A. (2018). Glutamine metabolism regulates FLIP expression and sensitivity to TRAIL in triple-negative breast cancer cells. Cell Death and Disease, 9(2), 205.
126. Vyas, S., Zaganjor, E., & Haigis, M. C. (2016). Mitochondria and Cancer. Cell, 166(3), 555-566.
127. Ashton, T. M., McKenna, W. G., Kunz-Schughart, L. A., & Higgins, G. S. (2018). Oxidative Phosphorylation as an Emerging Target in Cancer Therapy. Clinical Cancer Research: An Official Journal of the American Association for Cancer Research, 24(11), 2482–2490.
128. Rodríguez-Enríquez, S., Carreño-Fuentes, L., Gallardo-Pérez, J. C., Saavedra, E., Quezada, H., Vega, A., et al. (2010). Oxidative phosphorylation is impaired by prolonged hypoxia in breast and possibly in cervix carcinoma. The International Journal of Biochemistry & Cell Biology, 42(10), 1744–1751.
129. Smolková, K., Plecitá-Hlavatá, L., Bellance, N., Benard, G., Rossignol, R., & Ježek, P. (2011). Waves of gene regulation suppress and then restore oxidative phosphorylation in cancer cells. The International Journal of Biochemistry & Cell Biology, 43(7), 950–968.

130. Schieke, S. M., Phillips, D., McCoy, J. P., Aponte, A. M., Shen, R.-F., Balaban, R. S., & Finkel, T. (2006). The Mammalian Target of Rapamycin (mTOR) Pathway Regulates Mitochondrial Oxygen Consumption and Oxidative Capacity. Journal of Biological Chemistry, 281(37), 27643–27652.
131. Yuneva, M., Zamboni, N., Oefner, P., Sachidanandam, R., & Lazebnik, Y. (2007). Deficiency in glutamine but not glucose induces MYC-dependent apoptosis in human cells. The Journal of Cell Biology, 178(1), 93–105.
132. Hardie, D. G., & Alessi, D. R. (2013). LKB1 and AMPK and the cancer-metabolism link - ten years after. BMC biology, 11, 36.

133. Mazurek, S., Michel, A., & Eigenbrodt, E. (1997). Effect of Extracellular AMP on Cell Proliferation and Metabolism of Breast Cancer Cell Lines with High and Low Glycolytic Rates. Journal of Biological Chemistry, 272(8), 4941–4952.
134. Balko, J. M., Giltnane, J. M., Wang, K., Schwarz, L. J., Young, C. D., Cook, R. S., et al. (2014). Molecular profiling of the residual disease of triple-negative breast cancers after neoadjuvant chemotherapy identifies actionable therapeutic targets. Cancer Discovery, 4(2), 232–245.
135. Lee, K. M., Giltnane, J. M., Balko, J. M., Schwarz, L. J., Guerrero-Zotano, A. L., Hutchinson, K. E., et al. (2017). MYC and MCL1 Cooperatively Promote Chemotherapy-Resistant Breast Cancer Stem Cells via Regulation of Mitochondrial Oxidative Phosphorylation. Cell metabolism, 26(4), 633-647.e7.
136. Gao, P., Tchernyshyov, I., Chang, T. C., Lee, Y. S., Kita, K., Ochi, T., et al. V. (2009). c-Myc suppression of miR-23a/b enhances mitochondrial glutaminase expression and glutamine metabolism. Nature, 458(7239), 762-5.
137. Weinberg, F., & Chandel, N. S. (2009). Mitochondrial Metabolism and Cancer. Annals of the New York Academy of Sciences, 1177(1), 66–73.
138. Royle, J.F. (1839). Illustration of the botany and other branches of natural history of the Himalayan mountains and the flora of Cashmere. WC Allen & Co, eds, London.
139. Moermann, D.E., (1986). Medicinal plants of native America: University of Michigan, Ann Arbor, Museum of Anthropology, technical report No. 19.
140. Lombard, L.H., & The Maine Writers Research Club. (1952). Maine Indians in history and legends: Medicinal plants of our Maine Indians. Severn-Wylie-Jewel, eds, Portland.
141. King, J. (1844). New York Philosophical Medical Journal, 4, 159-161.
142. King, J. (1857. The discovery of podophyllin. College Journal of Medical Science, 2, 557-559.
143. Imbert, T. F. (1998). Discovery of podophyllotoxins. Biochimie, 80(3), 207–222.
144. Podwyssotzki, V. (1882). On the active constituents of podophyllin. American Journal of Pharmacy, 12, 102-115.
145. Kaplan, I.W. (1942). *Condylomata acuminata*. New Orleans Medical and Surgical Journal, 94,388–390.

146. Hartwell, J.L., & Shear, M.J. (1947). Chemotherapy of cancer: Classes of compounds under investigation, and active components of podophyllin. Cancer Research, 7, 716-717.
147. Stähelin, H. (1969). VM 26, a new podophyllotoxin glucoside derivative with anti-L1210 activity. Proceedings of the American Association for Cancer Research, 10, 86.
148. Ross, W., Rowe, T., Glisson, B., Yalowich, J., & Liu, L. (1984). Role of topoisomerase II in mediating epipodophyllotoxin-induced DNA cleavage. Cancer Research, 44(12 Pt 1), 5857–5860.
149. Noble, R. L. (1990). The discovery of the *Vinca* alkaloids--chemotherapeutic agents against cancer. Biochimie Et Biologie Cellulaire, 68(12), 1344–1351.
150. Noble, R. L., Beer, C. T., & Cutts, J. H. (1958). Role of chance observations in chemotherapy: *Vinca rosea*. Annals of the New York Academy of Sciences, 76(3), 882–894.
151. Moncrief, J. W., & Lipscomb, W. N. (1965). Structures of Leurocristine (Vincristine) and Vincaleukoblastine.1 X-Ray Analysis of Leurocristine Methiodide. Journal of the American Chemical Society, 87(21), 4963–4964.
152. Chabner, B.A., & Roberts, T.G. (2005). Timeline - Chemotherapy and the War on Cancer. Nature Reviews Cancer, 5, 65-72.
153. Diaz, J. F., & Andreu, J. M. (1993). Assembly of purified GDP-tubulin into microtubules induced by taxol and taxotere: Reversibility, ligand stoichiometry, and competition. Biochemistry, 32(11), 2747–2755.
154. Himes, R. H. (1991). Interactions of the *Catharanthus (Vinca*) alkaloids with tubulin and microtubules. Pharmacology & Therapeutics, 51(2), 257–267.
155. Wall, M. E., Wani, M. C., Cook, C. E., Palmer, K. H., McPhail, A. T., & Sim, G. A. (1966). Plant Antitumor Agents. I. The Isolation and Structure of Camptothecin, a Novel Alkaloidal Leukemia and Tumor Inhibitor from *Camptotheca acuminata*. Journal of the American Chemical Society, 88(16), 3888–3890.
156. Hsiang, Y. H., & Liu, L. F. (1988). Identification of mammalian DNA topoisomerase I as an intracellular target of the anticancer drug camptothecin. Cancer Research, 48(7), 1722–1726.

157. Loike, J. D., & Horwitz, S. B. (1976). Effects of podophyllotoxin and VP-16-213 on microtubule assembly *in vitro* and nucleoside transport in HeLa cells. Biochemistry, 15(25), 5435–5443.
158. Minocha, A., & Long, B. H. (1984). Inhibition of the DNA catenation activity of type II topoisomerase by VP16-213 and VM26. Biochemical and Biophysical Research Communications, 122(1), 165–170.
159. Long, B. H., & Stringfellow, D. A. (1988). Inhibitors of topoisomerase II: structure-activity relationships and mechanism of action of podophyllin congeners. Advances in Enzyme Regulation, 27, 223–256.
160. Chen, G. L., Yang, L., Rowe, T. C., Halligan, B. D., Tewey, K. M., & Liu, L. F. (1984). Non-intercalative antitumor drugs interfere with the breakage-reunion reaction of mammalian DNA topoisomerase II. The Journal of Biological Chemistry, 259(21), 13560–13566.
161. Afaq, F., Adhami, V. M., & Ahmad, N. (2003). Prevention of short-term ultraviolet B radiation-mediated damages by resveratrol in SKH-1 hairless mice. Toxicology and Applied Pharmacology, 186(1), 28–37.
162. Blanquer-Rosselló, M. del M., Hernández-López, R., Roca, P., Oliver, J., & Valle, A. (2017). Resveratrol induces mitochondrial respiration and apoptosis in SW620 colon cancer cells. Biochimica et Biophysica Acta (BBA) - General Subjects, 1861(2), 431–440.
163. Jang, M., Cai, L., Udeani, G. O., Slowing, K. V., Thomas, C. F., Beecher, C. W., et al. (1997). Cancer chemopreventive activity of resveratrol, a natural product derived from grapes. Science (New York, N.Y.), 275(5297), 218–220.
164. Kalra, N., Roy, P., Prasad, S., & Shukla, Y. (2008). Resveratrol induces apoptosis involving mitochondrial pathways in mouse skin tumorigenesis. Life Sciences, 82(7–8), 348–358.
165. Li, B., Hou, D., Guo, H., Zhou, H., Zhang, S., Xu, X., et al. (2017). Resveratrol sequentially induces replication and oxidative stresses to drive p53-CXCR2 mediated cellular senescence in cancer cells. Scientific Reports, 7(1), 208.

166. Park, D., Jeong, H., Lee, M. N., Koh, A., Kwon, O., Yang, Y. R., et al. H. (2016). Resveratrol induces autophagy by directly inhibiting mTOR through ATP competition. Scientific Reports, 6, 21772.
167. Reagan-Shaw, S., Afaq, F., Aziz, M. H., & Ahmad, N. (2004). Modulations of critical cell cycle regulatory events during chemoprevention of ultraviolet B-mediated responses by resveratrol in SKH-1 hairless mouse skin. Oncogene, 23(30), 5151–5160.
168. Kulkarni, S. S., & Cantó, C. (2015). The molecular targets of resveratrol. Biochimica et Biophysica Acta (BBA) - Molecular Basis of Disease, 1852(6), 1114–1123.
169. Gali-Muhtasib, H., Hmadi, R., Kareh, M., Tohme, R., & Darwiche, N. (2015). Cell death mechanisms of plant-derived anticancer drugs: beyond apoptosis. Apoptosis: An International Journal on Programmed Cell Death, 20(12), 1531–1562.
170. Aoki, H., Takada, Y., Kondo, S., Sawaya, R., Aggarwal, B. B., & Kondo, Y. (2007). Evidence that curcumin suppresses the growth of malignant gliomas *in vitro* and in vivo through induction of autophagy: role of Akt and extracellular signal-regulated kinase signaling pathways. Molecular Pharmacology, 72(1), 29–39.
171. Gossner, G., Choi, M., Tan, L., Fogoros, S., Griffith, K. A., Kuenker, M., & Liu, J. R. (2007). Genistein-induced apoptosis and autophagocytosis in ovarian cancer cells. Gynecologic Oncology, 105(1), 23–30.
172. Karna, P., Zughaier, S., Pannu, V., Simmons, R., Narayan, S., & Aneja, R. (2010). Induction of reactive oxygen species-mediated autophagy by a novel microtubule-modulating agent. The Journal of Biological Chemistry, 285(24), 18737–18748.
173. Larocque, K., Ovadje, P., Djurdjevic, S., Mehdi, M., Green, J., & Pandey, S. (2014). Novel Analogue of Colchicine Induces Selective Pro-Death Autophagy and Necrosis in Human Cancer Cells. PLOS ONE, 9(1), e87064.
174. Bhattacharya, S., Das, A., Datta, S., Ganguli, A., & Chakrabarti, G. (2016). Colchicine induces autophagy and senescence in lung cancer cells at clinically admissible concentration: potential use of colchicine in combination with autophagy inhibitor in cancer therapy. Tumour Biology: The Journal of the International Society for Oncodevelopmental Biology and Medicine, 37(8), 10653–10664.

175. D'Anneo, A., Carlisi, D., Lauricella, M., Puleio, R., Martinez, R., Di Bella, S., et al. (2013). Parthenolide generates reactive oxygen species and autophagy in MDA-MB231 cells. A soluble parthenolide analogue inhibits tumour growth and metastasis in a xenograft model of breast cancer. Cell Death & Disease, 4, e891.
176. Naasani, I., Seimiya, H., Yamori, T., & Tsuruo, T. (1999). FJ5002: a potent telomerase inhibitor identified by exploiting the disease-oriented screening program with COMPARE analysis. Cancer Research, 59(16), 4004–4011.
177. Pannu, V., Rida, P. C. G., Ogden, A., Clewley, R., Cheng, A., Karna, P., et al. (2012). Induction of robust de novo centrosome amplification, high-grade spindle multipolarity and metaphase catastrophe: a novel chemotherapeutic approach. Cell Death & Disease, 3, e346.
178. Sprouse, A. A., Steding, C. E., & Herbert, B.-S. (2012). Pharmaceutical regulation of telomerase and its clinical potential. Journal of Cellular and Molecular Medicine, 16(1), 1–7.
179. Wang, Y., Liu, Q., Liu, Z., Li, B., Sun, Z., Zhou, H., et al. (2012). Berberine, a genotoxic alkaloid, induces ATM-Chk1 mediated G2 arrest in prostate cancer cells. Mutation Research, 734(1–2), 20–29.
180. Watanabe, F. T., Chade, D. C., Reis, S. T., Piantino, C., Dall' Oglio, M. F., Srougi, M., & Leite, K. R. M. (2011). Curcumin, but not Prima-1, decreased tumor cell proliferation in the syngeneic murine orthotopic bladder tumor model. Clinics (Sao Paulo, Brazil), 66(12), 2121–2124.
181. Yu, R., Zhang, Z.-Q., Wang, B., Jiang, H.-X., Cheng, L., & Shen, L.-M. (2014). Berberine-induced apoptotic and autophagic death of HepG2 cells requires AMPK activation. Cancer Cell International, 14, 49.
182. Betancur-Galvis, L., Zapata, B., Baena, A., Bueno, J., Ruíz-Nova, C. A., Stashenko, E., & Mesa-Arango, A. C. (2011). Antifungal, cytotoxic and chemical analyses of essential oils of *Lippia origanoides* H.B.K grown in Colombia. Revista de La Universidad Industrial de Santander. Salud, 43(2), 141–148.
183. Pinto, C. da P., Rodrigues, V. D., Pinto, F. da P., Pinto, R. da P., Uetanabaro, A. P. T., Pinheiro, C. S. R., et al. (2013). Antimicrobial Activity of *Lippia* Species from

the Brazilian Semiarid Region Traditionally Used as Antiseptic and Anti-Infective Agents. Evidence Based Complement Alternative Medicine, 2013, 614501.

184. Barreto, H. M., Coelho, B. R. C., Menezes-Silva, S. M. P., Siqueira-Júnior, J. P., Coutinho, H. D. M., Lemos, I. C. S., et al. (2014). Light-mediated antibacterial activity of *Lippia origanoides* H.B.K. *in vitro*. Photochemical & Photobiological Sciences: Official Journal of the European Photochemistry Association and the European Society for Photobiology, 13(12), 1650–1654.
185. Vicuña, G. C., Stashenko, E. E., & Fuentes, J. L. (2010). Chemical composition of the *Lippia origanoides* essential oils and their antigenotoxicity against bleomycin-induced DNA damage. Fitoterapia, 81(5), 343–349.
186. López, M. A., Stashenko, E. E., & Fuentes, J. L. (2011). Chemical composition and antigenotoxic properties of *Lippia alba* essential oils. Genetics and Molecular Biology, 34(3), 479–488.
187. Pérez, S., Meckes, M., Pérez, C., Susunaga, A., & Zavala, M. A. (2005). Anti-inflammatory activity of *Lippia dulcis*. Journal of Ethnopharmacology, 102(1), 1–4.
188. Haldar, S., Kar, B., Dolai, N., Kumar, R. B. S., Behera, B., & Haldar, P. K. (2012). In vivo anti–nociceptive and anti–inflammatory activities of *Lippia alba*. Asian Pacific Journal of Tropical Disease, 2, S667–S670.
189. Riella, K. R., Marinho, R. R., Santos, J. S., Pereira-Filho, R. N., Cardoso, J. C., Albuquerque-Junior, R. L. C., & Thomazzi, S. M. (2012). Anti-inflammatory and cicatrizing activities of thymol, a monoterpene of the essential oil from *Lippia gracilis*, in rodents. Journal of Ethnopharmacology, 143(2), 656–663.
190. Abena, A. A., Diatewa, M., Gakosso, G., Gbeassor, M., Hondi-Assah, T., & Ouamba, J. M. (2003). Analgesic, antipyretic and anti-inflammatory effects of essential oil of *Lippia multiflora*. Fitoterapia, 74(3), 231–236.
191. Viana, G. S. B., Vale, T. G. do, Rao, V. S. N., & Matos, F. J. A. (1998). Analgesic and Anti-inflammatory Effects of Two Chemotypes of *Lippia alba*: a Comparative Study. Pharmaceutical Biology, 36(5), 347–351.
192. Mendes, S. S., Bomfim, R. R., Jesus, H. C. R., Alves, P. B., Blank, A. F., Estevam, C. S., et al. (2010). Evaluation of the analgesic and anti-inflammatory effects of the

essential oil of *Lippia gracilis* leaves. Journal of Ethnopharmacology, 129(3), 391–397.

193. Gomide, M. da S., Lemos, F. de O., Lopes, M. T. P., Alves, T. M. de A., Viccini, L. F., Coelho, C. M., et al. (2013). The effect of the essential oils from five different *Lippia* species on the viability of tumor cell lines. Revista Brasileira de Farmacognosia, 23(6), 895–902.
194. Montero-Villegas, S., Crespo, R., Rodenak-Kladniew, B., Castro, M. A., Galle, M., Cicció, J. F., et al. (2018). Cytotoxic effects of essential oils from four *Lippia alba* chemotypes in human liver and lung cancer cell lines. Journal of Essential Oil Research, 30(3), 167–181.
195. Oliveira, D.R., Leitão, G.G., Fernandes, P.D., & Leitão, S.G. (2014). Ethnopharmacological studies of *Lippia origanoides*. Revista Brasileira de Farmacognosia, 24(2), 206-214.
196. Arunasree, K. M. (2010). Anti-proliferative effects of carvacrol on a human metastatic breast cancer cell line, MDA-MB 231. Phytomedicine, 17(8), 581–588.
197. Dai, W., Sun, C., Huang, S., & Zhou, Q. (2016). Carvacrol suppresses proliferation and invasion in human oral squamous cell carcinoma. OncoTargets and Therapy, 9, 2297–2304.
198. Fan, K., Li, X., Cao, Y., Qi, H., Li, L., Zhang, Q., & Sun, H. (2015). Carvacrol inhibits proliferation and induces apoptosis in human colon cancer cells. Anti-Cancer Drugs, 26(8), 813–823.
199. Kang, S.-H., Kim, Y.-S., Kim, E.-K., Hwang, J.-W., Jeong, J.-H., Dong, X., et al. (2016). Anticancer Effect of Thymol on AGS Human Gastric Carcinoma Cells. Journal of Microbiology and Biotechnology, 26(1), 28–37.
200. Kumar, M. A. S., Nair, M., Hema, P. S., Mohan, J., & Santhoshkumar, T. R. (2007). Pinocembrin triggers Bax-dependent mitochondrial apoptosis in colon cancer cells. Molecular Carcinogenesis, 46(3), 231–241.
201. Legault, J., & Pichette, A. (2007). Potentiating effect of beta-caryophyllene on anticancer activity of alpha-humulene, isocaryophyllene and paclitaxel. The Journal of Pharmacy and Pharmacology, 59(12), 1643–1647.

202. Li, Y., Wen, J., Du, C., Hu, S., Chen, J., Zhang, S., et al. (2017). Thymol inhibits bladder cancer cell proliferation via inducing cell cycle arrest and apoptosis. Biochemical and Biophysical Research Communications, 491(2), 530–536.
203. Aristatile, B., Al-Assaf, A. H., & Pugalendi, K. V. (2013). Carvacrol suppresses the expression of inflammatory marker genes in D-galactosamine-hepatotoxic rats. Asian Pacific Journal of Tropical Medicine, 6(3), 205–211.
204. Liang, D., Li, F., Fu, Y., Cao, Y., Song, X., Wang, T., et al. (2014). Thymol inhibits LPS-stimulated inflammatory response via down-regulation of NF-κB and MAPK signaling pathways in mouse mammary epithelial cells. Inflammation, 37(1), 214–222.
205. Kingston, D.G.I. (2011). Modern Natural Products Drug Discovery and Its Relevance to Biodiversity Conservation. Journal of Natural Products, 74, 496-511.
206. Beutler, J.A. (2009). Natural Products as a Foundation for Drug Discovery. Current protocols in pharmacology. Current Protocols in Pharmacology, 46, 9.11.1–9.11.21.
207. Macgregor, P.F., Squire, J.A. (2002). Application of Microarrays to the Analysis of Gene Expression in Cancer. Clinical Chemistry, 48, 1170-1177.
208. Ghazalpour, A., Bennett, B., Petyuk, V.A., Orozco, L., Hagopian, R., & Mungrue, I.N. et al. (2011). Comparative Analysis of Proteome and Transcriptome Variation in Mouse. PLoS Genetics, 7, e1001393.
209. Ghaemmaghami, S., Huh, W., Bower, K., Howson, R.W., Belle, A., Dephoure, N. et al. (2003). Global Analysis of Protein Expression in Yeast. Nature, 425, 737-741.
210. Tian, Q., Stepaniants, S.B., Mao, M., Weng, L., Feetham, M.C., Doyle, M.J. et al. (2004). Integrated Genomic and Proteomic Analyses of Gene Expression in Mammalian Cells. Molecular and Cellular Proteomics, 3, 960-969.
211. Bantscheff, M., Schirle, M., Sweetman, G., Rick, J., & Kuster, B. (2007). Quantitative mass spectrometry in proteomics: a critical review. Analytical and Bioanalytical Chemistry, 389(4), 1017–1031.
212. Everley, P.A., Krijgsveld, J., Zetter, B.R., & Gygi, S.P. (2004). Quantitative cancer proteomics: stable isotope labeling with amino acids in cell culture (SILAC) as a tool for prostate cancer research. Cell Proteomics, 3, 729-735.

213. Grønborg, M., Kristiansen, T. Z., Iwahori, A., Chang, R., Reddy, R., Sato, N., et al. (2006). Biomarker discovery from pancreatic cancer secretome using a differential proteomics approach. Molecular & Cellular Proteomics: MCP, 5(1), 157–171.
214. Bose, R., Molina, H., Patterson, A. S., Bitok, J. K., Periaswamy, B., Bader, J. S., et al. (2006). Phosphoproteomic analysis of Her2/neu signaling and inhibition. Proceedings of the National Academy of Sciences of the United States of America, 103(26), 9773–9778.
215. Lawrence, R. T., Perez, E. M., Hernández, D., Miller, C. P., Haas, K. M., Irie, H. Y., et al. (2015). The proteomics landscape of triple-negative breast cancer. Cell Reports, 11(4), 630–644.
216. Dai, X., Li, T., Bai, Z., Yang, Y., Liu, X., Zhan, J., & Shi, B. (2015). Breast cancer intrinsic subtype classification, clinical use and future trends. American Journal of Cancer Research, 5(10), 2929–2943.
217. Gerhard, R., Ricardo, S., Albergaria, A., Gomes, M., Silva, A. R., Logullo, Â. F., et al. (2012). Immunohistochemical features of claudin-low intrinsic subtype in metaplastic breast carcinomas. The Breast, 21(3), 354–360.
218. Prat, A., Parker, J. S., Karginova, O., Fan, C., Livasy, C., Herschkowitz, J. I., et al. (2010). Phenotypic and molecular characterization of the claudin-low intrinsic subtype of breast cancer. Breast Cancer Research, 12(5), R68.
219. Basho, R.K., Gilcrease, M., Murthy, R.K., Helgason, T., Karp, D.D., Meric-Bernstam, F., et al. (2017). Targeting the PI3K/AKT/mTOR pathway for the treatment of mesenchymal triple-negative breast cancer: Evidence from a phase 1 trial of mTOR inhibition in combination with liposomal doxorubicin and bevacizumab. JAMA Oncology, 3,509–515.
220. Masuda, H., Baggerly, K. A., Wang, Y., Zhang, Y., Gonzalez-Angulo, A. M., Meric-Bernstam, F., et al. (2013). Differential Response to Neoadjuvant Chemotherapy Among 7 Triple-Negative Breast Cancer Molecular Subtypes. Clinical Cancer Research, 19(19), 5533–5540.
221. Xu, H., Chen, K., Jia, X., Tian, Y., Dai, Y., Li, D., et al. (2015). Metformin Use Is Associated With Better Survival of Breast Cancer Patients With Diabetes: A Meta-Analysis. The Oncologist, 20(11), 1236–1244.

222. Omarini, C., Guaitoli, G., Pipitone, S., Moscetti, L., Cortesi, L., Cascinu, S., & Piacentini, F. (2018). Neoadjuvant treatments in triple-negative breast cancer patients: where we are now and where we are going. Cancer Management and Research, 10; 91-103.

CHAPTER 2. *LIPPIA ORIGANOIDES* EXTRACT (LOE) INDUCES CELL CYCLE ARREST AND APOPTOSIS, AND SUPPRESSES NF-κB SIGNALING IN TNBC CELLS

A version of this chapter has been previously published in the International Journal of Oncology, 2017, 51(6):1801-1808. DOI: 10.3892/ijo.2017.4169

2.1 Abstract

Triple-negative breast cancer (TNBC) is an aggressive subtype making up 15-20 % of breast cancers diagnoses. TNBCs do not express hormone receptors for estrogen, progesterone, and human epidermal growth factor 2 (ER, PR, and Her2/neu respectively), and specific markers and targeted treatment options for this disease remain undiscovered. Towards identifying new compounds with potency against TNBC, we have tested an extract from the South American shrub *Lippia origanoides* (LOE) against TNBC and normal mammary cell lines for its effects on cell viability, and further described its mechanism of action in MDA-MB-231 cells, the standard *in vitro* TNBC model. TNBC cells exhibited a dose-dependent loss of viability in response to LOE treatment, which was greater than that observed in normal cells. Treatment with LOE also induced a significant shift to the G0/G1 phase of the cell cycle and a loss in Cyclin D1 and cIAP2 levels, and also induced apoptotic cell death concurrent with an induction of caspase-3/-8 activation. Pro-inflammatory NF-κB signaling through RIP1 contributes to proliferation and survival of TNBC cells, and LOE treatment was also shown to inhibit RIP1 protein levels in the MDA-MB-231 cell line. Together, our study provides evidence that LOE is a source of compounds with TNBC-specific potency, capable of inhibiting proliferation as well as inducing apoptosis in these aggressive cancer cells.

2.2 Introduction

The majority of breast cancers diagnosed are hormone-sensitive, with proliferation and survival mechanisms considerably dependent on signaling through overexpressed receptors for estrogen, progesterone, and/or human epidermal growth factor receptor 2 (i.e. ER, PR, and Her2/neu respectively). Treatment regimens against hormone-positive

breast cancers typically target hormone receptor signaling (e.g. tamoxifen, a selective estrogen receptor modulator, and trastuzumab, a monoclonal Her2-antibody) or attempt to inhibit enzymes involved in hormone synthesis (e.g. aromatase inhibitors such as letrozole) [1-3]. This has resulted in improved response rates and survival outcomes for hormone-positive breast cancers.

In contrast, 15-20 % of breast cancers are negative for expression of these three hormone receptors. Treatments for these 'triple-negative' breast cancers (TNBCs) are limited to cytotoxic chemotherapy which can lead to severe side-effects. In addition, TNBC tumors are associated with higher grade and the presence of unfavorable mitotic features at the time of diagnosis [4]. These tumors are often characterized by an invasive 'basal-like' phenotype with high expression levels of keratin 5 and 17, laminin, and fatty acid binding protein 7 [5-7]. In addition, TNBCs are associated with genetic aberrations and signaling anomalies (e.g. TP53 mutations, and the constitutive activation of pro-survival and inflammatory pathways such as MAPK and NF-κB respectively), which support their enhanced growth, survival and resistance to chemotherapy [8-11].

As mentioned in section 1.3.2., NF-κB activation can promote a pro-survival, proliferative, and inflammatory state by inducing expression of anti-apoptotic proteins such as Bcl-xL, cIAP1 and cIAP2, proteins involved in cell cycle progression such as Cyclin D1, and pro-inflammatory cytokines such as IL-6 and TNF-α [12-16]. Constitutive expression of NF-κB has also been shown to promote epithelial-mesenchymal transition in MCF10A cells by inducing Vimentin expression [17], and can transition RM22-F5 rat mammary carcinoma cells from a hormone-dependent phenotype to a hormone-independent, malignant phenotype [18]. Human TNBC models including MDA-MB-231 cells are often characterized by constitutive overexpression of activated NF-κB [19, 20]. Finally, aberrant NF-kB signaling may also lead to tumor initiation and progression. Transgenic mice overexpressing NF-kB p100/p52 under an inducible promoter were observed to have hyperplastic mammary gland growth and increased MMP-9 expression [21]. Targeting NF-κB signaling may thus be a potential avenue to new treatments for TNBC.

Plant-derived molecules have been a useful source of anti-cancer therapeutics. Plant-derived anti-cancer drugs widely used in the clinical setting include *Vinca* alkaloids, taxanes, epipodophyllotoxins and camptothecins. Following successful clinical trials, vincristine and docetaxel are now commonly utilized in combination chemotherapy regimens against advanced metastatic breast cancer [22, 23].

More recent studies have identified several plant-derived compounds with exerting pleiotropic anti-cancer effects. Plumbagin has been shown to inhibit the DNA-binding activity of NF-κB and induce apoptosis in MDA-MB-231 TNBC cells [24]. Treatment of MDA-MB-231 cells with halofuginone, a quinazolinone derivative from the Chinese herb *Dichroa febrifuga*, inhibited the expression of MMP-9 by suppressing nuclear translocation of the transcription factors NF-κB and AP1, leading to a reduction in migration and invasiveness of these cells [25]. In addition, curcumin and resveratrol, among others, have also been shown to possess potent anti-cancer effects [26-29]. These positive outcomes highlight the importance of fully uncovering the untapped clinical potential of natural compounds.

Here we report studying an extract from *Lippia origanoides*, a medicinal tropical plant native to South America for its potential anticancer effects on TNBC. Also known as "*oregano de monte*" or mountain oregano, infusions of the plant have been used traditionally to alleviate gastrointestinal ailments and as topical analgesics [30]. Towards a better understanding of *L. origanoides* actions and health benefits, the novel *L. origanoides* extract (LOE) used in this study was originally isolated by supercritical fluid extraction and analyzed using HPLC-MS [31, 32]. LOE was found to have numerous major components including pinocembrin, carvacrol, thymol and trans-β-caryophyllene. Studies using commercially available reagents of these compounds have shown they have pro-apoptotic and anti-proliferative effects on various cancer cell lines. For example, pinocembrin, a flavanone which comprises nearly 55% of the total LOE, has been shown to decrease viability and prevent epithelial-mesenchymal transition induced by TGF-β in Y-79 retinoblastoma cells [29]. Further, trans-β-caryophyllene and α-humulene, two sesquiterpenes present in the extract, were shown to synergize and inhibit cell growth and proliferation in MCF-7 breast cancer cells [33]. Strikingly, several components of LOE

have shown inhibitory effects on NF-κB signaling, a key survival and proliferative pathway in TNBC [34-38]. These reports support the hypothesis that *L. origanoides* may be a source of novel components that can effectively target aggressive breast cancer.

Our results reveal treatment with LOE lead to a G0/G1 phase arrest and apoptosis in MDA-MB-231 triple-negative breast cancer cells without promoting necrotic cell death. Further, we observed that cell cycle proteins and apoptotic markers, as well as key NF-κB regulatory molecules, are modulated by treatment with LOE, shedding light on a mechanism of action behind the anticancer effects of LOE. These data provide an important first step towards defining the potential utility of LOE in the identification and development of novel therapeutic strategies for TNBC.

2.3 Materials and Methods

2.3.1 Plant material and extract

Lippia origanoides plants were collected from the Chicamocha River Canyon (Los Santos, Santander, Colombia). Taxonomic identification of *L. origanoides* was performed by Dr. José Luis Fernández Alonso (National University, Bogotá, Colombia). The *L. origanoides* specimen (COL560259) was placed in the Colombian National Herbarium (Bogotá). Fresh leaves and stems from *L. origanoides* were used for extraction as previously described [32]. The extract was dissolved in methanol at a concentration of 50 mg/ml (stock solution), and then different extract concentrations were prepared in methanol for *in vitro* bioassays.

2.3.2 Cell culture

Triple-negative breast cancer (MDA-MB-231 and CRL-2321) and normal mammary epithelial (MCF10A) cell lines were obtained from the American Type Culture Collection. MCF10A-H cells, derived via H-ras transformation of MCF10A cells, were a kind gift from Dr. Barbara Stefanska, Purdue University. MDA-MB-231 cells were cultured in Dublecco's Modified Essential Medium (DMEM; Life Technologies, NY) supplemented with 10% fetal bovine serum (FBS; Atlanta Biologicals, GA), 100 IU/ml penicillin and 100 µg/ml streptomycin (Life Technologies, NY). MCF10A and MCF10A-

H cells were cultured in a 1:1 ratio of DMEM:Ham's F12 supplemented with 5% horse serum (HS; Atlanta Biologicals, GA), 20 ng/ml human epidermal growth factor (Sigma-Aldrich, MO), 0.5 mg/ml hydrocortisone (Sigma-Aldrich, MO), 100 ng/ml cholera toxin (Sigma-Aldrich, MO), 10 µg/ml bovine insulin (Sigma-Aldrich, MO), 100 IU/ml penicillin and 100 µg/ml streptomycin. CRL-2321 cells were cultured in Roswell Park Memorial Institute 1640 medium (RPMI 1640, Mediatech Inc., VA) supplemented with 10% FBS, 100 IU/ml penicillin and 100 µg/ml streptomycin.

2.3.3 Assessment of metabolic activity via MTT assay

MCF10A, MCF10A-H, MDA-MB-231 and CRL-2321 cells were seeded at 10^5 cells/well in 96-well plates and allowed to attach overnight. Spent media was then replaced with fresh media containing treatment dosages between 0.15 - 0.2 mg/ml LOE. Media in control wells was replaced with fresh media without additives (No-treatment, NT) or media containing the vehicle, methanol (Veh). Following 24 h treatment, 12 mM of MTT, 3-(4,5-dimethylthiazol-2-yl)-2,5-diphenyltetrazolium bromide (Life Technologies, NY), was added to the cells followed by incubation for 4 h at 37°C. Formazan crystals formed at the end of incubation period were dissolved using dimethyl sulfoxide (DMSO) and plates were read at 570 nm with a reference wavelength of 630 nm.

2.3.4 Assessment of cell cycle arrest via flow cytometry

For cell cycle assay, MDA-MB-231 were seeded in 6-well plates at a concentration of 6 x 10^5 cells/well. Cells were allowed to attach overnight followed by replacement of spent media with serum-free media after 24 hours to allow for synchronization of cell cycle. Cells were then treated in fresh media containing LOE at 0.06 mg/ml and 0.15 mg/ml. Controls were treated in triplicate with either serum-free media as a positive control or media containing the vehicle, methanol. At the end of 36 h of treatment, media was aspirated, cells were washed once with 1X Phosphate Buffered Saline (PBS) and collected via trypsinization. Samples were centrifuged at 3000 rpm for 5 min and supernatant was drained. Cell pellets were washed and resuspended in PBS containing 2.5 mM EDTA (1X PBS-EDTA buffer). Cells were then fixed by adding cell suspension drop-wise into microcentrifuge tubes containing 1 ml ice-cold 70% ethanol. Fixed cells

were stored at -20 °C until staining. For staining, fixed samples were centrifuged at 4000 rpm for 5 min and supernatant was drained following which cells were washed and resuspended in 200 µl 1X PBS-EDTA buffer. Samples were centrifuged at 4000 rpm for 5 min and supernatant was drained. Next, 200 µl MUSE® Cell Cycle Staining Reagent (EMD Millipore, MA) containing Propidium Iodide and RNase A was added to each sample. Samples were stored at room temperature for at least 30 min to allow for adequate staining before being run through an FC500 flow cytometer (Beckman Coulter, CA) at the Bindley Bioscience Center, Purdue University.

2.3.5 Assessment of apoptosis via flow cytometry

MDA-MB-231 were seeded in 12-well plates at a concentration of 2 x 10^5 cells/well. Cells were allowed to attach overnight followed by synchronization in serum-free media. Cells were then treated with fresh media containing LOE at 0.15 mg/ml and 0.30 mg/ml for 24 h in triplicate while controls were treated with media containing methanol. Cells collected via trypsinization and centrifuged and supernatant was removed. Next, 100 µl Muse™ Annexin V Dead Cell Assay stain (EMD Millipore, MA) was added to the cell pellet and samples were resuspended by gentle pipetting. Samples were incubated in the dark for 20 min, following which they were run through a Muse™ Cell Analyzer (EMD Millipore, MA) using manufacturer's protocol.

2.3.6 Caspase-3/7 activation assay

MDA-MB-231 cells were seeded at 10^5 cells/well in a 96-well plate and allowed to attach overnight. LOE and control treatments were prepared in fresh media containing 5 µM IncuCyte™ Caspase-3/7 apoptosis assay reagent and added to the cells, following which the plate was placed in an IncuCyte® ZOOM live-cell analyzer. Cells were imaged recurrently for 24 h and quantified for changes in caspase-3/7 activation via measurement of fluorescence intensity at a wavelength of 400 nm.

2.3.7 Western Blotting

MDA-MB-231 cells were seeded at 10^6 cells/well in 6-well plates and allowed to attach overnight. Cells were then treated with fresh media containing LOE at 0.06 or 0.15 mg/ml for 3 h, 6 h, 12 h and 24 h intervals. Treated cells were collected in RIPA buffer

and sonicated to obtain lysates. Cell lysates were cleared of debris by centrifugation and protein concentration of lysates was estimated via the bicinchoninic acid (BCA) assay. Next, 20 µg of protein from each sample was subjected to SDS-polyacrylamide gel electrophoresis, transferred onto a polyvinyl difluoride (PVDF) membrane and immunoblotted. Primary antibodies for Cyclin D1, cellular Inhibitor of Apoptosis Protein 2 (cIAP2), RIP1, cleaved caspase-8 and cleaved Poly-ADP Ribose Polymerase (PARP) were purchased from Cell Signaling Technologies, MA. Cleaved caspase-3 antibody was purchased from Epigenomics, WA. β-actin and β-tubulin antibodies were obtained from Sigma Aldrich, MO and Abcam, MA respectively. Quantification was carried out using ImageJ software [39].

2.3.8 Statistical Analysis

Data are presented as mean values with corresponding standard errors from various experiments. Analysis for statistical significance for MTT assay was carried out using One-way Analysis of Variance (ANOVA). Analysis for statistical significance for Western Blotting, Flow Cytometry and Caspase-3/-7 assay were carried out using Student's unpaired two-tailed t-test. Analysis for statistical significance for Immunofluorescence Microscopy was carried out using unpaired Wilcoxon signed-rank test.

2.4 Results

2.4.1 LOE decreases viability of TNBC cells.

In order to study the differential response of normal, invasive, and malignant triple-negative cells to LOE treatment, MCF10A, MCF10A-H, MDA-MB-231 and CRL-2321 cells were treated with increasing dosages of LOE for 24h and changes in cellular metabolic activity were quantified using the MTT assay and utilized as a reflection of cell viability (Figure 2.1).

Relative to control MCF10A cells, there was a dose-dependent decrease in cell viability of MDA-MB-231 cells. LOE at a concentration of 0.15 mg/ml resulted in 50% reduction in MDA-MB-231 cell viability while a higher dosage of 0.2 mg/ml resulted in a

95% reduction in MDA-MB-231 cell viability. Importantly, LOE impacted cell viability of MDA-MB-231, as well as the other triple-negative invasive and malignant cell lines (MCF10A-H and CRL-2321 respectively) to a much greater degree than in normal MCF10A mammary epithelial cells. In contrast with MDA-MB-231 cells, there was only a 20% decrease in cell viability of MCF10A cells with 0.15 mg/ml LOE treatment and a 40% decrease with 0.2 mg/ml LOE. Curiously, CRL-2321 cells demonstrated greater sensitivity than MDA-MB-231 cells in their initial response to low doses of LOE, but viability in this cell line did not decrease further with increasing dosage.

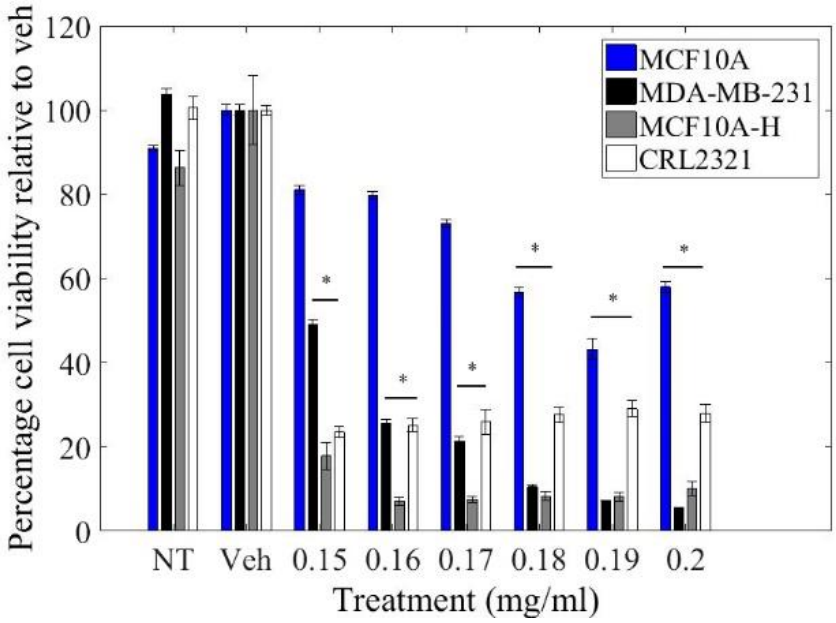

Figure 2.1 LOE impacts the viability of triple-negative breast cancer cells to a greater extent than normal-like cells. MDA-MB-231, MCF10A-H, CRL-2321 and MCF10A cells were seeded in 96-well plates and treated with indicated concentrations of LOE, Methanol (Veh) or left untreated (NT) for 24h and subjected to MTT assay. This was followed by absorbance reading at 570nm. n=10 replicates from 2 separate experiments; *significantly different from vehicle-treated $p < 0.0001$.

2.4.2 LOE induces cell cycle arrest in TNBC cells.

To quantify changes in cycle progression induced by LOE treatment, MDA-MB-231 cells were treated with LOE for 36 h. Control cells were treated with either serum-free media or growth media containing methanol. Cells were then collected and stained with Propidium Iodide followed by analysis using an FC500 flow cytometer. Representative raw data showing shifts in cell cycle phases under various treatments are shown in Figure 2.2A.

Treatment with LOE at 0.15 mg/ml induced a significant shift away from the replication stage (S-phase) of the cell cycle as compared to vehicle-treated cells (Figure 2.2B). Of the total cells counted, almost 20 % shifted away from the S-phase and toward the G0/G1 phase upon LOE treatment at 0.15 mg/ml. Further, there was a striking resemblance in the S-phase distribution between 0.15 mg/ml LOE-treated cells and serum-starved cells (0.15 mg/ml LOE: 79.78 % G0/G1; SF: 79.27 % G0/G1), corroborating that LOE induces a halt in cell cycle progression in MDA-MB-231 cells.

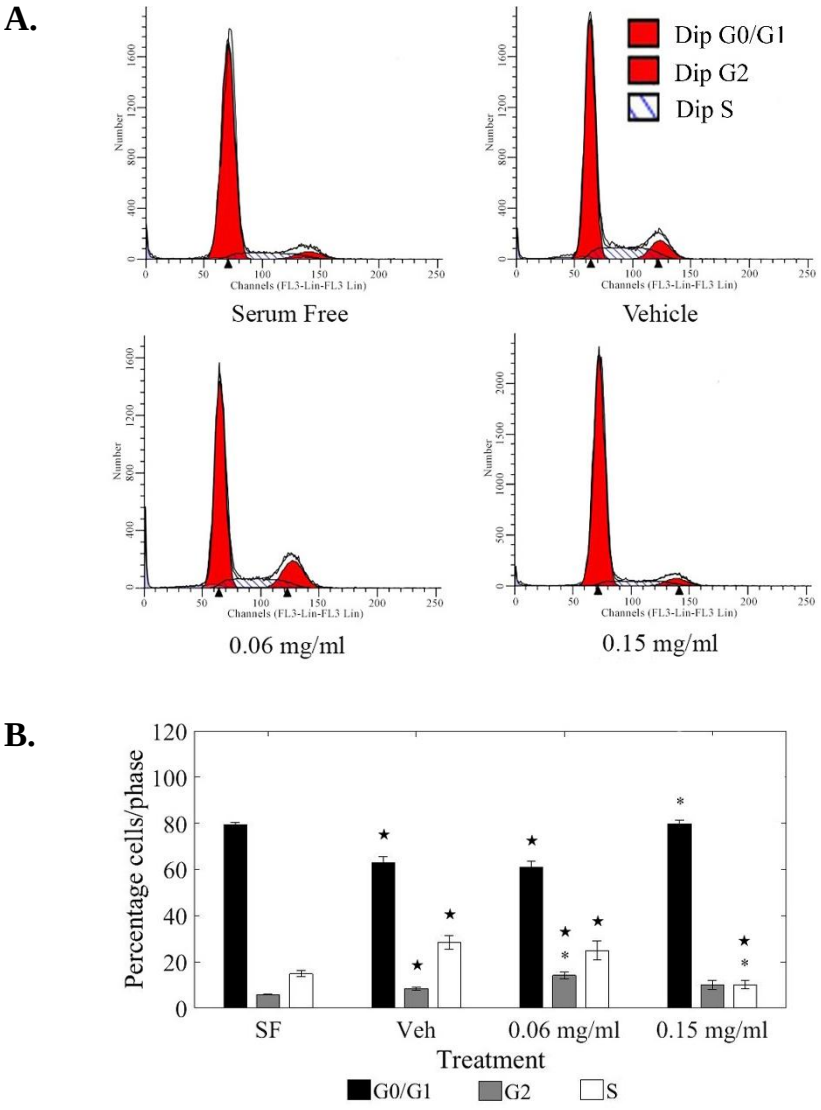

Figure 2.2 LOE induces G0/G1 phase arrest in MDA-MB-231 cells. MDA-MB-231 cells treated with indicated concentrations of LOE for 36h were stained with Propidium Iodide (PI) and differential staining was measured using an FC500 flow cytometer (Bindley Flow Cytometry Facility). **(A)** Representative plots of raw data indicating cell cycle stages from treatment groups. **(B)** Average distribution across different cell cycle stages from various treatment groups. SF: serum-free treatment. n=3; * significantly different from vehicle treatment $p<0.05$ ★ significantly different from serum free treatment $p<0.05$

2.4.3 LOE induces apoptosis in TNBC cells.

Cell death may take the form of apoptosis, a programmed and controlled process involving the degradation and clearance of cellular constituents; or necrosis, a traumatic and inflammatory process which leads to the expulsion of cellular material into the extracellular environment [40]. In order to analyze the impact of LOE on cell death in triple-negative breast cancer cells, MDA-MB-231 cells were treated with LOE for 24h. Cells were stained with Annexin V/7-Aminoactinomycin D and evaluated in a Muse Cell Analyzer (Merck Millipore, MA). Representative raw data from various treatments indicating shifts from live to early (EA) and late (LA) apoptosis as well as necrosis (Dead) is shown in Figure 2.3.

Treatment with LOE induced a significant decrease in live cells as well a significant increase in apoptosis but not necrosis in MDA-MB-231 cells. Furthermore, 40% of cells were apoptotic after 24h of 0.15 mg/ml LOE treatment while ~80% of cells underwent apoptosis after 0.3 mg/ml LOE treatment over the same time period.

A.

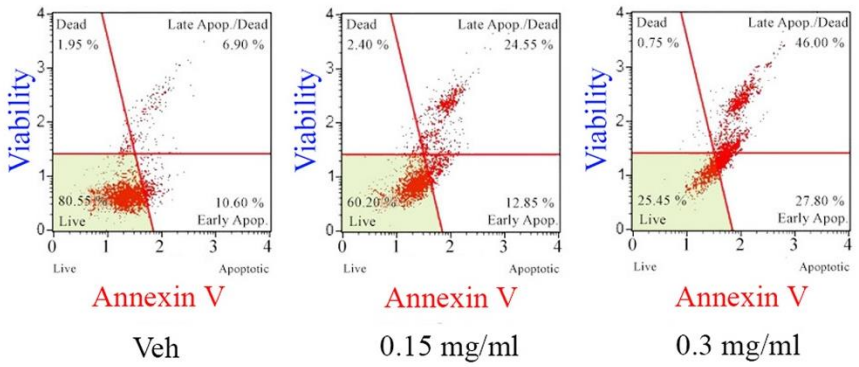

B.

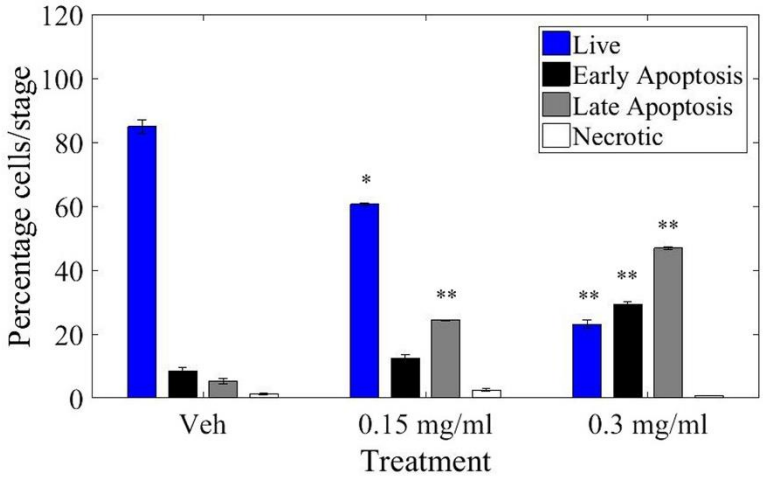

Figure 2.3 LOE induces apoptosis but not necrosis in MDA-MB-231 triple-negative breast cancer cells. MDA-MB-231 cells were treated with indicated concentrations of LOE for 24h and stained with Annexin-V/7-Aminoactinomycin D (7-AAD). This was followed by measurement of differential Annexin-V/7-AAD staining using a Muse™ Cell Analyzer. **(A)** Representative plots of raw data showing distribution of cells as Live, Early Apoptotic (EA), Late Apoptotic (LA) or Necrotic. **(B)** Quantified graph showing effect of LOE on apoptosis in MDA-MB-231 cells. N=3; Significant difference between LOE-treated cells and control (Vehicle-treated) cells is indicated as *$p<0.05$ **$p<0.005$.

2.4.4 LOE impacts critical regulators of cell cycle progression.

As seen from Figure 2.2B, LOE treatment induced a shift toward the G0/G1 phase and away from the S phase of the cell cycle in MDA-MB-231 cells. The progression from G0/G1 is mediated by Cyclin D1, with cellular inhibitor of apoptosis (cIAP) proteins playing a supportive role by suppressing apoptosis [41, 42]. As observed in Figure 2.4B, there was a significant (5-fold) decrease in Cyclin D1 protein at 24 h post-treatment. cIAP2 levels were significantly reduced by 40% after 12 h and by ~65% after 24 h.

Taken together, these results suggest that the halt in cell cycle progression observed upon treatment of MDA-MB-231 cells with LOE is brought about by its impact on Cyclin D1 and cIAP2 expression.

2.4.5 LOE induces apoptosis via caspase-8/-3 activation.

Based on the observation that LOE induces apoptosis and not necrosis in MDA-MB-231 cells (Figure 2.3B), our goal was to determine if LOE induces the extrinsic pathway of apoptosis via caspase-8 activation. As shown in Figure 2.5B, LOE induced the rapid cleavage of caspase-8 within 3 h post-treatment with PARP cleavage peaking at 6 h post-treatment.

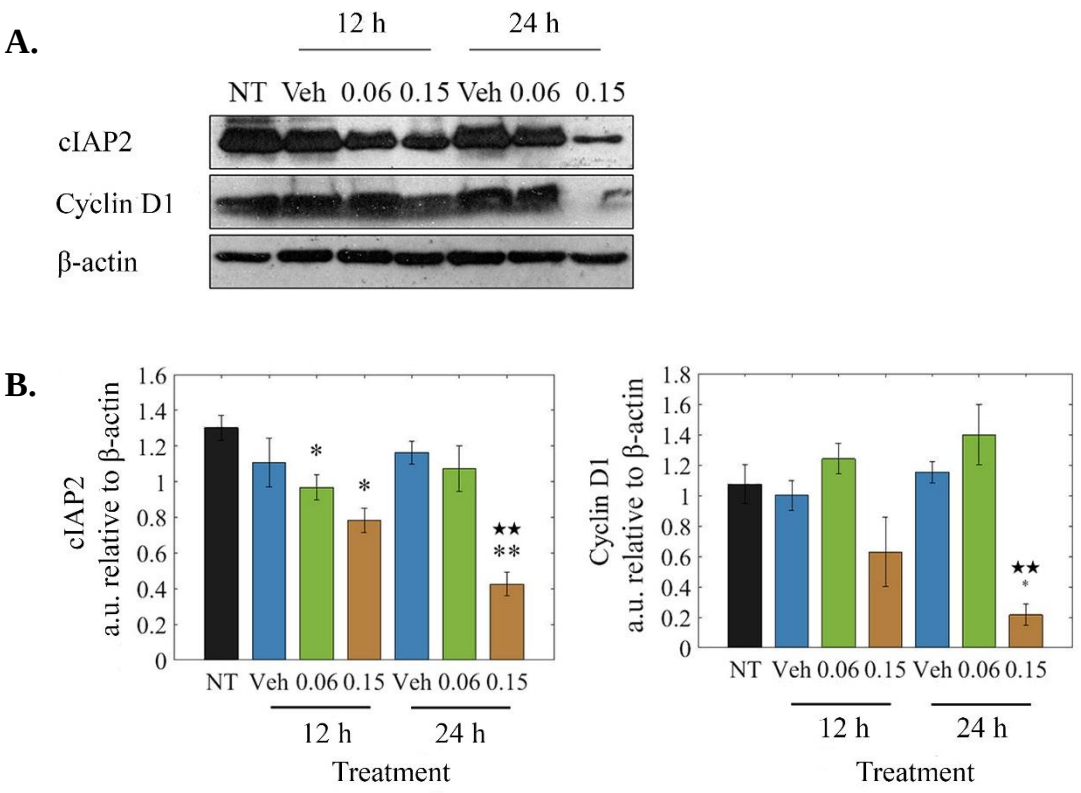

Figure 2.4. LOE inhibits markers of cell cycle progression and survival. MDA-MB-231 cells were treated with 0.06 and 0.15mg/ml of LOE for various time intervals. Cells were then lysed in RIPA buffer. Lysates were subjected to Western Blotting and probed for indicated proteins. **(A)** Representative blots of cytostatic markers Cyclin D1 and cIAP2. **(B)** Densitometry quantification of blots using ImageJ. Protein levels were normalized against β-actin and plotted as shown. n=3; Significant difference from untreated (NT) is indicated as *p<0.05 or **p<0.005; significant difference from Vehicle-treated (Veh) is indicated as ★p<0.05 or ★★p<0.005.

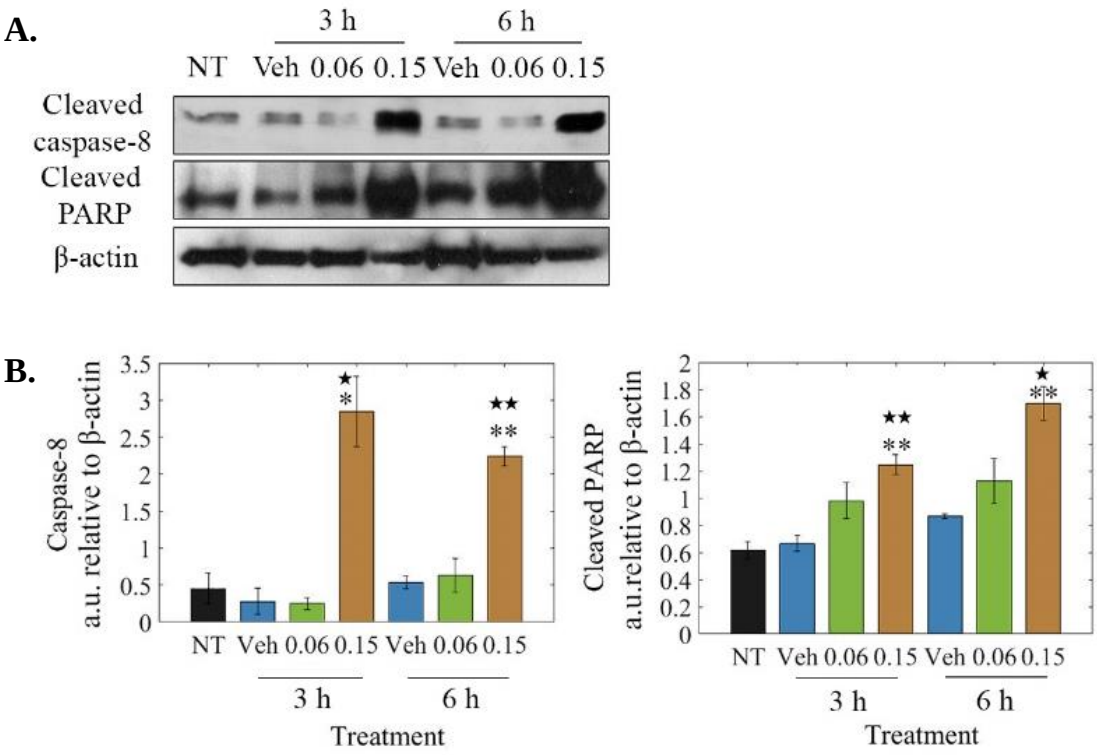

Figure 2.5 LOE induces apoptosis accompanied by caspase-8 activation and PARP cleavage. MDA-MB-231 cells treated with LOE for various time intervals were lysed and subjected to Western Blotting and probed for indicated proteins **(A)** Representative blots of apoptotic markers cleaved caspase-8, cleaved caspase-3 and cleaved PARP **(B)** Densitometry quantification of blots using ImageJ. Protein levels were normalized against β-actin and plotted as shown. n=3. Significant difference from untreated (NT) is indicated as *$p<0.05$ or **$p<0.005$; significant difference from Vehicle-treated (Veh) is indicated as $^{\star}p<0.05$ or $^{\star\star}p<0.005$.

To further understand apoptotic signaling, MDA-MB-231 cells were analyzed for executioner caspase-3/-7 activity via live cell imaging using the IncuCyte ZOOM system. These studies showed a marked visible increase in caspase-3/-7 activation upon LOE treatment. As quantified in Figure 2.6, there was a significant increase in caspase-3/-7 activity 3 h post-treatment with 0.15 mg/ml and 0.3 mg/ml LOE, with peak activity at approximately 10 h post-treatment. This was supported by Western Blotting time-course data, which indicated a peak in caspase-3 activity at 12 h post-treatment with 0.15 mg/ml LOE (Figure 2.6B).

2.4.6 LOE reduces RIP1 protein expression levels.

TNBC is often characterized by constitutive activation of NF-κB signaling via recruitment of key effector proteins by RIP1 [43, 44]. Immunoblotting revealed a significant decrease of ~ 40% in RIP1 protein levels in lysates from MDA-MB-231 cells treated with LOE for 9 h as compared to controls (Figure 2.7B).

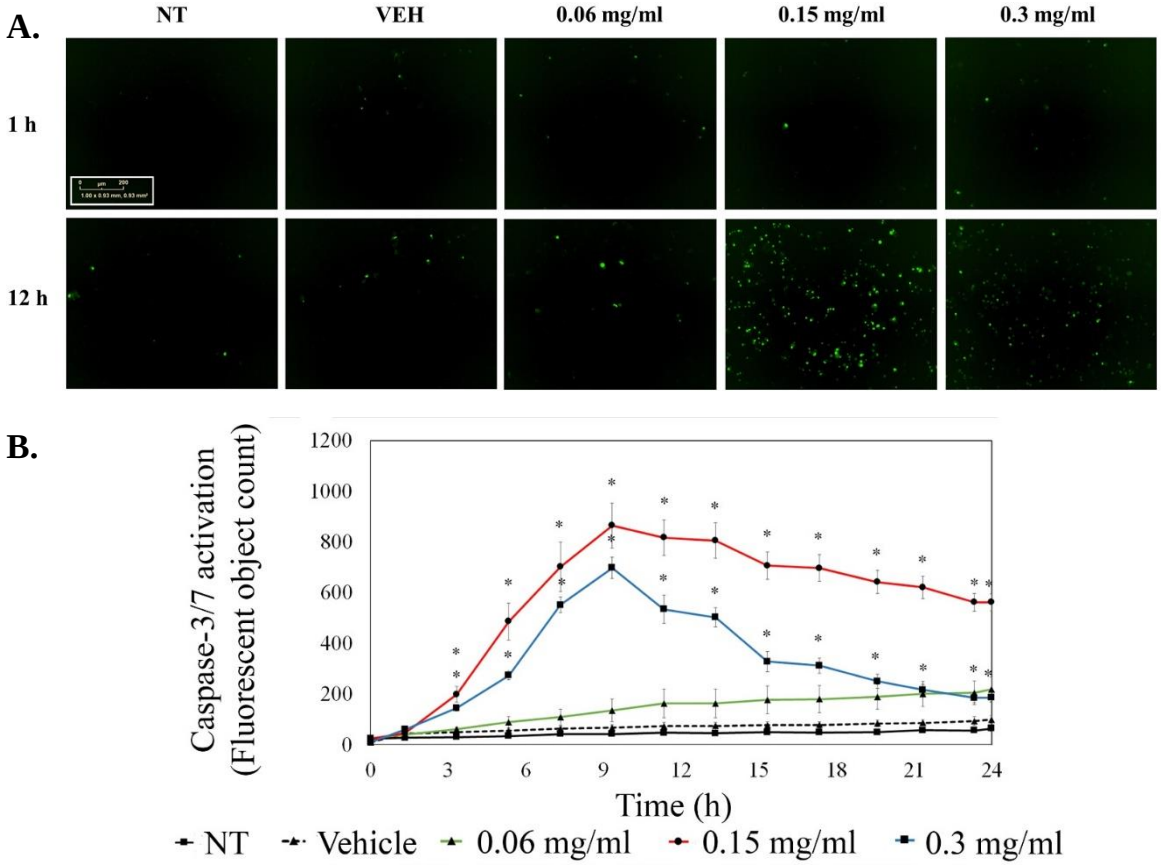

Figure 2.6 LOE induces executioner caspase-3/-7 activity in TNBC cells. (A) MDA-MB-231 cells incubated with full growth medium containing indicated treatments and IncuCyte™ Caspase-3/7 apoptosis assay reagent were imaged periodically over 24h in an IncuCyte® ZOOM live-cell analyzer to look at changes in caspase-3/-7 activity. **(B)** Activity was quantified as the mean Green Fluorescent Object Count/Image for each treatment group and plotted as shown. n=5; * significantly different from control (Vehicle-treated) cells; $p<0.005$.

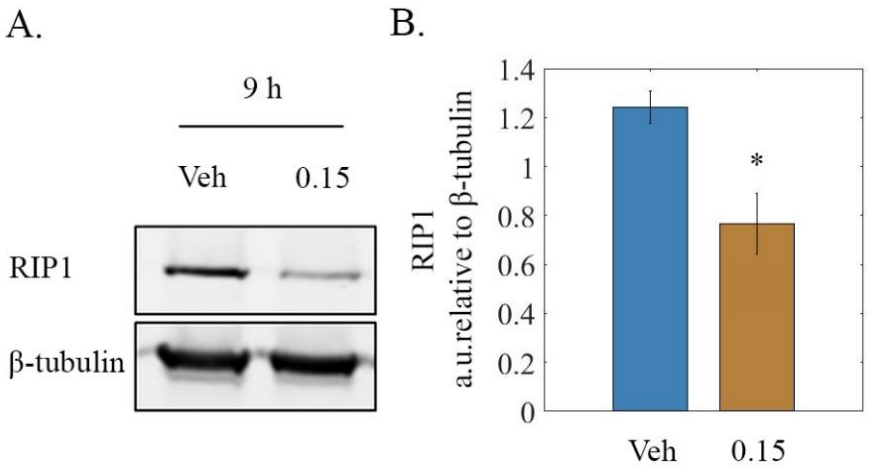

Figure 2.7 RIP1 protein levels are reduced upon treatment of TNBC cells with LOE. MDA-MB-231 cells were treated with 0.15 mg/ml LOE for 9 h and cell lysates were immunoblotted for RIP1. **(A)** Representative blots of RIP1 **(B)** Densitometry quantification of blots using ImageJ. Protein levels were normalized against β-tubulin and plotted as shown. N = average of 3 replicates run twice. Significant difference from Vehicle-treated cells is indicated as *$p<0.05$.

2.5 Discussion

TNBC continues to be a monumental concern in women's health issues. As our understanding of the mechanisms that govern the initiation and progression of breast cancer grows, it has become apparent that conventional chemotherapeutics are limited by their inability to target subtypes that are inherently more aggressive while being drug resistant. One such subtype is TNBC, which lacks expression of ER, PR and HER2/neu, thereby rendering TNBC resistant to conventional endocrine-targeted therapy. In this study we provide support that an extract from the tropical South American plant *L. origanoides* (LOE) may be a possible source for therapeutic agents against TNBCs.

2.5.1 LOE is a source of TNBC-specific cytotoxic compounds

In brief, we utilize the MTT metabolic activity assay to show LOE induces a dose-dependent decrease in the viability of MDA-MB-231 mammary adenocarcinoma cells, a universal standard *in vitro* model of highly invasive and drug resistant TNBC. This effect was much greater compared to normal-like MCF10A mammary epithelial cells (Figure 2.1). Our observation that LOE also significantly reduced cell viability in triple-negative Hras-transformed MCF10A invasive cells as well as the CRL-2321 cell-line, recently shown to be the best *in vitro* phenotypic representative of grade 3 TNBC tumors [45], further confirms its anti-TNBC effects. This observation suggests the LOE induces molecular actions that target pathways specific to cancer cells. We also note that while CRL-2321 cells have a greater sensitivity to low doses of LOE than MDA-MB-231 cells, higher dosages of LOE do not induce decreases in CRL-2321 viability beyond 80%. Previous studies have shown that cancer cell line subpopulations and sub-lines can exhibit a high degree of transcriptome and phenotypic variability leading to observable differences in metastatic activity [46] and drug sensitivity [47]. This suggests the possibility of heterogeneity within subpopulations of the CRL-2321 cell line allowing for compensatory survival pathways providing modest resistance to LOE treatment. The identification of novel mechanisms targeted by new small molecular inhibitors is of major interest in our continued studies of the actions of LOE.

2.5.2 LOE is a source of cell cycle inhibitors

Our study also quantified the molecular influences of the extract within cancer cells. Cyclin D1 is a protein which associates with cyclin-dependent kinase-4 and -6 (CDK-4 and -6) to form heterodimers that progress the cell cycle from G0/G1 to S phase [41]. In addition, inhibitor of apoptosis proteins (IAPs) prevent apoptosis and permit cell cycle progression via binding and possibly inactivating executioner caspases, i.e. caspase-3 and caspase-7 [42]. cIAP2 is known to be constitutively expressed in MDA-MB-231 cells, and has been shown to protect against death-inducing ligands such as TNF-α by possibly enhancing NF-κB signaling through RIP1 activation as well as by binding and inhibiting caspase-3 [43]. Here, we observed that LOE induced G0/G1 phase halt in MDA-MB-231 cells (Figure 2.2). Western blot analysis revealed the effects of LOE on cell cycle progression could be explained by a reduction in Cyclin D1 and cIAP2 levels upon treatment of the cells with the extract (Figure 2.3). These experiments begin to build an important framework for the actions of LOE on cell cycle regulation.

2.5.3 LOE is a source of apoptotic compounds

We next studied LOE's impact on MDA-MB-231 cell death. Upon triggering of the extrinsic pathway of apoptosis, procaspase-8 is activated via dimerization-induced auto-cleavage and subsequently cleaves and activates the master "executioner" caspase, caspase-3 [48, 49]. We revealed a potential mechanism behind the actions of the extract by showing LOE-induced apoptosis involved activation of caspase-8/-3 and cleavage of PARP (Figure 2.5 and 2.6), hallmarks of extrinsic apoptotic pathway activation [40]. Additionally, LOE induced apoptosis in these cells unaccompanied by necrotic cell death (Figure 2.3). As cancer therapy is focused on preventing damage to non-targeted tissue areas, this result provides additional support for LOE as a source for potential therapeutics with desirable characteristics.

2.5.4 LOE is a source of compounds targeting NF-κB signaling

In previous work, Stashenko et al. have characterized the major components of LOE [32]. However, it remains to be defined which component, or combination of components, is responsible for the extract's apoptotic effects. Furthermore, it is imperative that major

cellular pathways involved in LOE signal transduction be delineated. Based on previous studies involving components present in the LOE, one possible candidate pathway central to LOE-induced apoptosis is NF-κB signaling. Constitutive activation of this pathway has been previously linked to triple-negative breast cancer and blocking NF-κB signaling can spontaneously induce cell death via a caspase-8/-3-dependent mechanism or render cells susceptible to pro-apoptotic signals [44, 50, 51]. In normal cells, ligand binding to TNFR1 is followed by rapid activation of the extrinsic pathway of apoptosis. However, in contrast to normal cells, ligand binding to TNFR1 in TNBC cells instead activates NF-κB signaling via membrane-recruitment of the scaffold protein RIP1, a Ser/Thr kinase [43]. In brief, cIAP2 exerts E3 ubiquitin ligase activity to polyubiquitinate and activate RIP1, which goes on to phosphorylate the IKKα/β-NEMO complex. Active IKKs then phosphorylate IκB proteins which sequester p50/RelA (NF-κB) dimers to the cytoplasm, targeting the IkBs for polyubiquitination and subsequent degradation. This frees p50/RelA to translocate to the nucleus and act as a transcription factor for pro-survival genes such as Cyclin D1 and cIAPs [52, 53].

We hypothesized that components of LOE could interfere with NF-κB signaling, leading to a halt in the cell cycle and induction of apoptosis. Indeed, we showed LOE treatment resulted in a 40% decrease in protein levels of RIP1 in MDA-MB-231 cells (Figure 2.7B). This may, at least in part, be explained by our previous observation that LOE treatment induced activation of caspase-8/-3 (Figure 2.5 and 2.6). Active caspase-8 has previously been shown to cleave RIP-1, thereby inhibiting pro-survival NF-κB signaling and inducing apoptosis [54]. This result, coupled with our findings that LOE inhibits Cyclin D1 and cIAP2, proteins activated by NF-κB signaling, while simultaneously stimulating caspase-8 dependent cell death, a characteristic of NF-κB inhibition, sheds critical light on the mechanistic foreground of LOE action. All together, these data highlight the potential of *L. origanoides* extract and its major constituents as cancer therapeutics.

2.6 Summary

In summary, we have shown that LOE promotes apoptosis in TNBC cells, while having a much reduced impact on cell death in normal mammary cells. We also found that LOE reduces cell viability, alters the cell cycle and primarily leads to tumor cell apoptosis and not necrosis. Further, we established some of the mechanisms of LOE actions, showing that it suppresses markers of cell cycle progression and cell survival while inducing the extrinsic pathway of apoptosis via caspase-8/-3 activation. Finally, we reveal that levels of RIP1, an upstream effector of pro-survival NF-κB signaling, are reduced upon LOE treatment. These data collectively support that LOE can be a valuable source for development of novel anticancer agents. Moving forward, beyond fully describing the cellular mechanisms of LOE action, a top priority will be identifying the major component or combination of components responsible for its bioactivity. Plant-derived compounds offer a vast source of small molecule inhibitors that could be used both in their native state as well as chemically modified to optimize their pharmacological activity. The bio-reactivity of the LOE-treatment in TNBC cells *in vitro* supports the idea that future treatments for individual cancer subtypes lie in naturally-derived chemicals.

2.7 References

1. Jordan, V.C. (1992). The role of tamoxifen in the treatment and prevention of breast cancer. Current Problems in Cancer, 16, 134-176.
2. Buzdar, A., & Howell, A. (2001). Advances in aromatase inhibition, clinical efficacy and tolerability in the treatment of breast cancer. Clinical Cancer Research, 7, 2620-2635.
3. Romond, E.H., Perez, E.A., Bryant, J., Suman, V.J., Geyer, C.E. Jr., Davidson, N.E., et al. (2005). Trastuzumab plus adjuvant chemotherapy for operable HER2-positive breast cancer. New England Journal of Medicine, 353, 1673-1684.
4. Cakir, A., Gonul, I., & Uluoglu, O. (2012). A comprehensive morphological study for basal-like breast carcinomas with comparison to nonbasal-like carcinomas. Diagnostic Pathology, 7(1), 145.

5. Bertucci, F., Finetti, P., Cervera, N., Esterni, B., Hermitte, F., Viens, P., & Birnbaum, D. (2008). How basal are triple-negative breast cancers? International Journal of Cancer, 123(1), 236–240.
6. Rakha, E. A., El-Sayed, M. E., Green, A. R., Paish, E. C., Lee, A. H. S., & Ellis, I. O. (2007). Breast carcinoma with basal differentiation, a proposal for pathology definition based on basal cytokeratin expression. Histopathology, 50(4), 434–438.
7. Alluri, P., & Newman, L. A. (2014). Basal-like and triple-negative breast cancers, searching for positives among many negatives. Surgical oncology clinics of North America, 23(3), 567-77.
8. The Cancer Genome Atlas Network. (2012). Comprehensive molecular portraits of human breast tumors. Nature, 490, 61-70.
9. Qi, X., Yin, N., Ma, S., Lepp, A., Tang, J., Jing, W., et al. (2015). p38gamma MAPK is a therapeutic target for triple-negative breast cancer by stimulation of cancer stem-like cell expansion. Stem Cells, 33, 2738-2747.
10. Darvishi, B., Farahmand, L., Eslami-S, Z., & Majidzadeh-A, K. (2017). NF-κB as the main node of resistance to receptor tyrosine kinase inhibitors in triple-negative breast cancer. Tumor Biology, 39(6), 101042831770691.
11. Sero, J.E., Sailem, H.Z., Ardy, R.C., Almuttaqi, H., Zhang, T. & Bakal, C. (2015). Cell shape and the microenvironment regulate nuclear translocation of NF-kappaB in breast epithelial and tumor cells. Molecular Systems Biology, 11, 790.
12. Khoshnan, A., Tindell, C., Laux, I., Bae, D., Bennett, B. & Nel, A.E. (2000) The NF-kappaB cascade is important in Bcl-xL expression and for the anti-apoptotic effects of the Cd28 receptor in primary human CD4+ lymphocytes. Journal of Immunology, 165, 1743-1754.
13. Wang, C.Y., Mayo, M.W., Korneluk, R.G., Goeddel, D.V. & Baldwin, A.S. Jr. (1998). NF-kappaB antiapoptosis, induction of TRAF1 and TRAF2 and c-IAP1 and c-IAP2 to suppress caspase-8 activation. Science, 281, 1680-1683.
14. Huber, M.A., Azoitei, N., Baumann, B., Grünert, S., Sommer, A., Pehamberger, H. (2004). NF-kappaB is essential for epithelial-mesenchymal transition and metastasis in a model of breast cancer progression. Journal of Clinical Investigations, 114, 569-581, 2004.

15. Hartman, Z.C., Poage, G.M., den Hollander, P., Tsimelzon, A., Hill, J., Panupinthu, N., et al. (2013). Growth of triple-negative breast cancer cells relies upon coordinate autocrine expression of the pro-inflammatory cytokines IL-6 and IL-8. Cancer Research, 73, 3470-3480.
16. Hinz, M., Krappmann, D., Eichten, A., Heder, A., Scheidereit, C., & Strauss M, NF-kappaB function in growth control, regulation of Cyclin D1 Expression and G0/G1-to-S-phase transition. Molecular and Cellular Biology, 19, 2690-2698.
17. Li, C., Xia, W., Huo, L., Lim, S., Wu, Y., Hsu, J. L., et al. (2012). Epithelial-Mesenchymal Transition Induced by TNF- Requires NF- B-Mediated Transcriptional Upregulation of Twist1. Cancer Research, 72(5), 1290–1300.
18. Nakshatri, H., Bhat-Nakshatri, P., Martin, D.A., Goulet, R.J. Jr., & Sledge, G.W. Jr. (1997). Constitutive activation of NF-kappaB during progression of breast cancer to hormone-independent growth. Molecular and Cellular Biology, 17, 3629-3639.
19. Smith, S. M., Lyu, Y. L., & Cai, L. (2014). NF-κB Affects Proliferation and Invasiveness of Breast Cancer Cells by Regulating CD44 Expression. PLoS ONE, 9(9), e106966.
20. Matsumoto, G., Namekawa, J., Muta, M., Nakamura, T., Bando, H., Tohyama, K., et al. (2005). Targeting of nuclear factor kappaB pathways by dehydroxy-methyl-epoxyquinomicin, a novel inhibitor of breast carcinomas, antitumor and anti-angiogenic potential in vivo. Clinical Cancer Research, 11(3),1287-93.
21. Connelly, L., Robinson-Benion, C., Chont, M., Saint-Jean, L., Li, H., Polosukhin, V.V., et al. (2007). A transgenic model reveals important roles for the NF-kappaB alternative pathway (p100/p52) in mammary development and links to tumorigenesis. Journal of Biological Chemistry, 282,10028–10035.
22. Thomas, G.W., Muss, H.B., Jackson, D.V., McCulloch, J., Ramseur, W., McFarland, J., et al. (1994). Vincristine with high-dose etoposide in advanced breast cancer, a phase II trial of the Piedmont Oncology Association. Cancer Chemotherapy and Pharmacology, 35(2),165-8.
23. Stemmler, H.J., Gutschow, K., Sommer, H., Malekmohammadi, M., Kentenich, C.H., Forstpointner, R., et al. (2001). Weekly docetaxel (Taxotere) in patients with metastatic breast cancer. Annals of Oncology, 12(10),1393-8.

24. Ahmad, A., Banerjee, S., Wang, Z., Kong, D., & Sarkar, F.H. (2008). Plumbagin-induced apoptosis of human breast cancer cells is mediated by inactivation of NF-kappaB and Bcl-2. Journal of Cellular Biochemistry, 105, 1461-1471.
25. Jin, M.L., Park, S.Y., Kim, Y.H., Park, G., & Lee, S. (2014) Halofuginone induces the apoptosis of breast cancer cells and inhibits migration via downregulation of matrix metalloproteinase-9. International Journal of Oncology, 44, 309-318.
26. Pozo-Guisado, E., Merino, J.M., Mulero-Navarro, S., Lorenzo-Benayas, M.J., Centeno, F., Alvarez-Barrientos, A., & Fernandez-Salguero, P.M. (2005) Resveratrol-induced apoptosis in MCF-7 human breast cancer cells involves a caspase-independent mechanism with downregulation of Bcl-2 and NF-kappaB. International Journal of Cancer, 115, 74-84.
27. Singh., S, & Aggarwal, B.B. (1995). Activation of transcription factor NF-kappaB is suppressed by curcumin (diferuloylmethane). The Journal of Biological Chemistry, 270, 24995-25000.
28. Tse, A.K., Wan, C.K., Shen, X.L., Yang, M., & Fong, W.F. (2005). Honokiol inhibits TNF-alpha-stimulated NF-kappaB activation and NF-kappaB-regulated gene expression through suppression of IKK activation. Biochemical Pharmacology, 70, 1443-1457.
29. Chen, K.S., Shi, M.D., Chien, C.S., & Shih, Y.W. (2014). Pinocembrin suppresses TGF-betta1-induced epithelial-mesenchymal transition and metastasis of human Y-79 retinoblastoma cells through inactivating alphavbetta3 integrin/FAK/p38alpha signaling pathway. Cell Biosciences, 4, 41.
30. Pascual, M.E., Slowing, K., Carretero, E., Sanchez Mata, D., & Villar, A. (2001) *Lippia*, traditional uses, chemistry and pharmacology, a review. Journal of Ethnopharmacology, 76, 201-214.
31. Stashenko, E.E., Martínez, J.R., Ruíz, C.A., Arias, G., Durán, C., Salgar, W., & Cala, M. (2010). *Lippia origanoides* chemotype differentiation based on essential oil GC-MS and principal component analysis. Journal of Separation Science, 33, 93-103.

32. Stashenko, E.E., Martínez, J.R., Cala, M.P., Durán, D.C., & Caballero, D. (2013). Chromatographic and mass spectrometric characterization of essential oils and extracts from *Lippia* (Verbenaceae) aromatic plants. Journal of Separation Science, 36, 192-202.
33. Legault, J., & Pichette, A. (2007). Potentiating effect of beta-caryophyllene on anticancer activity of alpha-humulene, isocaryophyllene, and paclitaxel. Journal of Pharmacy and Pharmacology, 59, 1643-1647.
34. Aristatile, B., Al-Assaf, A.H., & Pugalendi, K.V. (2013). Carvacrol suppresses the expression of inflammatory marker genes in D-galactosamine-hepatotoxic rats. Asian Pacific Journal of Tropical Medicine. 6(3),205-11.
35. Greiner, J.F., Müller, J., Zeuner, M.T., Hauser, S., Seidel, T., Klenke, C., et al. (2013). 1,8-Cineol inhibits nuclear translocation of NF-κB p65 and NF-κB-dependent transcriptional activity. Biochimica et Biophysica Acta, 1833(12),2866-78.
36. Lee, J.C., Kundu, J.K., Hwang, D.M., Na, H.K., & Surh, Y.J. (2007). Humulene inhibits phorbol ester-induced COX-2 expression in mouse skin by blocking activation of NF-kappaB and AP-1, IkappaB kinase and c-Jun-N-terminal kinase as respective potential upstream targets. Carcinogenesis, 28(7),1491-8.
37. Liang, D., Li, F., Fu, Y., Cao, Y., Song, X., Wang, T., et al. (2014). Thymol inhibits LPS-stimulated inflammatory response via down-regulation of NF-κB and MAPK signaling pathways in mouse mammary epithelial cells. Inflammation, 37(1),214-22.
38. Kim, C., Cho, S.K., Kim, K.D., Nam, D., Chung, W.S., Jang, H.J., et al. (2014). β-Caryophyllene oxide potentiates TNFα-induced apoptosis and inhibits invasion through down-modulation of NF-κB-regulated gene products. Apoptosis 19(4),708-18.
39. Schneider, C.A., Rasband, W.S. & Eliceiri, K.W. (2012). NIH Image to ImageJ, 25 years of image analysis. Nature Methods, 9, 671-675.
40. Portt, L., Norman, G., Clapp, C., Greenwood, M., & Greenwood, M.T. (2011). Anti-apoptosis and cell survival, a review. Biochimica Biophysica Acta, 1813,238-59.
41. Baldin,V., Lukas, J., Marcote, M.J., Pagano, M., & Draetta, G. (1993). Cyclin D1 is a nuclear protein required for cell cycle progression in G1. Genes and Development, 7, 812-821.

42. Salvesen, G.S., & Duckett, C.S. (2002). IAP proteins, blocking the road to death's door. Nature Reviews Molecular Cell Biology, 3, 401-410.
43. Bertrand, M.J., Milutinovic, S., Dickson, K.M., Ho, W.C., Boudreault, A., Durkin, J., et al. (2008). cIAP1 and cIAP2 facilitate cancer cell survival by functioning as E3 ligases that promote RIP1 ubiquitination. Molecular Cell, 30, 689-700.
44. Yamaguchi, N., Ito, T., Azuma, S., Ito, E., Honma, R., Yanagisawa, Y., et al. (2009). Constitutive activation of nuclear factor-kappaB is preferentially involved in the proliferation of basal-like subtype breast cancer cell lines. Cancer Science, 100, 1668-1674.
45. Grigoriadis, A., Mackay, A., Noel, E., Wu, P.J., Natrajan, R., Frankum, J., Reis-Filho, J.S., Tutt, A. (2012). Molecular characterisation of cell line models for triple-negative breast cancers. BMC Genomics, 13,619.
46. Nguyen, A., Yoshida, M., Goodarzi, H., & Tavazoie, S.F. (2016). Highly variable cancer subpopulations that exhibit enhanced transcriptome variability and metastatic fitness. Nature Communications 7,11246.
47. Leung, E., Kannan, N., Krissansen, G.W., Findlay, M.P., & Baguley, B.C. (2010). MCF-7 breast cancer cells selected for tamoxifen resistance acquire new phenotypes differing in DNA content, phospho-HER2 and PAX2 expression, and rapamycin sensitivity. Cancer Biology and Therapy, 1,9(9),717-24.
48. Peter, M.E., & Krammer, P.H. (2003). The CD95(APO-1/Fas) DISC and beyond. Cell Death and Differentiation, 10, 26-35.
49. Beaudouin, J., Liesche, C., Aschenbrenner, S., Horner, M., & Eils, R. (2013). Caspase-8 cleaves its substrates from the plasma membrane upon CD95-induced apoptosis. Cell Death and Differentiation, 20, 599-610.
50. Yamamoto, M., Taguchi, Y., Ito-Kureha, T., Semba, K., Yamaguchi, N., & Inoue, J. (2013). NF-kappaB non-cell-autonomously regulates cancer stem cell populations in the basal-like breast cancer subtype. Nature Communications, 4, 2299.
51. Micheau, O., & Tschopp, J. (2003). Induction of TNF receptor I-mediated apoptosis via two sequential signaling complexes. Cell, 114, 181-190.

52. Guttridge, D.C., Albanese, C., Reuther, J.Y., Pestell, R.G., & Baldwin, A.S. Jr. (1999). NF-kappaB controls cell growth and differentiation through transcriptional regulation of Cyclin D1. Molecular and Cellular Biology, 19, 5785-5799.
53. You, M., Ku, P.T., Hrdličková, R., & Bose, H.R. Jr. (1997). ch-IAP1, a member of the inhibitor-of-apoptosis protein family, is a mediator of the antiapoptotic activity of the v-Rel oncoprotein. Molecular and Cellular Biology, 17, 7328-7341.
54. Lin, Y., Devin, A., Rodriguez, Y., & Liu, Z. (1999). Cleavage of the death domain kinase RIP by Caspase-8 prompts TNF-induced apoptosis. Genes and Development, 13(19),2514-2526.

CHAPTER 3. PROTEOMIC ANALYSIS REVEALS *LIPPIA ORIGANOIDES* EXTRACT (L42) TARGETS MITOCHONDRIAL METABOLISM IN TRIPLE-NEGATIVE BREAST CANCER CELLS

A version of this chapter has been previously published in the Journal of Proteome Research, 2018, 17(10):3370-3383. DOI: 10.1021/acs.jproteome.8b00255

3.1 Abstract

Recent studies indicate triple-negative breast cancers possesses an altered metabolic state with higher rates of glycolysis, mitochondrial oxidative phosphorylation, and increased generation and utilization of tricarboxylic acid cycle intermediates. Here we utilized label-free quantitative proteomics to gain insight into the anti-cancer mechanisms of a methanolic extract from the Central American plant *Lippia origanoides* on MDA-MB-231 triple-negative breast cancer cells. The *L. origanoides* extract dysregulated mitochondrial oxidative phosphorylation by targeting Complex I of the electron transport chain and suppressed cellular metabolism by targeting key tricarboxylic acid cycle enzymes and mitochondrial lipid and amino acid metabolic pathways. Our study also revealed treatment with the extract activated the stress response, and pathways related to cell cycle progression and DNA repair. Overall, our results reveal new compelling evidence that the extract from *Lippia origanoides* triggers rapid irreversible apoptosis in MDA-MB-231 cells by effectively 'starving' the cells of metabolites and ATP. We continue to study the specific bioactive components of the extract in the search for novel, highly effective mitochondrial inhibitors to selectively target triple-negative breast cancer.

3.2 Introduction

As mentioned in section 1.4., the initial discovery of anticancer drugs from natural sources prompted the NIH to begin screening natural extracts using *in vitro* cancer models to isolate and identify their bioactive compounds [1, 2]. Such extracts have often shown inhibitory effects on the viability and proliferation of cancer cells while remaining

relatively harmless to normal cells, and non-toxic *in vivo* [3-5]. Bioassay-driven fractionation and target-identification schemes have led to the discovery of several drugs, notably the *Vinca* alkaloids and taxanes; however, this is both time-consuming and very expensive [6, 7]. In addition, the use of Western-blots, PCR, and ELISA to identify the effects of treatments on specific signaling pathways does not provide information on off-target effects, which is a major drawback when dealing with complex mixtures of compounds. The advent of cDNA microarray-driven biomarker identification techniques provided a more holistic picture of the cell- and tissue-wide effects of chemotherapy [8]. Unfortunately, microarrays have the limitation of only providing information on fluctuations in mRNA levels, which are often disproportional to corresponding changes in protein expression [9-11]. Hence, it is critical that new techniques are developed to more efficiently screen natural extracts for their effects on the entire proteome on a cell- and tissue-wide basis. Realizing this goal will greatly expedite the identification of viable new cancer targets.

Recently, there has been tremendous interest in targeting cancer cell metabolism as a new therapeutic strategy, given that the most recognized hallmark of cancer cells is increased aerobic glycolysis, a phenomenon termed the Warburg effect [12, 13]. In particular, TNBCs are known to have an altered metabolic profile with elevated uptake and utilization of glucose [14, 15], glutamine [16-18], and TCA cycle intermediates [19], as well as increased fatty acid β-oxidation [20]. We speculate that this allows for the heightened growth, proliferation and invasiveness observed in TNBCs by providing alternative sources of ATP generation. For these reasons, identifying specific targets and novel small molecule inhibitors against TNBC metabolism is of considerable clinical importance.

As shown in Chapter 2, the *Lippia origanoides* extract (LOE), had substantial anti-proliferative and pro-apoptotic effects on several TNBC cells lines, while remaining relatively non-toxic to normal mammary epithelial cells [21]. In testing multiple extracts from *Lippia* and other species, we discovered a new extract from a different chemotype of the same species possessed an even higher potency against TNBC cells while retaining reduced toxicity against normal cells. Hence, this extract, termed ‘L42’, was used in the

present study to determine its proteome-wide effects on MDA-MB-231 TNBC cells. We applied precursor ion (MS1) intensity based label-free quantitation (LFQ) via LC-MS/MS, which is becoming the method of choice to study cell functional responses at the proteome level [22-26], to determine relative changes in protein abundances due to L42 treatment.

In brief, we quantified 2,407 proteins, of which 519 were significantly dysregulated upon L42 treatment. The majority of down-regulated proteins were mitochondrial, and known to play critical roles in cellular metabolism pathways, including the TCA cycle, β-oxidation of fatty acids, and glutamine utilization. Core subunits of Complex I and the mitochondrial ribosome were down-regulated upon treatment, providing evidences of the disruptive effects of L42 on mitochondrial activity and function.

Considering these actions, Chapter 3 provides critical and holistic mechanistic insight into the TNBC-specific inhibitory effects of L42, and proposes that L42 is a novel source of potent mitochondrial-specific inhibitors for tumor metabolism-based cancer therapy.

3.3 Materials and Methods

3.3.1 Cell culture

MDA-MB-231 triple-negative breast cancer and MCF10A normal mammary epithelial cell lines were obtained from the American Type Culture Collection. MDA-MB-231 cells were cultured in Dulbecco's Modified Essential Medium (DMEM; Life Technologies, NY, USA) supplemented with 10 % fetal bovine serum (FBS; Atlanta Biologicals, GA, USA), 100 IU/ml penicillin and 100 µg/ml streptomycin (Life Technologies, NY, USA). MCF10A cells were cultured in a 1:1 ratio of DMEM:Ham's F12 supplemented with 5 % horse serum (HS; Atlanta Biologicals, GA, USA), 20 ng/ml human epidermal growth factor (Sigma-Aldrich, MO, USA), 0.5 mg/mL hydrocortisone (Sigma-Aldrich, MO), 100 ng/ml cholera toxin (Sigma-Aldrich, MO, USA), 10 µg/mL bovine insulin (Sigma-Aldrich, MO, USA), 100 IU/ml penicillin and 100 µg/ml streptomycin.

3.3.2 L42 extract preparation

The extract from *Lippia origanoides* (COL 560267) was prepared as described previously [27]. Briefly, 200 g of finely ground *L. origanoides* plant material (leaves and stems) was placed in the extraction chamber of a Thar SFE-2000-2-FMC50 (Thar Instruments, PA, USA) and subjected to supercritical CO_2 extraction at 50 MPa and 333 K at the Universidad Industrial de Santander, Bucaramanga, Colombia. The material deposited on the walls of the chamber was collected, and 250 mg of this extracted material was dissolved in 5 ml of methanol, sonicated for 15 min, and centrifuged at 10000 rpm for a further 15 min. The 50 mg/ml stock solution of the supernatant collected (L42) was used in the present study.

3.3.3 Assessment of cell viability using MTT assay

MCF10A and MDA-MB-231 cells were seeded at 10^4 cells/well in 96-well plates and allowed to attach. Spent media was then replaced with treatment media containing either L42 or methanol (vehicle control, VEH). Following 24, 48 and 72 h treatments, 20 µl of 12 mM MTT (Life Technologies, NY, USA), was added to the cells followed by incubation overnight at 37 °C. Formazan crystals formed at the end of incubation period were dissolved using dimethyl sulfoxide (DMSO) and cell viability was determined as a measure of absorbance at 570 nm.

3.3.4 Western blotting

MDA-MB-231 cells were seeded at 10^6 cells/well in 6-well plates and allowed to attach overnight, then treated with fresh media containing L42 (0.15 mg/ml) or vehicle (methanol) for 12 h. Treated cells were collected in RIPA buffer and sonicated, following which samples were centrifuged to obtain lysates. Protein concentrations of lysates were estimated via the bicinchoninic acid (BCA) assay (Thermo Fisher, IL, USA). 20 µg of protein from each sample was mixed with 4X sample buffer and boiled, and denatured proteins were loaded and run via SDS-PAGE, then transferred onto a polyvinyl difluoride (PVDF) membrane and immunoblotted. Primary antibodies for Cyclin D1 and cleaved caspase-8 were purchased from Cell Signaling Technologies, MA, USA. GLS and β-actin antibodies were purchased from Abcam, MA, USA and Sigma-Aldrich, MO, USA

respectively. β-tubulin antibody was purchased from the Developmental Studies Hybridoma Bank, University of Iowa, IA, USA. Densitometric quantification was carried out using ImageJ software.

3.3.5 LC-MS/MS: sample preparation and analysis

Protein extraction: 3 x 10^6 MDA-MB-231 cells, treated with L42 or vehicle control (N = 3 replicates/ treatment), were collected via scraping, centrifuged and then washed twice with ice-cold 1X PBS. Samples were centrifuged at 3,000 rpm for 5 min after each wash, and pelleted cells were re-suspended in 100 µl of 100 mM ammonium bicarbonate (ABC). Samples were then homogenized at 35,000 psi using a barocycler (Pressure Biosciences, MA, USA) with high-pressure time of 20 s followed by low-pressure time of 10 s, for each cycle for a total of 90 cycles.

Homogenized samples were centrifuged at 14,000 rpm for 20 min at 4 °C and the soluble fraction (SF, supernatant) and membrane-fraction (MF, pellet) were collected separately. SF was subjected to bicinchoninic acid (BCA) assay to measure protein concentration. A total of 100 µg of SF was made up to 100 µl using Milli Q water and then precipitated using 5 volumes of cold (-20 °C) acetone overnight to allow for protein precipitation. For pellet (membrane fraction, MF), 10 µl of urea/DTT was added and MF samples were placed in 37 °C rotary shaker for 1 h to reduce and denature proteins. Denatured MF samples were then mixed with 10 µl alkylation mixture (195 µl acetonitrile (ACN), 1 µl triethylphosphine, and 4 µl 2-iodoethanol) and placed for a further 1 h in 37 °C shaker. MF samples were then dried in vacuum centrifuge (Labconco, MO, USA) for 1 h after which the dry protein pellets were stored at -20 °C until further use. Precipitated SF samples were centrifuged at 14,000 rpm for 20 min and pellets were dried in vacuum centrifuge briefly, after which SF samples were also subjected to reduction, denaturation and alkylation as described previously.

Protein digestion and solid phase extraction (SPE): Lys-C/trypsin (Promega, WI, USA) vial containing 20 µg of the mixture was dissolved by adding 400 µl of 25 mM ABC to 80 µl of each sample (both SF and MF) to achieve enzyme:substrate ratio of 1:25. Samples were then transferred to a barocycler for digestion. Proteins were digested for 1 h at 50 °C at 20 kpsi using a program set at high pressure for 50 s followed by a low

(atmospheric) pressure setting for 10 s per cycle, for a total of 60 cycles. Digested peptides were desalted using C18 SPE columns using a protocol provided by the manufacturer. Clean peptides were eluted using 50 µl 80 % ACN/ 0.1 % FA/ 20 % Milli Q, and elution step was repeated twice. Eluates were dried in a vacuum centrifuge following which the clean, dry peptides were stored at -20 °C until further use.

LC-MS/MS analysis: Samples were analyzed by reverse-phase HPLC-ESI-MS/MS using the Dionex UltiMate 3000 RSLC nano System (Thermo Fisher Scientific) coupled to the Q-Exactive High Field (HF) Hybrid Quadrupole Orbitrap MS (Thermo Fisher Scientific) and a Nano- electrospray Flex ion source (Thermo Fisher Scientific). Peptides were re-suspended in 3 % ACN/ 0.1 % FA/ 97 % milliQ formic acid, and loaded onto a trap column (300 µm ID x 5 mm) packed with 5 µm 100 Å PepMap C18 medium and washed using a flow rate of 5 µl/ min with 98 % purified water/ 2 % acetonitrile (ACN)/ 0.01 % formic acid (FA). The trap column was then switched in-line with the analytical column after 5 minutes. Peptides were separated using a reverse phase Acclaim PepMap RSLC C18 (75 µm x 15 cm) analytical column using a 120-min method at a flow rate of 300 nl/min. The analytical column was packed with 2 µm 100 Å PepMap C18 medium (Thermo Fisher Scientific). Mobile phase A consisted of 0.01 % FA in water and a mobile phase B consisted of 0.01 % FA in 80 % ACN. The linear gradient started at 5 % B and reached 30 % B in 80 min, 45 % B in 91 min, and 100 % B in 93 min. The column was held at 100% B for the next 5 min before being brought back to 5 % B and held for 20 min to equilibrate the column.

Sample was injected into the QE HF through the Nanospray Flex™ Ion Source fitted with an emission tip from Thermo Scientific. Column temperature was maintained at 35 ˚C. MS data were acquired with a Top 20 data-dependent MS/MS scan method. The full scan MS spectra were collected over 300-1,650 m/z range with a maximum injection time of 100 ms, a resolution of 120,000 at 200 m/z, spray voltage of 2 and AGC target of 1 ×106. Fragmentation of precursor ions was performed by high-energy C-trap dissociation (HCD) with the normalized collision energy of 27 eV. MS/MS scans were acquired at a resolution of 15,000 at m/z 200. The dynamic exclusion was set at 20 s to avoid repeated scanning of identical peptides.

Three biological sample replicates from each treatment were utilized for LC-MS/MS, each run as a single technical replicate, which was sufficient for good statistical power. Instrument optimization and recalibration was carried out at the start of each batch run using the Pierce calibration solution. The sensitivity of the instrument was also monitored using an *E. coli* digest at the start of the sample run.

Bioinformatics: MS/MS data was processed using MaxQuant (v1.6.1.0, [28]) with the spectra matched against the Uniprot *Homo sapiens* fasta (http://www.uniprot.org/; 26,232 entries, state 10/25/17) concatenated with a common contaminants database and a reverse decoy database. MS/MS spectra from Soluble (SF) and Membrane (MF) fractions from each sample were combined during MaxQuant analysis. The cleavage enzyme used was set as Trypsin/P; LysC while allowing for up to 2 missed cleavages. Mass error was set to 10 ppm for precursor ions and 20 ppm for fragment ions. Variable modifications included were oxidation of methionine and acetylation of N-terminal amino acids, with alkylation of cysteine residues set as a fixed modification and oxidation of methionine was defined as a variable modification. Estimated False Discovery Rate (FDR) threshold was set to 1 % both at the peptide and protein level. The 'unique plus razor peptides' were used for peptide quantitation. Razor peptides are non-unique peptides assigned to the protein group with most other peptides.

After MaxQuant searches, proteins without any LFQ intensity and without any MS/MS counts were filtered out. MaxQuant results were exported to Data Analysis and Extension Tool (DAnTE) [29], and analyzed for Pearson correlations coefficients, and visualized using heatmaps generated by Heatmapper [30]. The complete RAW proteomics data files, peptide sequence files, protein identification files, parameters used, LC-MS/MS methodology, and Supplementary Tables have been deposited in the MassIVE public proteomics data repository and can be accessed at ftp://massive.ucsd.edu/MSV000082159.

3.3.6 Proteomics data analysis*:*

We identified 3,061 proteins across all 3 replicates from both treatment groups. Proteins identified and quantified in ≥ 2 replicates in both treatment groups were retained, and zero-fill proteins (i.e. proteins identified in all replicates of one treatment group, and not

found in any replicates of the other) were also retained, leaving 2,407 proteins for further analyses. Bioinformatics analysis was performed using the R statistical software. LFQ intensities of identified proteins were converted to $\log_2$ values and averaged across replicates. The difference in average $\log_2$ values [$\Delta\log_2$ (LFQ intensity)] between proteins from L42-treated and control-treated groups was used as a measure of fold change. Proteins with fold-change values $\Delta\log2 < -0.5$ or $\Delta\log2 > 0.5$, and $p < 0.05$ (Student's unpaired, two-tailed, t-test) were considered to be significantly regulated by L42 treatment.

GO enrichment analysis: Upon L42 treatment, 519 proteins were significantly changed, of which 293 were found to be down-regulated and 226 were up-regulated (See Supplementary Table 3.1C). Gene ontology enrichment analysis was performed by comparing the total pool of 2,407 quantified proteins to down-regulated proteins (Blue font, Supplementary Table 3.1C) and up-regulated (Red font, Supplementary Table 3.1C) using the GOrilla software tool (for biological process, localization and function enrichment) [31, 32] and DAVID 6.8 (for pathway enrichment using the KEGG database) [33, 34]. GO terms with an FDR q-value (Bejamini-Hochberg corrected p-value) < 0.05 were considered significant.

STRING Interaction Analysis: Proteins were further divided into lists (Fatty Acid Metabolism, Amino Acid Metabolism, Oxidative Phosphorylation etc.) based on pathway enrichment, and lists were mapped for possible interactions using the STRING interaction database tool [35]. Interactions were considered significant only at confidence scores of ≥ 0.9 (highest confidence). Mitochondrial localization was also displayed using the STRING enrichment analysis feature for Cellular Component.

Pathway visualization: Pathways were downloaded using the WikiPathways app (v3.3.1) [36] onto Cytoscape software (v3.6.0) [37]. Pathway proteins found in Supplementary Table 3.1C were highlighted, with the extent of up- or down-regulation portrayed using a blue-red gradient indicating $\Delta\log2$ values.

3.3.7 Validation experiment: mitochondrial membrane potential assay

MDA-MB-231 cells were seeded at 10^4 cells/well in 96-well plates and allowed to grow to 70 % confluency, following which cells were treated with L42 (0.15 mg/ml) or vehicle for 8 h. At the end of the treatment period, media was aspirated gently and 200 nM TMRE (Abcam, MA) prepared in fresh media was added to the cells. Following a 30 min incubation period at 37 °C, TMRE media was gently aspirated and cells were washed with 200 µl 1X PBS/ 0.2 % BSA. 100 µl of the same was then added to the cells prior to imaging with a Zeiss Axiovert 200m fluorescence microscope.

3.3.8 Statistical analysis

Cell viability data from the MTT assay was analyzed using JMP 12 (SAS) software. Box Cox transformation ($\lambda = 0.403$) was performed on data to satisfy the normality and equal variance assumptions for Analysis of Variance (ANOVA), which was used to test for overall statistical significance, $p < 0.0001$. An F-test was then performed to measure significance of different effects (individual and crossed), $p < 0.0001$. Significant difference between different levels for third level interaction (Treatment*Time*Cell Line) was then assessed using Tukey's Honest Significant Difference test (Tukey's HSD). The complete report is summarized in Supplementary Table 3.2.

Western Blotting data acquired using denistometric analysis via ImageJ software was subjected to Student's t-test [38]. Statistical analysis for Immunofluorescence Microscopy was performed using an unpaired, two-tailed Mann-Whitney Test.

3.3.9 Data availability

RAW proteomics data files, peptide sequence files, protein identification files, parameters used, LC-MS/MS methodology, and Supplementary Tables have been deposited in the MassIVE public proteomics data repository and can be accessed using the link ftp://massive.ucsd.edu/MSV000082159.

3.4 Results

3.4.1 Effect of L42 on TNBC cell viability.

To investigate the effects of L42 on cell viability of triple-negative and normal mammary epithelial cells, MDA-MB-231 (TNBC) and MCF10A (normal) cells were treated with increasing dosages of L42 for 24, 48 and 72 h, following which the cells were analyzed for viability using the MTT assay. As summarized in the Tukey HSD Report from Supplementary Table 3.2, we observed that L42 induced a significant decrease in viability of MDA-MB-231 cells at 0.09 mg/ml while a dose of 0.13 mg/ml was required to induce a significant reduction in MCF10A viability at 24 h (Figure 3.1A). Importantly, at this time-point, 0.12 mg/ml L42 reduced cell viability in MDA-MB-231 cells to 51%, with no loss of viability in MCF10A cells. At doses ≥ 0.09 mg/ml, at both 48 h and 72 h time-points, MDA-MB-231 cell viability was significantly reduced upon L42 treatment compared to MCF10A viability, even at the highest dosage of 0.15 mg/ml. At the end of 72 h, a single dose of 0.15 mg/ml L42 was seen to reduce MDA-MB-231 viability to < 2 %. Replacing treatment media after 24 h with fresh media did not rescue MDA-MB-231 cell viability (Figure 3.1B)

As a reduction in cell viability may be explained by either cell death or slowing of cell proliferation, we studied the effects of L42 on known effectors of these pathways. Similar to LOE (See Figure 2.4B and Figure 2.5B), L42 treatment of MDA-MB-231 cells induced a significant loss of Cyclin D1 while inducing Caspase-8 activation (Figure 3.1C). These results indicate that L42 dysregulates both proliferative as well as survival pathways to induce apoptosis in TNBC cells.

3.4.2 Overview of proteome analysis and LC-MS reproducibility.

The multi-component nature of L42 could conceivably induce the dysregulation of multiple cellular pathways to bring about its apoptotic effects, and so we sought to study its actions on the proteome landscape of TNBC cells (see Figure 3.2A for workflow). Reproducibility of peptide intensity is critical for accurate MS1 based label free quantitation [26]. We obtained quantifiable data for 2,407 proteins. To assess the accuracy, we ran 3 technical replicates of a complex *E. coli* digest. The average CV of

peptide intensity was 16.7 % (Figure 3.2B), and the median CV was 15.4% (Supplementary Table 3.3). In addition, accuracy was confirmed by analyzing log2 intensity values of Supplementary Table 3.1C proteins which showed high correlation ($R2 \geq 0.99$) between MDA-MB-231 biological replicates from each treatment group (Figure 3.2C). Correlation between replicates from all 2,407 proteins was also similarly high (Figure 3.2D).

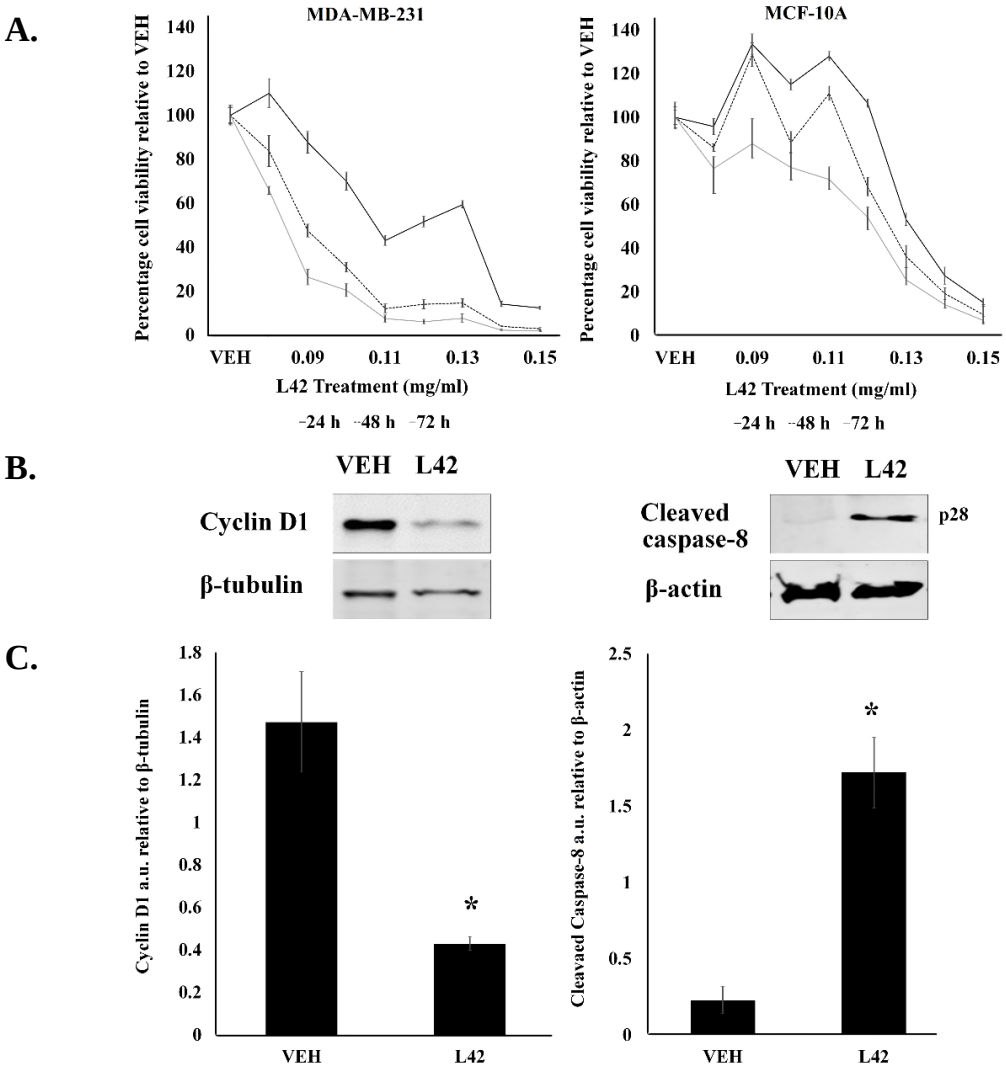

Figure 3.1 L42 inhibits survival and induces apoptosis in MDA-MB-231 cells. A. MDA-MB-231 and MCF10A cells were seeded in 96-well plates and treated with indicated concentrations of L42 or vehicle control (VEH) for 24, 48 and 72 h and subjected to MTT assay. This was followed by absorbance reading at 570 nm. N = 5 replicates; Significance was determined using Tukey's HSD test (see Supplementary Table 3.2), $p < 0.0001$. **B.** MDA-MB-231 cells were treated with 0.15 mg/ml of L42 for various time intervals and lysates were probed for indicated proteins by Western Blot. (*Upper panel)* Representative blots of Cyclin D1 and Caspase-8. (*Lower panel)* Densitometry quantification of blots using ImageJ. Protein levels were normalized against β-actin and plotted as shown. N = 3; * significant difference from VEH, $p < 0.05$.

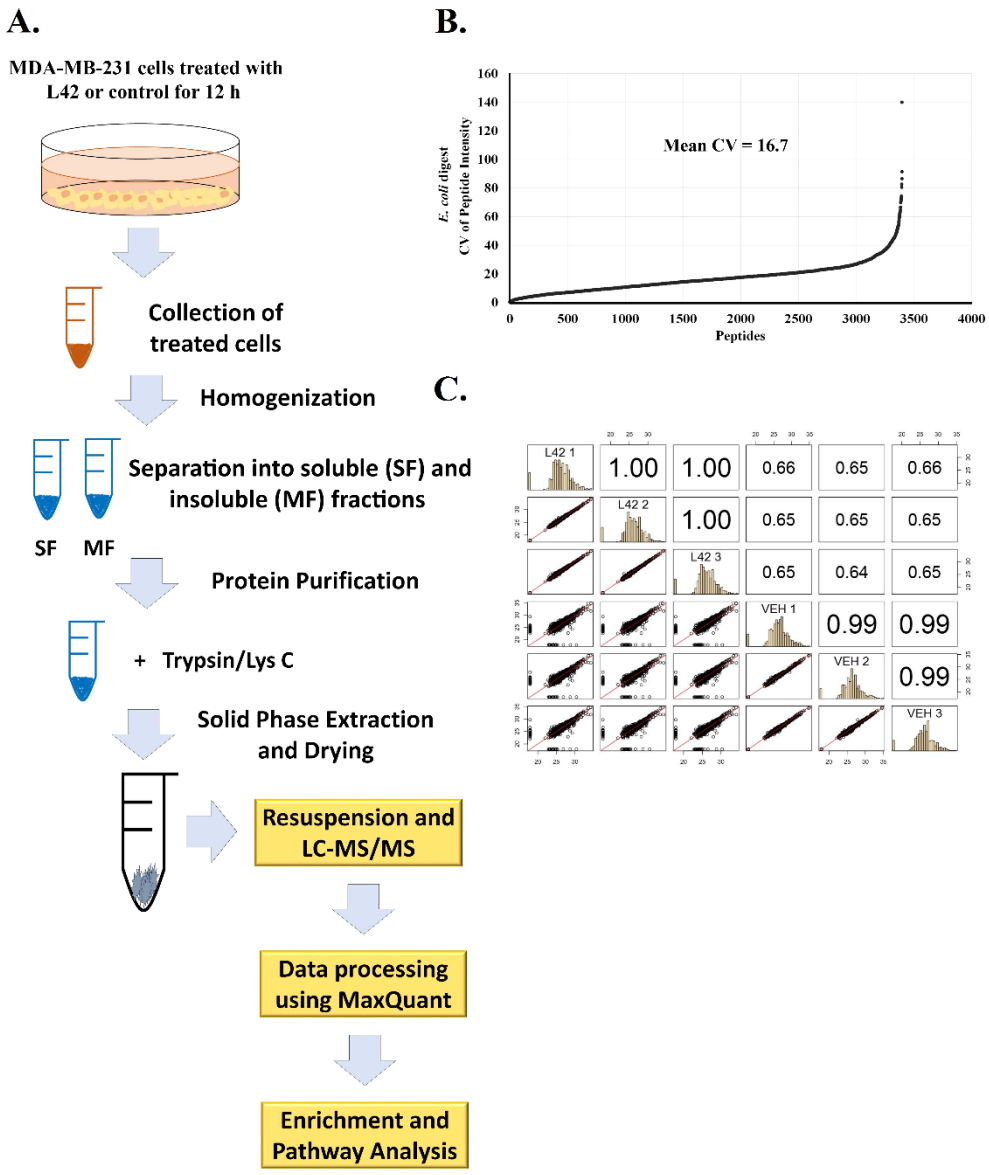

Figure 3.2 Experimental design for proteomics analysis. A. *Proteomics workflow*. **B.** CV % plot of peptide intensity from technical replicates of an *E. coli* tryptic digest. N = 3. **C.** Correlation plot of 519 significantly changed proteins (Supplementary Table 3.1C). R^2-values are consistent, and values between replicates within treatments is noticeably higher than those between replicates across treatments, indicating good experimental reproducibility. N = 3 biological replicates from each treatment group.

3.4.3 Functional classification of identified proteins.

To obtain an overall assessment of the effects of L42 on TNBC cells, proteins from Table 3.1C were divided into separate lists of significantly up-regulated (Red font, Supplementary Table 3.1C) and down-regulated (Blue font, Supplementary Table 3.1C) proteins. GO enrichment for cellular localization, function and process was performed using the GOrilla tool and expression levels of replicates of proteins from significantly enriched terms were averaged and visualized with heat-maps. L42 was found to significantly down-regulate components of oxidoreductase (part of the electron transport chain) and TCA cycle complexes, both localized to the mitochondria, as well as both large and small mitochondrial ribosomal subunits (Figure 3.3A). Further, the functional terms enriched consisted of mitochondrial enzymes significantly down-regulated by L42 treatment (Figure 3.3B). Finally, Figure 3.3C shows with striking clarity that L42 suppressed multiple mitochondrial functions including the TCA cycle, oxidative phosphorylation and protein translation. Interestingly, L42 treatment was also seen to up-regulate proteins involved in stress response, cell cycle regulation and DNA repair (Figure 3.3D).

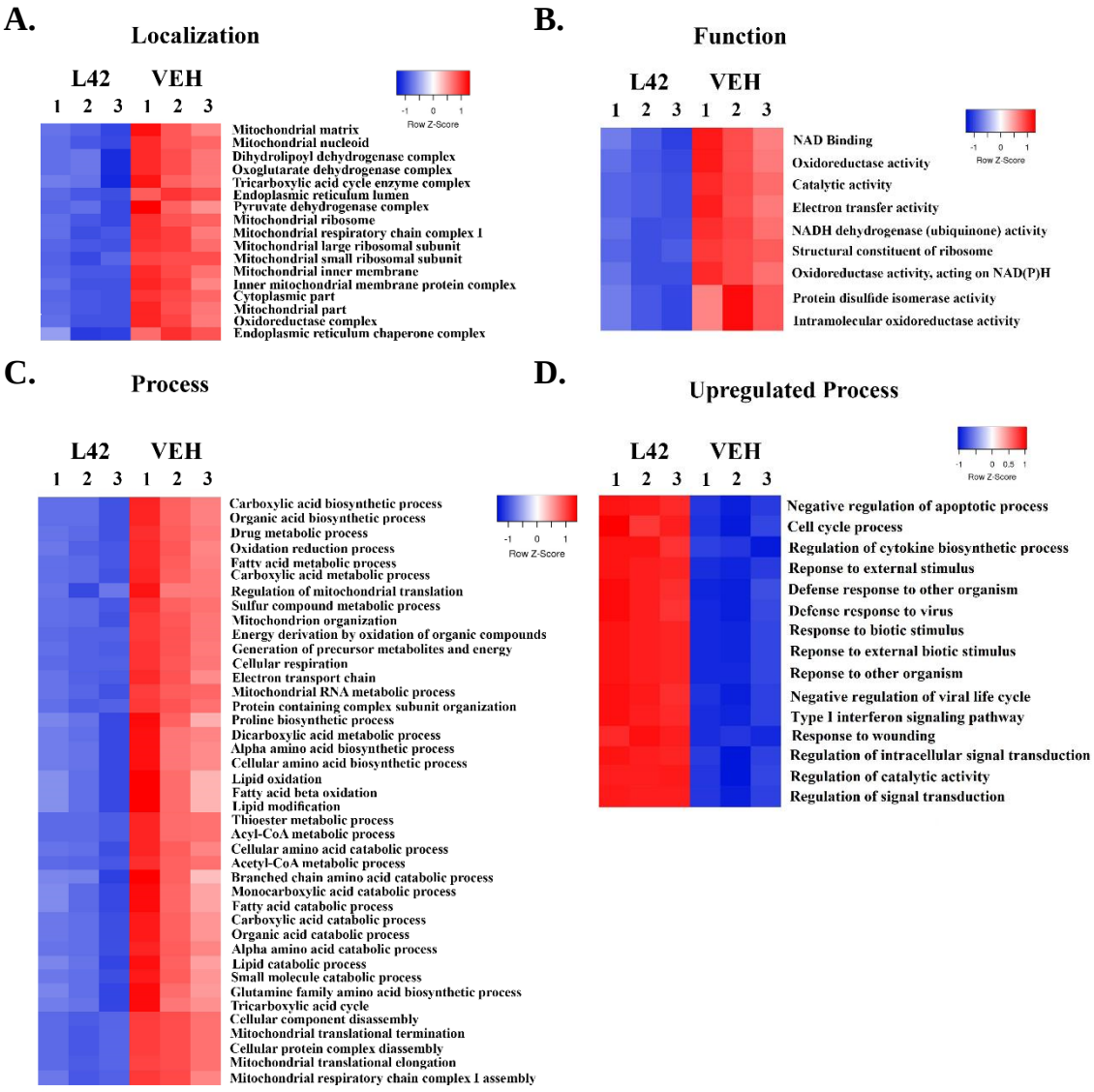

Figure 3.3 GO enrichment analysis of L42-regulated proteins. Significantly upregulated (Red font, Supplementary Table 3.1C) and down-regulated (Blue font, Supplementary Table 3.1C) proteins were compared to the pool of 2,407 identified proteins to identify enrichment of Localization, Function, and Biological process. **A-C.** GO enrichment for significant downregulation. **D.** GO enrichment for significant upregulation *(only observed for biological process)*. Enrichment analysis was performed using GOrilla software and average protein fold-change/replicate/GO term was calculated and visualized using heatmaps generated by Heatmapper.

3.4.4 L42 disrupts metabolism in MDA-MB-231 TNBC cells.

We next examined whether L42 modulated the altered metabolic pathways of TNBC cells. GO pathway enrichment analysis using the KEGG pathway database revealed that L42 strongly suppressed proteins involved in lipid and amino acid metabolism (Figure 3.4A) and STRING analysis provided evidence for interaction between these proteins (Figure 3.4B) and confirmed their mitochondrial localization. Of particular note are the losses of enzymes such as acetyl-CoA acetyltransferease 1 (ACAT1) and AMPK-activated protein kinase 1 (AMPK1) which are key to pyruvate and fatty acid β-oxidation respectively [39, 40]. This was also accompanied by a significant reduction of glutaminase (GLS) and the glutamine transporter solute carrier family 1 member 5 (SLC1A5). Given that targeting glutamine metabolism has emerged as an avenue for TNBC therapy [16], we validated the loss of GLS expression by Western Blot (Figure 3.4C).

Figure 3.4 Hierarchical clustering of differentially-expressed proteins. Significantly changed (Supplementary Table 3.1C) proteins were compared to the pool of 2,407 identified proteins to identify pathway enrichment using DAVID 6.8 software, with the pathways matched to the KEGG database. **A.** Heatmaps of Lipid Metabolism (Top, GO terms included: "Fatty Acid Metabolism", "Fatty Acid Elongation", and "Fatty Acid Degradation") and Amino Acid Metabolism (Bottom, GO terms included: "Amino Acid Biosynthesis", "Valine, Leucine and Isoleucine Degradation", "Tryptophan Metabolism", and "Lysine Metabolism"). **B.** STRING interaction analysis of proteins from Lipid Metabolism (Top) and Amino Acid Metabolism (Bottom), with coloring indicating localization to mitochondria (Red: Mitochondrial matrix, Blue: Mitochondrial inner membrane, Green: Mitochondrial unspecified). Shown are interactions at highest confidence i.e. confidence score ≥ 0.9. **C.** Validation of GLS levels. (Left) Densitometry quantification of blots using ImageJ. GLS levels were normalized against β-actin and plotted as shown. N = 3. Significant difference from VEH is indicated as $*p<0.05$. (Right) Representative western blot showing expression of glutaminase (GLS) in MDA-MB-231 cells treated with L42 (0.15 mg/ml) or vehicle control (VEH) for 12 h.

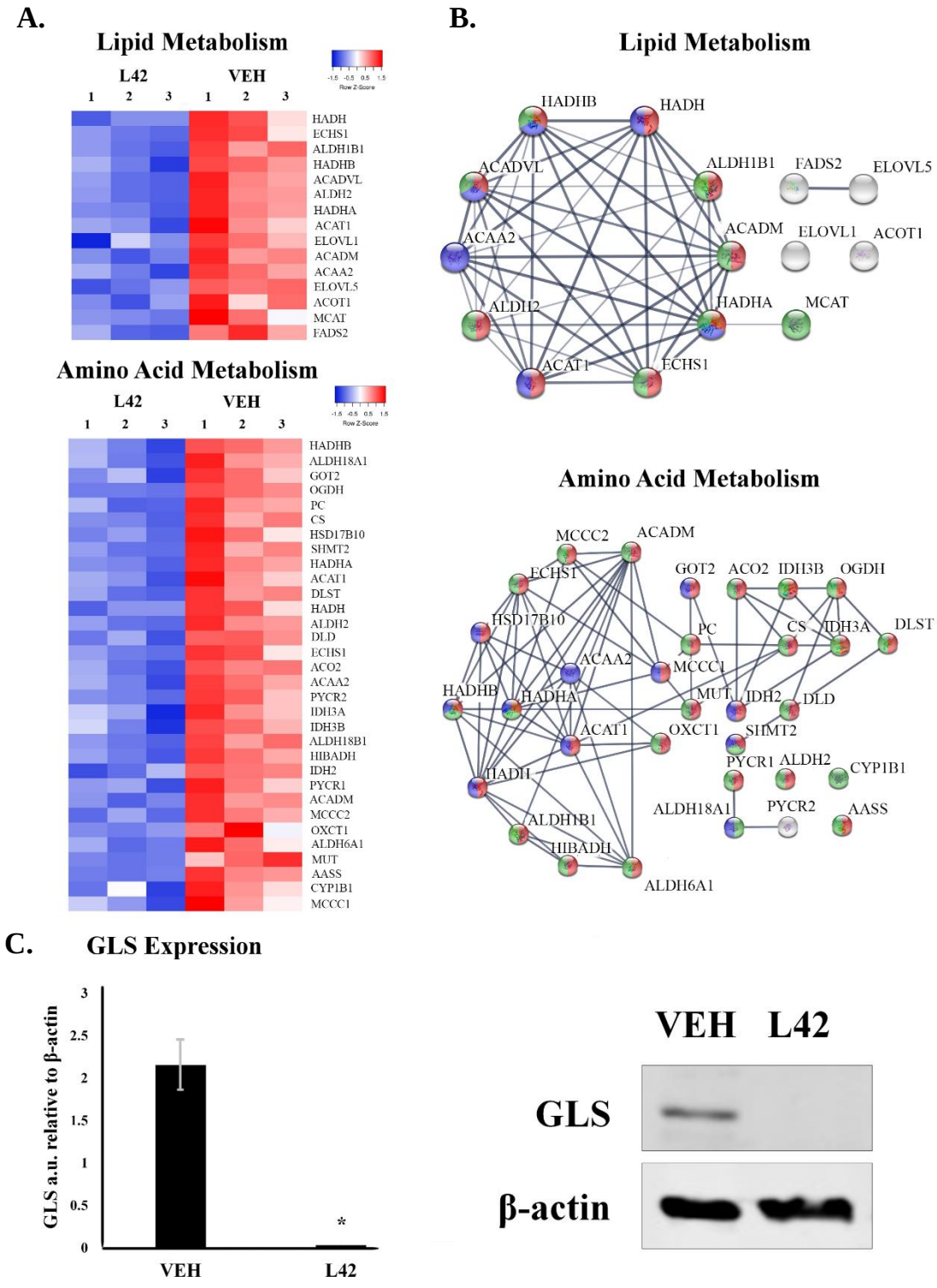

Figure 3.5 Hierarchical clustering of differentially-expressed proteins.

3.4.5 L42 impacts expression of TCA cycle enzymes.

Targeting the TCA cycle has recently generated interest as a novel route to cancer therapy, in light of the observation that several TCA enzymes are mutated or dysregulated in cancer cells [41]. Based on our GO analysis reflecting enrichment of TCA cycle enzymes among the significantly down-regulated proteins, we compared the expression levels of individual TCA cycle enzymes between L42- and control-treated MDA-MB-231 cells. The full extent of TCA cycle suppression by L42 is made apparent in Figure 3.5A, with substantial reductions in expression of multiple enzymes. As shown in Figure 3.5B, L42 severely cripples the TCA cycle by inducing significant reductions in nearly all TCA enzymes. In particular, the all subunits of the α-ketoglutarate dehydrogenase complex (α-KGHDC) complex were down-regulated, with the key component oxoglutarate decarboxylase (OGDH) exhibiting a nearly 2-fold reduction in protein levels.

3.4.6 L42 dysregulates Complex I of the Electron Transport Chain.

Based on our GO analysis revealing down-regulation of proteins involved in oxidative phosphorylation, we evaluated the impact of L42 on the specific complexes of the ETC. We found L42 diminished expression of all the core subunits of Complex I, while also suppressing subunits of Complex IV (Figure 3.6A). Comparison of expression levels between L42- and control-treated groups shows the marked down-regulation of multiple ETC complexes, with Complex I being particularly affected (Figure 3.6B).

A.

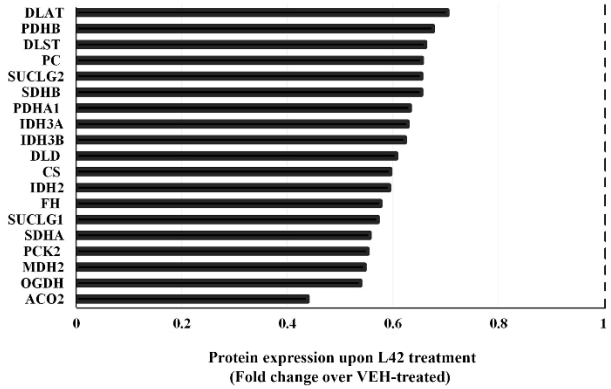

B.

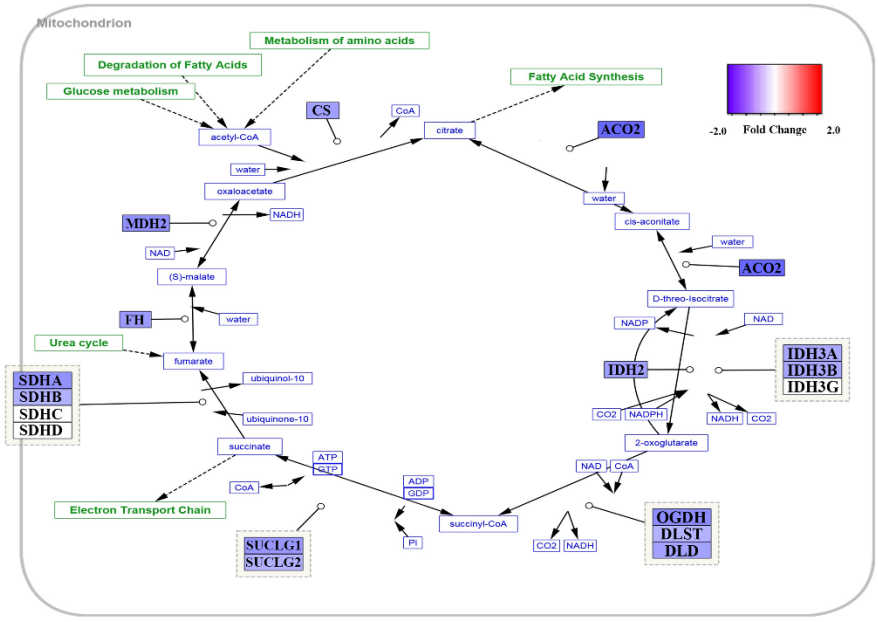

Figure 3.6. Identification of TCA cycle proteins inhibited by L42 in MDA-MB-231 cells. A. Bar graph showing relative protein fold-change between treatment groups for the GO term "Citrate cycle" from KEGG pathway analysis. **B.** Significantly changed (Supplementary Table 3.1C) proteins were uploaded onto Cytoscape software (v3.6.0) and matched to the TCA cycle using the WikiPathways app (v3.3.1), with degree of shading of matching proteins set as a measure of fold-change (see key).

A.

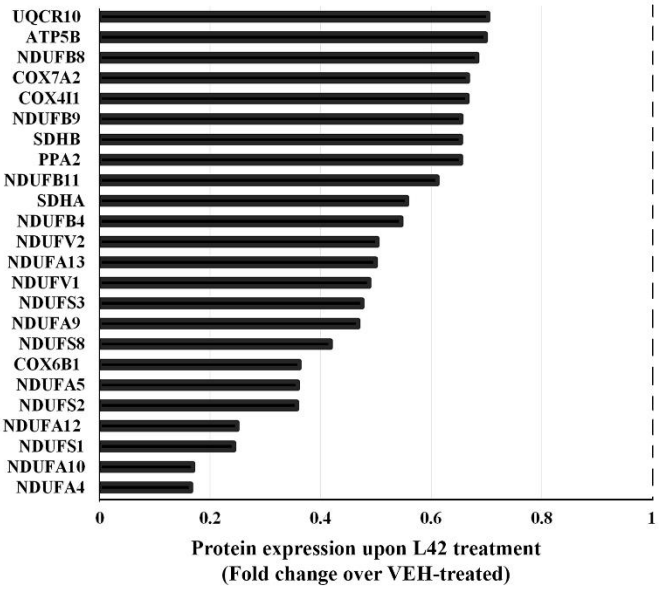

B.

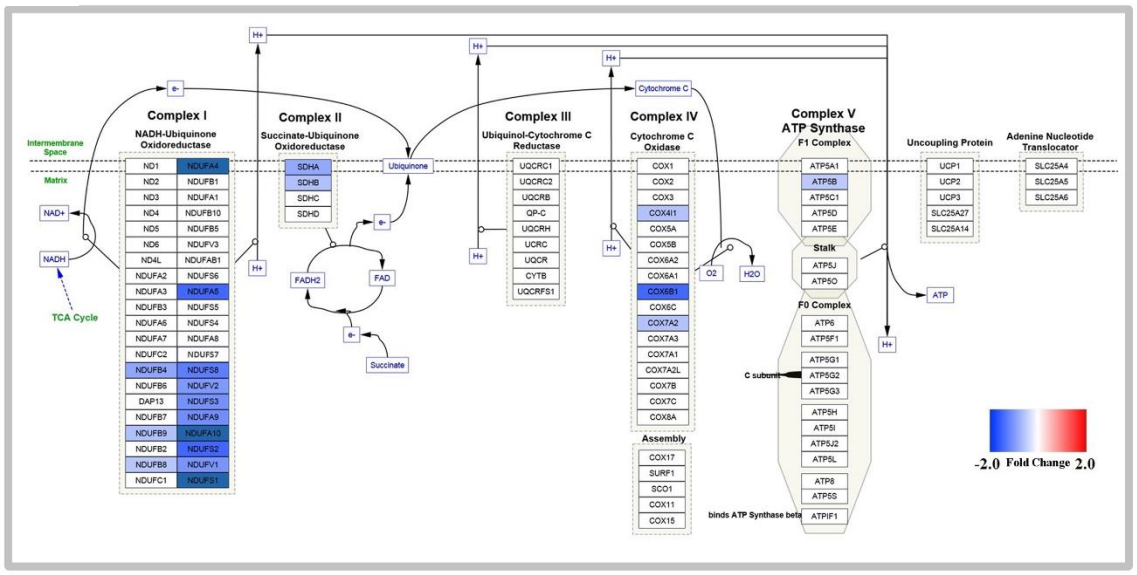

Figure 3.7 Identification of ETC proteins inhibited by L42 in MDA-MB-231 cells. A. Bar graph showing relative protein fold-change between treatment groups for the GO term "Oxidative Phosphorylation" from KEGG pathway analysis. **B.** Significantly changed (Supplementary Table 3.1C) proteins were uploaded onto Cytoscape software (v3.6.0) and matched to the Electron Transport Chain pathway using the WikiPathways app (v3.3.1), with degree of shading of matching proteins set as a measure of fold-change (see key).

3.4.7 L42 disrupts mitochondrial membrane potential in TNBC cells

A major role of the ETC is maintenance of the mitochondrial membrane potential [42], the loss of which disrupts the proton motive force required for ATP production, and is a well-known trigger for apoptosis [43]. Our proteomics data strongly indicated that L42 induces apoptosis in TNBC cells by restricting oxidative phosphorylation through ETC inhibition. To confirm this, we utilized a trimethylrhodamine, ethyl ester (TMRE)-based staining assay to assess the status of the mitochondrial membrane potential in L42-treated TNBC cells. As shown in Figure 3.7A, vehicle-treated MDA-MB-231 cells showed robust staining with TMRE indicating intact and viable mitochondria, while L42-treated cells displayed a significant 50 % reduction in TMRE staining (Figure 3.7B).

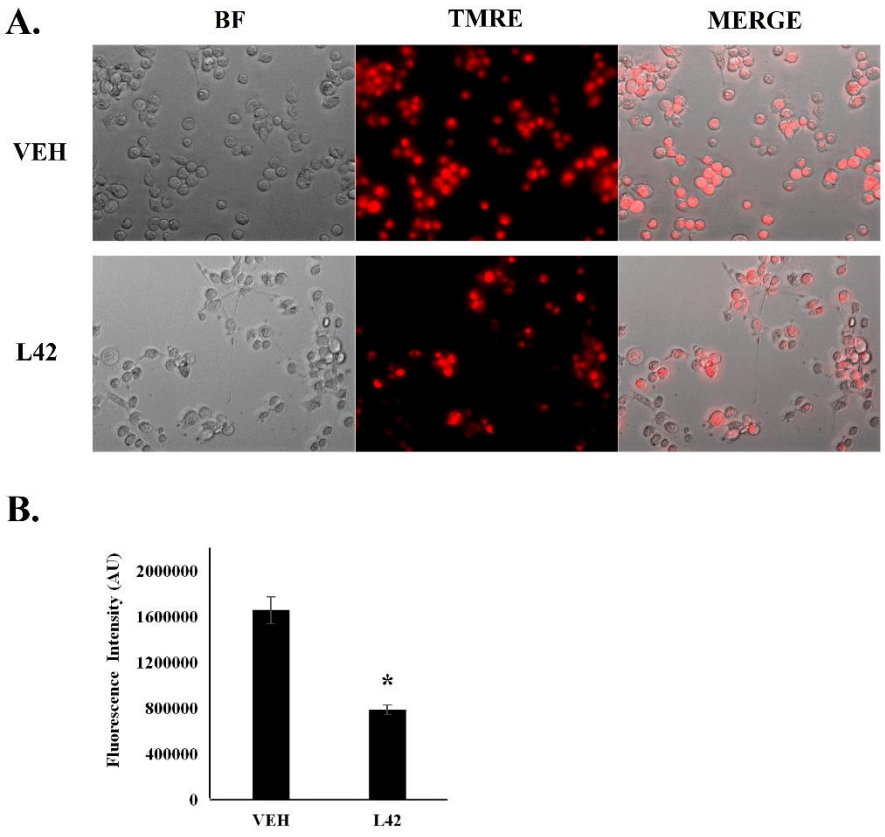

Figure 3.8 Assessment of mitochondrial membrane potential upon L42 treatment. A. MDA-MB-231 cells were treated with L42 (0.15 mg/ml) or vehicle for 8 h and stained using 200 nM TMRE. Samples were imaged using a Zeiss Axiovert 200m fluorescence microscope. **B.** Mitochondrial membrane potential was measured as the relative TMRE fluorescent staining intensity between L42 and Vehicle-treated cells, quantified using ImageJ. Statistical analysis was performed using an unpaired, two-tailed Mann-Whitney Test. A minimum of 250 cells were analyzed from a total of 4 replicates. *$p < 0.00001$.

3.5 Discussion

3.5.1 L42 inhibits survival and induces apoptosis in TNBC cells

Our study focused on elucidating the effects of an extract from the plant *Lippia origanoides*, on the proteome of MDA-MB-231 TNBC cells. TNBCs are a particularly aggressive, drug-resistant subtype of breast cancer with no known therapeutic targets. Our previous research revealed that a *Lippia* extract had significant cytostatic and apoptotic effects on TNBC cells with much reduced cytotoxicity against normal mammary cells [21].

We reasoned that, since TNBC cells are known to have an altered metabolic profile which includes heightened glycolysis and glutamine uptake, as well as generation of TCA cycle intermediates, it was possible that the extract suppressed such metabolism to selectively induce cell death in these cells. Through testing of extracts from other *L. origanoides* chemotypes, we identified the L42 extract, which demonstrated an even more potent dose-dependent cytotoxicity against TNBC cells while retaining a reduced effect on normal cells (Figure 3.1A). L42 induced rapid, sustained and irreversible loss of viability in MDA-MB-231 cells. L42 also inhibited Cyclin D1 (regulator of G0/G1 cell cycle phase transition [44]) protein levels and induced Caspase-8 (extrinsic apoptosis pathway marker [45]) activation (Figure 3.1B). These results shed light on the mechanism by which L42 reduced TNBC cell viability but were insufficient to explain its specificity. It was our intention to achieve a molecular understanding of the cancer cell selectivity of L42 through quantitative proteomics.

3.5.2 L42 inhibits mitochondrial function and metabolism in TNBC cells.

We utilized LFQ to study the effects of a complex mixture, L42, on the TNBC proteome landscape (Figure 3.2A). Data analysis revealed the LFQ data was remarkably reproducible, with highly consistent quantitation achieved across replicates from both treatment groups (Figure 3.2B). 2,407 proteins were quantified, with 519 proteins significantly changed quantitatively between L42- and control-treated groups. L42 was found to down-regulate proteins predominantly localized to various mitochondrial complexes and compartments (Figure 3.3). Also apparent was that L42 inhibited

expression of proteins involved in oxidoreductase, iron sulfur-binding, NADH dehydrogenase activity, and electron transport chain activity; all further indicative of its mitochondrial-specificity.

This comprehensive and rapid loss of mitochondrial proteins required for sustained cellular growth and proliferation could be expected to induce compensatory pathways to prolong survival. The observation that L42 treatment induced stress response, cell cycle, and DNA repair pathways is therefore not surprising (Figure 3.3B). However, these cellular responses were insufficient to significantly bolster viability, which continued to decrease up to 72 h post-treatment (Figure 3.1A). Together, these results led us to further examine the nature of L42's effects on mitochondrial metabolism.

3.5.3 L42 extensively inhibits the TCA Cycle in TNBC cells.

The TCA cycle (coupled to oxidative phosphorylation) provides a major alternative route of ATP production for cancer cells compared to the inefficient process of anaerobic glycolysis. TCA cycle intermediates are made readily available in TNBC cells by upregulation of fatty acid β-oxidation and amino acid uptake and degradation [16-20]. We found that L42 downregulated several enzymes involved in mitochondrial amino acid catabolism and fatty acid oxidation, effectively cutting off sources of acetyl CoA for the TCA cycle (Figure 3.4). It has recently been revealed that Glutaminase (GLS), an enzyme involved in the conversion of glutamine to glutamate (the rate-limiting step in glutamine utilization), is necessary for TNBC growth *in vitro* and *in vivo* [16]. In support of its actions on regulating TCA cycle substrate availability, we observed L42 reduced GLS levels, a result validated by Western Blotting (Figure 3.4C).

It is recognized that the rate-limiting enzyme of the TCA cycle is α-KGHDC, a complex consisting of oxoglutarate dehydrogenase (OGDH), dihydrolipoamide S-succinyltransferase (DLST), and dihydrolipoamide dehydrogenase (DLD) [46]. Both OGDH and DLST are implicated in cancer cell proliferation and survival, and targeting α-KGHDC has become an exciting prospect for metabolism-based cancer therapy [41]. L42 severely disrupted the TCA cycle by down-regulating almost every enzyme involved in the process, and reduced the expression of OGDC, DLST and DLD, (Figure 3.5). Together, these results provide conclusive evidence that L42 treatment impacts the TCA

cycle in TNBC cells, and strongly suggests the resulting depletion of ATP could contribute to the observed rapid apoptotic process.

3.5.4 L42 induces loss of NADH dehydrogenase (Complex I) expression

The electron transport chain (ETC) is critical for the generation of ATP via oxidative phosphorylation, and also maintains the mitochondrial membrane potential ($\Delta\Psi m$) via the transfer of protons across the membrane by Complex I and Complex IV (cytochrome c oxidase) [42]. The maintenance of $\Delta\Psi m$ is crucial for cellular integrity, and depolarization of the membrane potential is a known catalyst for apoptosis [43]. For these reasons, suppressing oxidative phosphorylation via electron transport chain (ETC) inhibition has shown promise in cancer therapy. Metformin and Phenformin, both small molecule Complex I inhibitors, were shown to reduce cell proliferation in HCT116 human colon cancer cells [47]. In addition, AG311, also a Complex I inhibitor, induced rapid ATP depletion, mitochondrial depolarization, and necrosis in breast cancer cell lines, and also retarded tumor growth and metastases in mouse models of breast cancer without exhibiting any obvious toxicity [48].

We studied the effects of L42 on the electron transport chain, the major source of ATP in the cell. L42 diminished expression of Complex I as well as Complex IV, down-regulating several of their core subunits (Figure 3.6). Together, these two complexes produce the proton gradient necessary for ATP production through ATP synthase, and their severe down-regulation by L42 leads to rapid energy depletion in the cell and subsequent apoptosis. In order to validate our proteomics data, we stained control- and L42-treated MDA-MB-231 cells with trimethylrhodamine, ethyl ester (TMRE). TMRE is a positively-charged fluorescent dye which readily stains active mitochondria via their negative charge that is maintained by the functioning ETC. Disruption of ETC activity leads to depolarization of the mitochondrial membrane and loss of TMRE staining. Indeed, L42-treated MDA-MB-231 cells showed significantly reduced TMRE staining, confirming impaired ETC function in these cells (Figure 3.7).

3.6 Summary

Our observation that L42 extensively downregulated mitochondrial proteins in TNBC cells is significant for a number of reasons. It is well known that mitochondria are the metabolic centers in cells, responsible for ATP production via oxidative phosphorylation (OXPHOS) through the electron transport chain (ETC), while also housing the TCA cycle as well as key enzymes involved in amino acid metabolism and fatty acid oxidation [49-52]. Recent studies have implicated dysregulated mitochondrial function as key to the acquisition of drug resistance in several forms of cancer; with targeting of mitochondrial metabolism emerging as a novel route to cancer therapy. For example, inhibiting mitochondrial protein synthesis and OXPHOS using tigecycline and imatinib was shown to eradicate tyrosine kinase inhibitor-resistant CML leukemic stem cells (CML LSCs) [53]. In addition, AraC (cytarabine, a nucleoside analogue)-resistant AML cells from patient-derived xenografts (PDX) were shown to have significantly higher OXPHOS signatures than AraC-sensitive cells, and targeting OXPHOS along with AraC treatment was shown to be an effective combinatorial treatment [54]. In a recent study on TNBC, Lee et al. discovered that targeting of MYC and myeloid-cell leukemia 1 (MCL1) protein, along with hypoxia-inducible factor 1α (HIF-1α), inhibited mitochondrial OXPHOS and drug resistance of cancer stem cells (CSCs) [55]. These studies strongly suggest that targeting the mitochondria may be an effective method of treating aggressive cancer and overcoming drug resistance [56].

Our study reveals suppression of TNBC metabolism to be a potentially powerful, and as-yet unexploited, therapeutic approach. We hypothesize that the combined inhibitory effects of L42 on TCA cycle enzymes, Acetyl CoA production, and OXPHOS via ETC Complex I inhibition could trigger a cellular famine, which also provides an explanation as to why L42 selectively affects MDA-MB-231 TNBC cells, which are known to be highly metabolically active, as compared to normal mammary epithelial MCF10A cells.

The difficulty of isolating bioactive components from complex mixtures and identifying their cellular targets has limited the utility of studies on naturally-derived extracts. Here, we show that the comprehensive landscape of information gleaned from

proteomics experiments both validates and advocates for the use of LFQ via LC-MS/MS in the discovery of new cancer drugs from complex mixtures, as well as sheds light on their mechanisms of action. The dose-dependent loss of cancer cell viability in response to L42-treatment is comparable to responses commonly seen with the use of single compounds. Our subsequent studies will focus on identifying the composition of L42, and describing its effects *in vivo*.

3.7 References

1. Mann, J. (2002). Natural Products in Cancer Chemotherapy, Past, Present and Future. Nature Reviews Cancer, 2, 143-148.
2. Chabner, B.A., & Roberts, T.G. (2005). Timeline - Chemotherapy and the War on Cancer. Nature Reviews Cancer, 5, 65-72.
3. Milajerdia, A., Djafarian, K., & Hosseinia, B. (2016). The toxicity of saffron (*Crocus sativus* L.) and its constituents against normal and cancer cells. Journal of Nutrition and Intermediary Metabolism, 3, 23-32.
4. Graidist, P., Martla, M., & Sukpondma, Y. (2015). Cytotoxic Activity of *Piper cubeba* Extract in Breast Cancer Cell Lines. Nutrients, 7, 2707-2718.
5. Konarikova, K., Jezovicova, M., Kerestes, J., Gbelcova, H., Durackova, Z., & Zitnanova, I. (2015). Anticancer Effect of Black Tea Extract in Human Cancer Cell Lines. Springerplus, 4, 4-127
6. Kingston, D.G.I. (2011). Modern Natural Products Drug Discovery and Its Relevance to Biodiversity Conservation. Journal of Natural Products, 74, 496-511.
7. Beutler, J.A. (2009). Natural Products as a Foundation for Drug Discovery. Current protocols in pharmacology. Current Protocol in Pharmacology, 46, 9.11.1–9.11.21
8. Macgregor, P.F., & Squire, J.A. (2002). Application of Microarrays to the Analysis of Gene Expression in Cancer. Clinical Chemistry, 48, 1170-1177.
9. Ghazalpour, A., Bennett, B., Petyuk, V.A., Orozco, L., Hagopian, R., Mungrue, I.N. et al. (2011). Comparative Analysis of Proteome and Transcriptome Variation in Mouse. PLoS Genetics, 7, e1001393.
10. Ghaemmaghami, S., Huh, W., Bower, K., Howson, R.W., Belle, A., Dephoure, N. et al. (2003). Global Analysis of Protein Expression in Yeast. Nature, 425, 737-741.

11. Tian, Q., Stepaniants, S.B., Mao, M., Weng, L., Feetham, M.C., Doyle, M.J. et al. (2004). Integrated Genomic and Proteomic Analyses of Gene Expression in Mammalian Cells. Molecular and Cellular Proteomics, 3, 960-969.
12. Warburg, O. (1956). Origin of Cancer Cells. Science, 123, 309-314.
13. Teicher, B.A., Linehan, W.M., & Helman, L.J. (2012). Targeting Cancer Metabolism. Clinical Cancer Research, 18, 5537-5545.
14. Shen, L.L., O'shea, J.M., Kaadige, M.R., Cunha, S., Wilde, B.R., Cohen, A.L. et al. (2015). Metabolic Reprogramming in Triple-Negative Breast Cancer through Myc Suppression of TXNIP. Proceedings of the National Academy of Sciences U.S.A., 112, 5425-5430.
15. Lim, S.O., Li, C.W., Xia, W.Y., Lee, H.H., Chang, S.S., Shen, J. et al. (2016). EGFR Signaling Enhances Aerobic Glycolysis in Triple-Negative Breast Cancer Cells to Promote Tumor Growth and Immune Escape. Cancer Research, 76, 1284-1296.
16. Lampa, M., Arlt, H., He, T., Ospina, B., Reeves, J., Zhang, B.L. et al. Glutaminase Is Essential for the Growth of Triple-Negative Breast Cancer Cells with a Deregulated Glutamine Metabolism Pathway and Its Suppression Synergizes with Mtor Inhibition. PLoS One. 2017, 12, e0185092
17. Goode, G., Gunda, V., Chaika, N.V., Purohit, V., Yu, F., Singh, P.K. Muc1 Facilitates Metabolomic Reprogramming in Triple-Negative Breast Cancer. PLoS One 2017, 12, e0176820
18. Van Geldermalsen, M., Wang, Q., Nagarajah, R., Marshall, A.D., Thoeng, A., Gao, D. et al. Asct2/Slc1a5 Controls Glutamine Uptake and Tumour Growth in Triple-Negative Basal-Like Breast Cancer. Oncogene. 2016, 35, 3201-3208.
19. Kanaan, Y.M., Sampey, B.P., Beyene, D., Esnakula, A.K., Naab, T.J., Ricks-Santi, L.J. et al. Metabolic Profile of Triple-Negative Breast Cancer in African-American Women Reveals Potential Biomarkers of Aggressive Disease. Cancer Genomics Proteomics. 2014, 11, 279-294.
20. Wright, H.J., Hou, J., Xu, B., Cortez, M., Potma, E.O., Tromberg, B.J., Razorenova, O.V. CDCP1 regulates lipid metabolism in TNBC. Proc. Natl. Acad. Sci. U.S.A. 2017, 8, 114 (32)

21. Raman, V., Fuentes-Lorenzo, J.L., Stashenko, E.E., Levy, M., Levy, M.M., Camarillo, I.G. *Lippia origanoides* Extract Induces Cell Cycle Arrest and Apoptosis and Suppresses Nf-Kappa B Signaling in Triple-Negative Breast Cancer Cells. Int. J. Oncol. 2017, 51, 1801-1808.
22. Aryal, U.K., McBride, Z., Chen, D., Xie, J., Szymanski, D.B. Analysis of protein complexes in *Arabidopsis* leaves using size exclusion chromatography and label-free protein correlation profiling. J. Proteomics. 2017, 166, 8-18.
23. Bantscheff, M., Schirle, M., Sweetman, G., Rick, J., Kuster, B. Quantitative Mass Spectrometry in Proteomics, A Critical Review. Anal. Bioanal. Chem. 2007, 389, 1017-1031.
24. Patel, V.J., Thalassinos, K., Slade, S.E., Connolly, J.B., Crombie, A., Murrell, J.C. et al. A Comparison of Labeling and Label-Free Mass Spectrometry-Based Proteomics Approaches. J. Proteome Res. 2009, 8, 3752-3759.
25. Michalski, A., Damoc, E., Hauschild, J.P., Lange, O., Wieghaus, A., Makarov, A. et al. Mass Spectrometry-Based Proteomics Using Q Exactive, a High-Performance Benchtop Quadrupole Orbitrap Mass Spectrometer. Mol. Cell. Proteomics. 2011, 10, M111.
26. Cox, J., Hein, M.Y., Luber, C.A., Paron, I., Nagaraj, N., Mann, M. MaxLFQ allows accurate proteome-wide label-free quantification by delayed normalization and maximal peptide ratio extraction. Mol. Cell. Proteomics. 2014, 13, 2513-26.
27. Stashenko, E.E., Martinez, J.R., Cala, M.P., Duran, D.C., Caballero, D. Chromatographic and Mass Spectrometric Characterization of Essential Oils and Extracts from *Lippia* (Verbenaceae) Aromatic Plants. J. Sep Sci. 2013, 36, 192-202.
28. Cox, J., Mann, M. Maxquant Enables High Peptide Identification Rates, Individualized P.P.B.-Range Mass Accuracies and Proteome-Wide Protein Quantification. Nat. Biotechnol. 2008, 26, 1367-1372.
29. Polpitiya, A.D., Qian, W.J., Jaitly, N., Petyuk, V.A., Adkins, J.N., Camp, D.G. 2nd, Anderson G.A., Smith, R.D. DAnTE, a statistical tool for quantitative analysis of -omics data. Bioinformatics. 2008, 24, 1556-8.

30. Babicki, S., Arndt, D., Marcu, A., Liang, Y., Grant, J.R., Maciejewski, A., Wishart, D.S. Heatmapper, web-enabled heat mapping for all. Nucleic Acids Res. 2016, 44, W147-W153.
31. Eden, E., Navon, R., Steinfeld, I., Lipson, D., Yakhini, Z. Gorilla, A Tool for Discovery and Visualization of Enriched Go Terms in Ranked Gene Lists. BMC Bioinformatics. 2009, 10, 48.
32. Eden, E., Lipson, D., Yogev, S., Yakhini, Z. Discovering Motifs in Ranked Lists of DNA Sequences. PLoS Comput. Biol. 2007, 3, 508-522.
33. Huang, D.W., Sherman, B.T., Lempicki, R.A. Systematic and Integrative Analysis of Large Gene Lists Using David Bioinformatics Resources. Nat. Protoc. 2009, 4, 44-57.
34. Huang, D.W., Sherman, B.T., Lempicki, R.A. Bioinformatics Enrichment Tools, Paths toward the Comprehensive Functional Analysis of Large Gene Lists. Nucleic Acids Res. 2009, 37, 1-13.
35. Jensen, L.J., Kuhn, M., Stark, M., Chaffron, S., Creevey, C., Muller, J. et al. String 8-a Global View on Proteins and Their Functional Interactions in 630 Organisms. Nucleic Acids Res. 2009, 37, D412-D416.
36. Slenter, D.N., Kutmon, M., Hanspers, K., Riutta, A., Windsor, J., Nunes, N. et al. Wikipathways, A Multifaceted Pathway Database Bridging Metabolomics to Other Omics Research. Nucleic Acids Res. 2018, 46, D661-D667.
37. Shannon, P., Markiel, A., Ozier, O., Baliga, N.S., Wang, J.T., Ramage, D. et al. Cytoscape, A Software Environment for Integrated Models of Biomolecular Interaction Networks. Genome Res. 2003, 13, 2498-2504.
38. Schneider, C.A., Rasband, W.S. & Eliceiri, K.W. (2012). NIH Image to ImageJ, 25 years of image analysis. Nature Methods, 9, 671-675.
39. Fan, J., Lin, R.T., Xia, S.Y., Chen, D., Elf, S.E., Liu, S.P. et al. Tetrameric Acetyl-Coa Acetyltransferase 1 Is Important for Tumor Growth. Mol. Cell. 2016, 64, 859-874.
40. Hardie, D.G., Pan, D.A. Regulation of Fatty Acid Synthesis and Oxidation by the Amp-Activated Protein Kinase. Biochem. Soc. Trans. 2002, 30, 1064-1070.
41. Anderson, N.M., Mucka, P., Kern, J.G., Feng, H. The emerging role and targetability of the TCA cycle in cancer metabolism. Protein Cell. 2017, 9, 216-237.

42. Mitchell, P. Coupling of Phosphorylation to Electron and Hydrogen Transfer by a Chemi-Osmotic type of Mechanism. Nature. 1961, 191,144–148
43. Ly, J.D., Grubb, D.R., Lawen, A. The Mitochondrial Membrane Potential (Delta Psi M) in Apoptosis, an Update. Apoptosis. 2003, 8, 115-128.
44. Baldin, V., Lukas, J., Marcote, M.J., Pagano, M., Draetta, G. Cyclin D1 Is a Nuclear-Protein Required for Cell-Cycle Progression in G(1). Genes Dev. 1993, 7, 812-821.
45. Muzio, M., Chinnaiyan, A.M., Kischkel, F.C., Orourke, K., Shevchenko, A., Ni, J. et al. Flice, a Novel Fadd-Homologous Ice/Ced-3-Like Protease, Is Recruited to the Cd95 (Fas/Apo-1) Death-Inducing Signaling Complex. Cell. 1996, 85, 817-827.
46. Lai, J.C.K., Cooper, A.J.L. Brain Alpha-Ketoglutarate Dehydrogenase Complex - Kinetic-Properties, Regional Distribution, and Effects of Inhibitors. J. Neurochem. 1986, 47, 1376-1386.
47. Wheaton, W.W., Weinberg, S.E., Hamanaka, R.B., Soberanes, S., Sullivan, L.B., Anso, E. et al. Metformin Inhibits Mitochondrial Complex I of Cancer Cells to Reduce Tumorigenesis. Elife. 2014, 3, e02242.
48. Bastian, A., Thorpe, J.E., Disch, B.C., Bailey-Downs, L.C., Gangjee, A., Devambatla, R.K.V. et al. A Small Molecule with Anticancer and Antimetastatic Activities Induces Rapid Mitochondrial-Associated Necrosis in Breast Cancer. J. Pharmacol. Exp. Ther. 2015, 353, 392-404.
49. Bertram, R., Pedersen, M.G., Luciani, D.S., Sherman, A. A Simplified Model for Mitochondrial ATP Production. J. Theor. Biol. 2006, 243, 575-586.
50. Nunes-Nesi, A., Araujo, W.L., Obata, T., Fernie, A.R. Regulation of the Mitochondrial Tricarboxylic Acid Cycle. Curr. Opinion Plant Biol. 2013, 16, 335-343.
51. Shah, Y.M., Lyssiotis, C.A. Mitochondrial Amino Acid Metabolism Provides Vulnerabilities in Mutant Kras-Driven Cancers. Gastroenterology. 2016, 151, 798-801.
52. Currie, E., Schulze, A., Zechner, R., Walther, T.C., Farese, R.V. Cellular Fatty Acid Metabolism and Cancer. Cell Metab. 2013, 18, 153-161.
53. Kuntz, E.M., Baquero, P., Michie, A.M., Dunn, K., Tardito, S., Holyoake, T.L. et al. Targeting Mitochondrial Oxidative Phosphorylation Eradicates Therapy-Resistant Chronic Myeloid Leukemia Stem Cells. Nat. Med. 2017, 23, 1234.

54. Farge, T., Saland, E., De Toni, F., Aroua, N., Hosseini, M., Perry, R. et al. Chemotherapy-Resistant Human Acute Myeloid Leukemia Cells Are Not Enriched for Leukemic Stem Cells but Require Oxidative Metabolism. Cancer Discov. 2017, 7, 716-735.
55. Lee, K.M., Giltnane, J.M., Balko, J.M., Schwarz, L.J., Guerrero-Zotano, A.L., Hutchinson, K.E. et al. Myc and Mcl1 Cooperatively Promote Chemotherapy-Resistant Breast Cancer Stem Cells Via Regulation of Mitochondrial Oxidative Phosphorylation. Cell Metab. 2017, 26, 633.
56. Bosc, C., Selak, M.A., Sarry, J.E. Resistance Is Futile, Targeting Mitochondrial Energetics and Metabolism to Overcome Drug Resistance in Cancer Treatment. Cell Metab. 2017, 26, 705-707.

CHAPTER 4. ANALYSIS OF COMPOSITION AND *IN VIVO* TOXICITY OF *LIPPIA* EXTRACTS

4.1 Abstract

Chapter 2 and Chapter 3 described our investigations into the *in vitro* effects and mechanisms of action of the *Lippia origanoides* chemotype-variant extracts LOE and L42. Here, we analyzed the composition of L42 via GC/MS to identify likely bioactive components that mediate its apoptotic effects on TNBC cells. L42 was found to contain 30 different components, with the major peaks identified as the oxygenated monoterpenes carvacrol and thymol. This is in contrast to LOE, which was previously shown by the Stashenko lab to contain the flavonoid pinocembrin as the major component. However, MDA-MB-231 cells treated with pinocembrin or carvacrol showed no significant difference in viability, indicating that minor components and/or synergistic effects potentiate the apoptotic effects of these extracts. In addition, *in vivo* toxicity assays showed no significant adverse effects in NSG mice treated with intra-peritoneal injections of L42. Collectively, these studies provide strong support for i) further exploring the individual and synergistic apoptotic effects of L42 components on TNBC cells, and ii) studying the ability of L42 to prevent tumor growth and progression *in vivo.*

4.2 Introduction

We have previously shown that *Lippia origanoides* extract LOE induced apoptosis in multiple TNBC cell lines accompanied by NF-κB inhibition and caspase-8 activation (*see Chapter 2*) [1]. Compositional analysis of the extract by the Fuentes lab revealed it to contain 16 components (Table 4.2), many of which have also been shown to inhibit NF-κB signaling and induce apoptosis in *in vitro* and *in vivo* models of cancer [2-13, 21-23]. Subsequently, we observed that an *L. origanoides* extract from a different chemotype, L42, showed even greater potency against TNBC cells *in vitro* (*see Chapter 3*) [14]. L42 treatment of TNBC cells induced significant loss of expression of mitochondrial enzymes necessary for cellular metabolism [14]. Similar to LOE, L42 also induced loss of RIP1, Cyclin D1 and cIAP2, and activated caspase-8, leading to rapid, irreversible cell death

(Figure 4.1). We hypothesized that the similar downstream molecular effects of the extracts on TNBC cells would be consistent with a conservation of composition across the two chemotypes. Accordingly, we performed GC/MS analysis of L42 to compare its components with those from LOE (Table 4.1), and were able to identify 30 compounds present in the extract. While several of these compounds were shared with LOE, including thymol, carvacrol, caryophyllene, and humulene, L42 also contained multiple unique compounds, many of which have not been studied in the context of cancer.

Major components identified in LOE and L42 have been previously shown to possess anti-cancer effects. The flavonoid pinocembrin makes up ~ 55 % of LOE, and as mentioned in Chapter 2, was observed to inhibit epithelial-mesenchymal and transition and reduce cell viability in Y-79 retinoblastoma cells [7]. Pinocembrin also induced apoptosis in HCT-116 colon cancer cells by triggering the loss of mitochondrial membrane potential accompanied by caspase-3/-9 activation and cytochrome c release [11]. The oxygenated monoterpene carvacrol, found in significant quantities in both L42 and LOE, has also shown inhibitory effects on NF-κB signaling and induced apoptosis in multiple cancer cell lines [2-6]. We therefore investigated the effects of these components on MDA-MB-231 cell viability.

Investigations into plant-derived extracts as a source of cancer therapeutics are supported by a number of studies observing them to be non-toxic to normal cells as well as *in vivo* [15-17]. To serve as a foundation for future studies investigating the benefits of L42 for prevention of cancer initiation and progression, we performed toxicity tests of L42 in the C57BL/6 mouse model, with no adverse reactions recorded over the period of observation.

Taken together, our results provide a detailed composition of L42, and suggest that its apoptotic effects are modulated by minor components or require multiple components working synergistically. We also validate the safety of L42 for use as a treatment in future studies of TNBC *in vivo*.

4.3 Materials and Methods

4.3.1 Plant material and extract

Lippia origanoides plants were collected from the Chicamocha River Canyon (Los Santos, Santander, Colombia). Taxonomic identification of *L. origanoides* was performed by Dr. José Luis Fernández Alonso (National University, Bogotá, Colombia). Fresh leaves and stems from *L. origanoides* specimens (LOE: COL560259; L42: COL560267) were used for extraction as previously described [18]. Briefly, 200 g of finely ground *L. origanoides* plant material was placed in the extraction chamber of a Thar SFE-2000-2-FMC50 (Thar Instruments, PA, USA) and subjected to supercritical CO_2 extraction at 50 MPa and 333 K at the Universidad Industrial de Santander, Bucaramanga, Colombia. The material deposited on the walls of the chamber was collected, and 250 mg of this extracted material was dissolved in 5 ml of methanol, sonicated for 15 min, and centrifuged at 10,000 rpm for a further 15 min. The 50 mg/ml stock solutions of the supernatants collected from each specimen (LOE: COL560259; L42: COL560267) were used in the present study.

4.3.2 GC/MS analysis of *L. origanoides* extracts

20 µl of L42 stock solution was dried in a speedvac (Labconco, MO, USA) for 30 min. The dried pellet was resuspended in 40 uL methoxyamination reagent (10 mg/ml methoxyamine HCl in anhydrous pyridine, prepared daily), then incubated at 37°C for 90 min. A second sample prepared as above was derivatized by trimethylsilylation by incubating with 70 µl N-Methyl-N-(trimethylsilyl) trifluoroacetamide (MSTFA) for 30 min at 37°C.

GC/MS/MS analyses of both derivatized and non-derivatized samples were performed at the Metabolite Profiling Facility (MPF), Purdue University, using a Thermo TSQ 8000 triple quadrupole mass spectrometer coupled to a Thermo Trace 1310 GC. Data acquisition and analysis was performed using the Chromeleon software tool, and peaks were identified via spectral matching to the NIST compound library.

4.3.3 MTT cell viability assay

MDA-MB-231 cells were seeded at 10^5 cells/well in 96-well plates and allowed to attach overnight. Spent media was then replaced with fresh media containing carvacrol (Sigma-Aldrich, MO, USA) dosages between 60 - 85 μM. Media in control wells was replaced with fresh media without additives (No-treatment, NT) or media containing the vehicle, methanol (Veh). Following 24 h treatment, 12 mM of MTT, 3-(4,5-dimethylthiazol-2-yl)-2,5-diphenyltetrazolium bromide (Life Technologies, NY), was added to the cells followed by incubation for 4 h at 37°C. Formazan crystals formed at the end of incubation period were dissolved using dimethyl sulfoxide (DMSO) and plates were read at 570 nm with a reference wavelength of 630 nm.

4.3.4 *In vivo* toxicity study

Female virgin C57BL/6 mice were acquired from the Purdue Biological Evaluation Facility and housed at the Purdue Animal Housing Facility. Animals were provided rat chow and water *ad libitum*. At Day 0, mice (n = 3 per treatment group) were intraperitoneally injected with a single 200 μl dose of control (20% v/v methanol/1X PBS), or 100 mg/kg BW L42 (high dose), or 50 mg/kg BW L42 (medium dose), or 25 mg/kg BW L42 (low dose). In order to keep dosage volumes consistent within treatment groups, mice with similar weights were grouped together. Animals were periodically monitored for changes in body weight and adverse reactions over the course of 2 weeks, at the end of which all animals were sacrificed via isoflurane anesthesia followed by cervical dislocation. All experimental procedures were conducted under Purdue Animal Care and Use Committee (PACUC) ethical regulations.

4.3.5 Histological analysis of mouse mammary gland

Left inguinal mammary glands were removed from mice post-sacrifice, and fixed in 10 % formalin for 48 h prior to being transferred to the Purdue Histology Research Laboratory. Tissues were placed in a Sakura Tissue-VIP6 tissue processor for dehydration through graded ethanol solutions. Next, dehydrated tissues were cleared in xylene and paraffin-fixed using Leica Paraffin Plus. 4 μm microsections were taken using a Themo Shandon Finesse Me microtome, and the sections were then mounted on charged slides and dried

for 1 h at 60°C in an oven. Slides were then placed on a Leica ST5010-CV5030 autostainer, deparaffinized in 3 changes of xylene and rehydrated using graded ethanols to water. Slides were then stained using Gill's II hematoxylin, blued, and eosin/phloxine B mixture. Finally, slides were dehydrated, cleared in xylene and coverslipped in a toluene-based mounting media. Slides were imaged at 10X and 40X magnification using a DSC-F717 camera (Carl-Zeiss) attached to an inverted brightfield microscope (VWR International). The author acknowledges the assistance of the Purdue University Histology Research Laboratory, a core facility of the NIH-funded Indiana Clinical and Translational Science Institute

4.4 Results

4.4.1 GC/MS reveals compositional differences in L42 and LOE

In order to understand if the increased potency exhibited by L42 over LOE on MDA-MB-231 TNBC cell viability was due to compositional differences between the two extracts, we performed GC/MS analysis of L42. Figure 4.1. shows the GC/MS spectra of L42, with Table 4.1 describing the composition of L42 identified by matching the spectra to the NIST compound library. Compared to the composition of LOE, which has 15 identified components (Table 4.2, taken with permission from Castellanos et al. [17]), L42 is a more complex extract, with 32 components. However, 7 components (ρ-cymene, D-limonene, γ-terpinene, thymol, carvacrol, trans-β-caryophyllene, and α-humulene) are shared between the two extracts (*components highlighted in red*, Table 4.1 and Table 4.2).

4.4.2 Major components of LOE and L42 do not induce loss of viability in TNBC cells.

GC/MS analysis by Castellanos et al. revealed that the flavanone pinocembrin makes up 54.9 % of LOE [19]. In addition, analysis of L42 at the MPF revealed carvacrol to be the major component of this extract, followed by ρ-cymene and thymol. We tested the major component of each of these extracts for their effects on MDA-MB-231 cell viability. Interestingly, while no significant effect on viability was observed for carvacrol (Figure

4.2), pinocembrin appeared to significantly *increase* the viability of these cells (*not shown*).

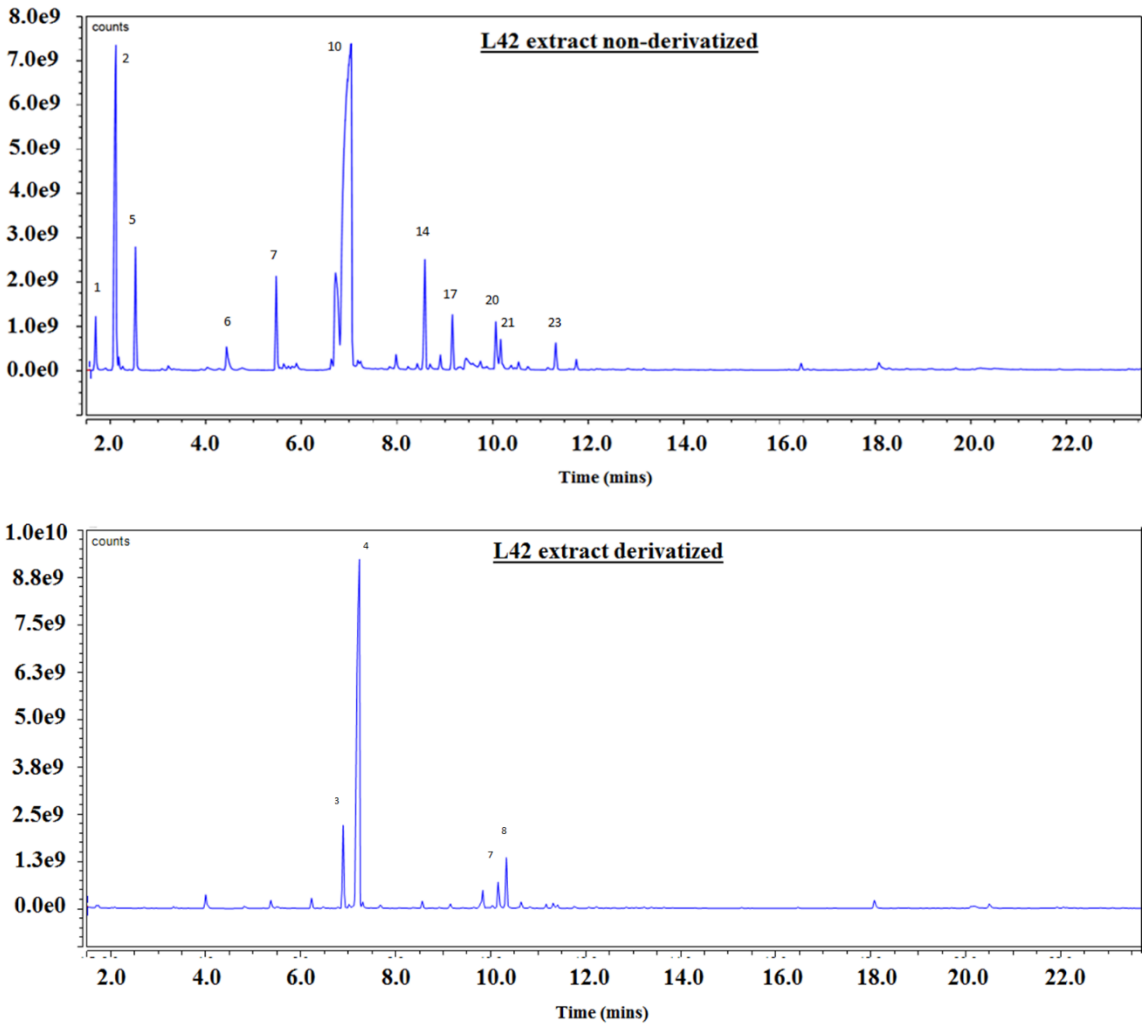

Figure 4.1 GC/MS spectra of L42. *(upper panel)* Spectra of L42 run without TMS derivatization using N-Methyl-N-(trimethylsilyl) trifluoroacetamide (MSTFA). *(lower panel)* Spectra of L42 run after derivatization using MSTFA. Numbers on major peaks indicate component identified in Table 4.1

Table 4.1 Composition of L42. Peaks from GC/MS spectra of non-derivatized and derivatized L42 (Figure 4.1) were searched against the NIST compound library based on retention times, and the respective components were identified. Components in red are shared between L42 and LOE (See Table 4.2).

Peak No.	Non-derivatized	Peak No.	Derivatized
1	ß-Myrcene	1	Boric acid, 3TMS derivative
2	**ρ-Cymene**	2	5-Hydroxy-5-methyl-2-phenyl-3-isoxazolidinone ditms pk1
3	**D-Limonene**	3	**Thymol, TMS derivative**
4	Eucalyptol	4	**Carvacrol, TMS derivative**
5	**γ-Terpinene**	5	**trans-β-Caryophyllene**
6	3-Cyclohexen-1-ol, 4-methyl-1-(1-methylethyl)-, (R)-	6	**α-Humulene**
7	Benzene, 2-methoxy-4-methyl-1-(1-methylethyl)-	7	(2-(tert-Butyl)-4-methoxyphenoxy)-TMS
8	Benzene, 1-methoxy-4-methyl-2-(1-methylethyl)-	8	tert-Butylhydroquinone, 2TMS derivative
9	Thymoquinone	9	Caryophyllene oxide
10	**Thymol**	10	4-tert-Butylcatechol, 2TMS derivative
11	1,3-Dioxolane, 2,2-dimethyl-4,5-di-1-propenyl-	11	Palmitic Acid, TMS derivative
12	Phenol, 2-methyl-5-(1-methylethyl)-, acetate	12	Stearic acid, TMS derivative
13	1H-3a,7-Methanoazulene, 2,3,4,7,8,8a-hexahydro-3,6,8,8-tetramethyl-, [3R-(3a,3aß,7ß,8aa)]-		
14	**trans-β-Caryophyllene**		
15	Cubenene		
16	cis-a-Bergamotene		
17	**α-Humulene**		
18	p-Cymene-2,5-diol		
19	Benzene, 1-(1,5-dimethyl-4-hexenyl)-4-methyl-		
20	Phenol, 3-(1,1-dimethylethyl)-4-methoxy-		
21	1H-Benzocycloheptene, 2,4a,5,6,7,8,9,9a-octahydro-3,5,5-trimethyl-9-methylene-, (4aS-cis)-		
22	Naphthalene, 1,2,3,4-tetrahydro-1,6-dimethyl-4-(1-methylethyl)-, (1S-cis)-		
23	Caryophyllene oxide		
24	(1R,3E,7E,11R)-1,5,5,8-Tetramethyl-12-oxabicyclo[9.1.0]dodeca-3,7-diene		
25	Naphthalene, 1,2,3,4,4a,5,6,7-octahydro-4a-methyl-		
26	Palmitic Acid, TMS derivative		

Table 4.2 Composition of LOE. Peaks from GC/MS spectra of non-derivatized LOE. Components in red are shared between L42 and LOE (See Table 4.1). (*Taken with permission from Castellanos et. al [17]*)

Peak No.	LOE composition (non-derivatized)
1	α-Phellandrene
2	**ρ-Cymene**
3	**Limonene**
4	β-Phellandrene
5	1,8-Cineole
6	**γ-Terpinene**
7	Borneol
8	**Thymol**
9	**Carvacrol**
10	α-Copaene
11	**trans-β-caryophyllene**
12	**α-Humulene**
13	γ-Muurolene
14	δ-Cadinene
15	Pinocembrin

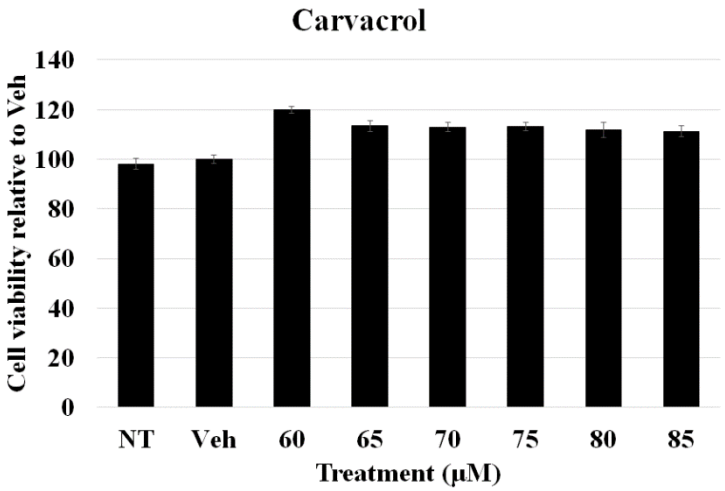

Figure 4.2. Effect of carvacrol on TNBC cell viability. MDA-MB-231 cells were treated with 60 – 85 μM carvacrol for 24 h, then tested for viability using the MTT assay. Plot shows viability relative to vehicle (methanol)-treated cells.

4.4.3 L42 is well-tolerated *in vivo* upon IP administration

As a precursor to future experiments testing the effects of L42 on preventing tumorigenesis and inhibiting tumor growth *in vivo*, we performed a Maximum Tolerated Dose (MTD) study using high (100 mg/kg BW), medium (50 mg/kg BW), and low (25 mg/kg BW) of L42 intraperitoneally injected into female C57BL/6 mice. This strain of mice was chosen due to possession of an intact immune system, which allowed for observation of any immune reactions to components, toxins, or pathogens that may have been present in the extract.

Immediately after injection, mice from 'high' and 'medium' dosage groups exhibited slightly unsteady gait and dragging of the hind limb. However, these mice quickly recovered 30 min post-injection, and mice from all groups remained bright, alert, and responsive (BAR) throughout the duration of the study period (Table 4.3).

Mice were also monitored for changes in body weight during the 2-week observational period following IP injection. As can be seen from Figure 4.3, mice from all treatment groups exhibited no significant change in body weight during this time, confirming that L42 is well-tolerated among mice with intact immune systems.

Table 4.3 L42 does not induce adverse effects in C57BL/6 mice. Female virgin C57BL/6 mice were intraperitoneally injected with L42 at 100 mg/kg BW (High dose), or 50 mg/kg BW (Medium dose), or 25 mg/kg BW (Low dose) or Control, and monitored for adverse effects over the course of 2 weeks. BAR: Bright, alert, and responsive. *Mouse number reflects ID number assigned to mouse at the start of experiment; numbers are not sequential because mice were grouped based on body weight, not assigned number.*

	9/11/2018						9/12/2018	9/13/2018	9/14/2018	9/17/2018	9/19/2018	9/21/2018	9/25/2018
	20 min	30 min	1 hr (11:25)	2 hr (12:25	3 hr (1:25)	7h (5:25)							
CTRL													
mouse number	comments	comments	comments	comments	comments	comments	comments	comments	comments	comments	comments	comments	comments
1	BAR	BAR	BAR	BAR	BAR	BAR	BAR	BAR	BAR	BAR	BAR	BAR	BAR
3	BAR	BAR	BAR	BAR	BAR	BAR	BAR	BAR	BAR	BAR	BAR	BAR	BAR
4	BAR	BAR	BAR	BAR	BAR	BAR	BAR	BAR	BAR	BAR	BAR	BAR	BAR
HIGH													
2	unsteady gait, dragging back legs	active when stimulated	BAR	BAR	BAR	BAR	BAR	BAR	BAR	BAR	BAR	BAR	BAR
5	resting	resting	BAR	BAR	BAR	BAR	BAR	BAR	BAR	BAR	BAR	BAR	BAR
6	unsteady gait, dragging back legs	active when stimulated	BAR	BAR	BAR	BAR	BAR	BAR	BAR	BAR	BAR	BAR	BAR
MED													
7	active when stimulated	BAR	BAR	BAR	BAR	BAR	BAR	BAR	BAR	BAR	BAR	BAR	BAR
8	resting	resting	BAR	BAR	BAR	BAR	BAR	BAR	BAR	BAR	BAR	BAR	BAR
9	active when stimulated	BAR	BAR	BAR	BAR	BAR	BAR	BAR	BAR	BAR	BAR	BAR	BAR
LOW													
10	BAR	BAR	BAR	BAR	BAR	BAR	BAR	BAR	BAR	BAR	BAR	BAR	BAR
11	BAR	BAR	BAR	BAR	BAR	BAR	BAR	BAR	BAR	BAR	BAR	BAR	BAR
12	BAR	BAR	BAR	BAR	BAR	BAR	BAR	BAR	BAR	BAR	BAR	BAR	BAR

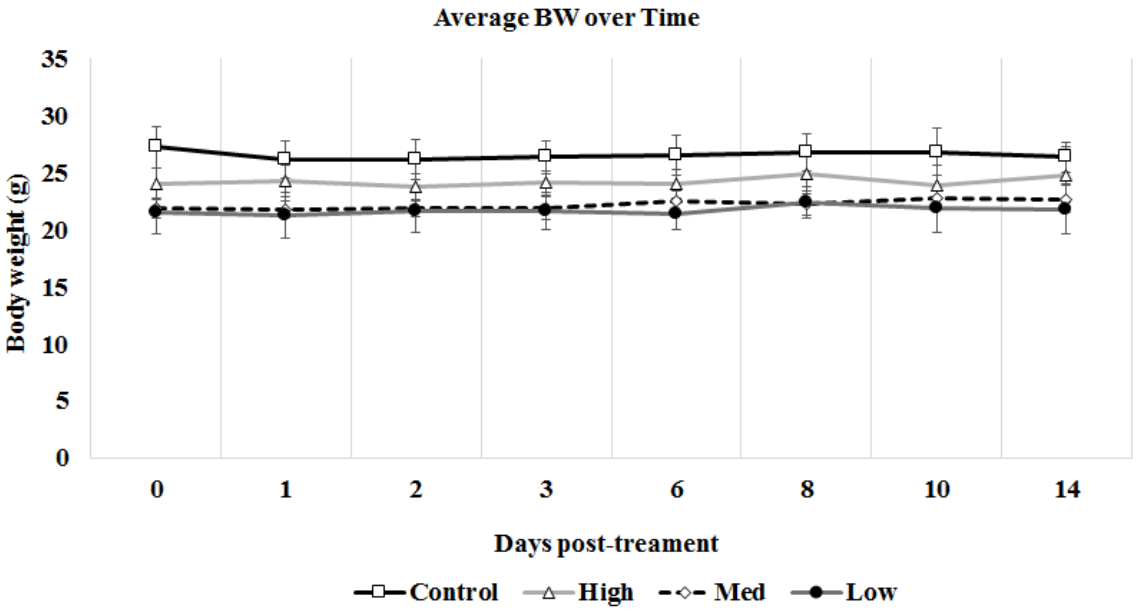

Figure 4.3 C57BL/6 mice do not exhibit weight loss upon L42 administration. Female virgin C57BL/6 mice were intraperitoneally injected with L42 at 100 mg/kg BW (High dose), or 50 mg/kg BW (Medium dose), or 25 mg/kg BW (Low dose) or Control, and weighed at indicated days post-treatment over the course of 2 weeks.

4.4.4 IP injection of L42 is non-toxic to mouse mammary glands

In order to identify any potential adverse effects that L42 may have on the mammary gland, the left inguinal mammary glands were isolated from C57BL/6 mice 2 weeks post-IP injection of L42. H&E staining of mammary gland sections from control-treated and L42-treated mice showed no significant pathological differences (Figure 4.4, *left*). Specifically, the lactiferous ducts were intact, and surrounded by adipocytes of uniform size with peripheral nuclei, and there were no visible signs of an immune response such as the infiltration of polymorphonuclear neutrophils (PMNs), a common characteristic of inflammation [20]. A closer examination of the lactiferous ducts also revealed no differences in ductal morphology (Figure 4.4, *right*). Ducts from both groups showed a single layer of polarized luminal epithelial cells lining the ductal lumen, with a thin stromal layer forming the basement membrane. Mammary glands from both groups were also free of necrotic cells and damage to lymph nodes (*not shown*).

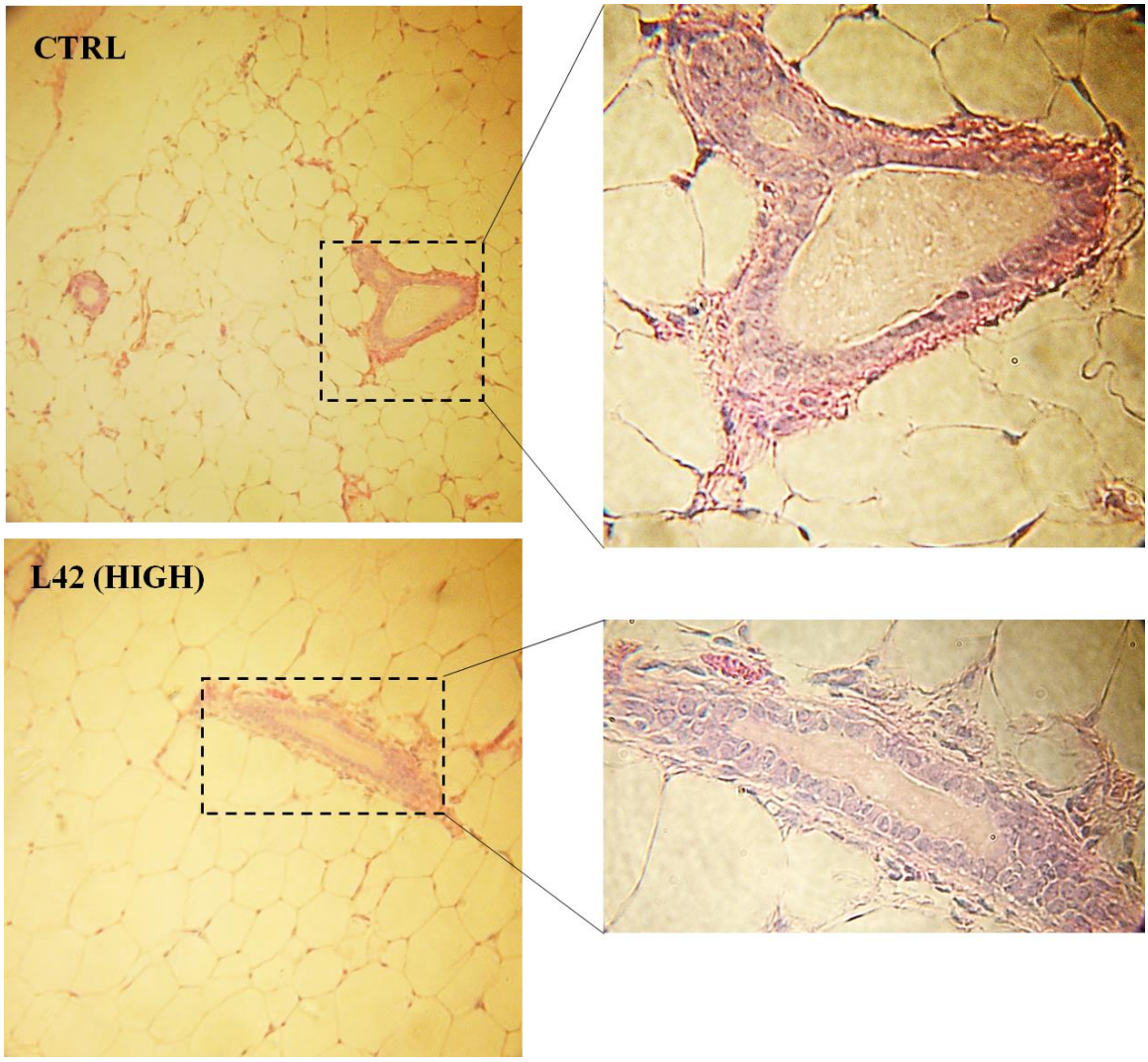

Figure 4.4 Mammary glands from C57BL/6 mice do not show pathological differences upon L42 administration. Mammary glands from control- and L42-treated mice were fixed and H&E stained. (*Left*) Representative mammary glands from control (CTRL)- and L42 (100 mg/kg BW, HIGH dose)-treated mice showing intact lactiferous glands (boxed), adipocytes with peripheral nuclei, and no sign of inflammation. (*Right*) Magnified lactiferous glands showing normal phenotype from both groups, i.e. a single layer of luminal epithelial cells attached to a stroma-rich basement membrane, surrounding the ductal lumen.

4.5 Summary

In Chapter 2 and 3, the *Lippia origanoides* extracts LOE and L42 were shown to exert potent apoptotic effects against TNBC cells, with reduced effects on normal mammary epithelial cells *in vitro*. Our investigations shed light on their mechanisms of action. Both LOE and L42 significantly reduced RIP1 levels and induced caspase-8 activation, which support the inhibition of NFκB signaling as a common apoptotic mechanism of the extracts. However, L42 also showed significant inhibitory effects on mitochondrial metabolism, and showed greater potency against MDA-MB-231 TNBC cells than LOE. In order to understand the reasons behind the similarities and differences in the effects of LOE and L42, the composition of L42 was analyzed by GC/MS, and compared to that of LOE (previously revealed by Castellanos et al. [19]).

As can be seen from Table 4.1 and 4.2, LOE and L42 share multiple major components including carvacrol, thymol, α-humulene, trans-β-caryophyllene, and ρ-cymene; all of which have been shown to block NFκB signaling in previous studies [2, 13, 21-23]. However, L42 was shown to contain twice the number of components as LOE, with 32 identified in total. It cannot be ruled out that the added potency of L42 against TNBC cells is due to synergism between components not found in LOE.

The major components of LOE and L42 were the flavanone pinocembrin, and the monoterpene carvacrol, respectively. MDA-MB-231 TNBC cells were treated with these components individually, to determine if they were sufficient for the apoptotic effects exhibited by the extracts. As can be seen from Figure 4.2, carvacrol had no effect on MDA-MB-231 viability, while surprisingly, pinocembrin *increased* cell viability (*not shown*), possibly by stimulating proliferation or cellular oxidoreductase activity (as the MTT assay measures oxidoreductase activity to assess viability). These results point to synergism between *Lippia* components as a requirement for apoptosis induction in TNBC cells. Further experiments using individual *L. origanoides* components alone or in combinations, as well as bioassay-driven fractionation methods, may be required to isolate the bioactive components (BACs) from these extracts. Also, in collaboration with the Purdue Proteomics Facility and Metabolomics Profiling Facility, we are also developing LC/MS and GC/MS-based tools to identify BACs and their cellular protein

binding partners, thereby improving on existing techniques while reducing the time requirements.

Our studies have revealed that *L. origanoides* extracts are capable of inhibiting NFκB signaling, an inflammatory pathway often constitutively activated in TNBC [1, 24, 25], while also targeting mitochondrial metabolism, a major source of ATP for proliferating cancer cells [26-28]. These extracts as a whole may have multiple health benefits including anti-inflammation, anti-tumorigenic, and anti-tumor progression effects *in vivo*. To serve as a foundation to such future studies, we performed a Maximum Tolerated Dose study of L42 to assess its toxicity in the C57BL/6 mouse model. These mice showed no significant adverse effects upon IP administration of up to 100 mg/kg BW L42 (Figure 4.3), and mammary glands from L42-treated and control group mice showed no histopathological differences (Figure 4.4), indicating that L42 is non-toxic *in vivo* and can be safely used at high dosages in future studies.

Taken together, these results provide a compositional basis for the similarities and differences seen in the effects of LOE and L42, while also indicating that the apoptotic effects of these extracts on TNBC cells may be due to multi-component action. Finally, our MTD study supports the safe use of L42 in future *in vivo* research investigating its ability to prevent TNBC initiation and progression.

4.6 References

1. Raman, V., Lorenzo, J. L. F., Stashenko, E. E., Levy, M., Levy, M. M., & Camarillo, I. G. (2017). *Lippia origanoides* extract induces cell cycle arrest and apoptosis and suppresses NF-κB signaling in triple-negative breast cancer cells. International Journal of Oncology, 51(6), 1801–1808.
2. Aristatile, B., Al-Assaf, A. H., & Pugalendi, K. V. (2013). Carvacrol suppresses the expression of inflammatory marker genes in D-galactosamine-hepatotoxic rats. Asian Pacific Journal of Tropical Medicine, 6(3), 205–211.
3. Arunasree, K. M. (2010). Anti-proliferative effects of carvacrol on a human metastatic breast cancer cell line, MDA-MB 231. Phytomedicine, 17(8), 581–588.

4. Dai, W., Sun, C., Huang, S., & Zhou, Q. (2016). Carvacrol suppresses proliferation and invasion in human oral squamous cell carcinoma. OncoTargets and Therapy, 9, 2297–2304.
5. Fan, K., Li, X., Cao, Y., Qi, H., Li, L., Zhang, Q., & Sun, H. (2015). Carvacrol inhibits proliferation and induces apoptosis in human colon cancer cells. Anti-Cancer Drugs, 26(8), 813–823.
6. Kang, S.-H., Kim, Y.-S., Kim, E.-K., Hwang, J.-W., Jeong, J.-H., Dong, X., et al. (2016). Anticancer Effect of Thymol on AGS Human Gastric Carcinoma Cells. Journal of Microbiology and Biotechnology, 26(1), 28–37.
7. Chen, K.S., Shi, M.D., Chien, C.S., & Shih, Y.W. (2014). Pinocembrin suppresses TGF-betta1-induced epithelial-mesenchymal transition and metastasis of human Y-79 retinoblastoma cells through inactivating alphavbetta3 integrin/FAK/p38alpha signaling pathway. Cell Biosciences, 4, 41.
8. Legault, J., & Pichette, A. (2007). Potentiating effect of beta-caryophyllene on anticancer activity of alpha-humulene, isocaryophyllene and paclitaxel. The Journal of Pharmacy and Pharmacology, 59(12), 1643–1647.
9. Li, Y., Wen, J., Du, C., Hu, S., Chen, J., Zhang, S., et al. (2017). Thymol inhibits bladder cancer cell proliferation via inducing cell cycle arrest and apoptosis. Biochemical and Biophysical Research Communications, 491(2), 530–536.
10. Ahmad, A., Banerjee, S., Wang, Z., Kong, D., & Sarkar, F.H. (2008). Plumbagin-induced apoptosis of human breast cancer cells is mediated by inactivation of NF-kappaB and Bcl-2. Journal of Cellular Biochemistry, 105, 1461-1471.
11. Kumar, M. A. S., Nair, M., Hema, P. S., Mohan, J., & Santhoshkumar, T. R. (2007). Pinocembrin triggers Bax-dependent mitochondrial apoptosis in colon cancer cells. Molecular Carcinogenesis, 46(3), 231–241.
12. Jin, M.L., Park, S.Y., Kim, Y.H., Park, G., & Lee, S. (2014) Halofuginone induces the apoptosis of breast cancer cells and inhibits migration via downregulation of matrix metalloproteinase-9. International Journal of Oncology, 44, 309-318.
13. Liang, D., Li, F., Fu, Y., Cao, Y., Song, X., Wang, T., et al. (2014). Thymol inhibits LPS-stimulated inflammatory response via down-regulation of NF-κB and MAPK signaling pathways in mouse mammary epithelial cells. Inflammation, 37(1), 214–222.

14. Raman, V., Aryal, U. K., Hedrick, V., Ferreira, R. M., Fuentes Lorenzo, J. L., Stashenko, E. E., et al. (2018). Proteomic Analysis Reveals That an Extract of the Plant *Lippia origanoides* Suppresses Mitochondrial Metabolism in Triple-Negative Breast Cancer Cells. Journal of Proteome Research, 17(10), 3370–3383.
15. Milajerdia, A., Djafarian, K., & Hosseinia, B. (2016). The toxicity of saffron (*Crocus sativus L*.) and its constituents against normal and cancer cells. Journal of Nutrition and Intermediary Metabolism, 3, 23-32.
16. Graidist, P., Martla, M., & Sukpondma, Y. (2015). Cytotoxic Activity of *Piper cubeba* Extract in Breast Cancer Cell Lines. Nutrients, 7, 2707-2718.
17. Konarikova, K., Jezovicova, M., Kerestes, J., Gbelcova, H., Durackova, Z., & Zitnanova, I. (2015). Anticancer Effect of Black Tea Extract in Human Cancer Cell Lines. Springerplus, 4, 4-127
18. Stashenko, E.E., Martínez, J.R., Cala, M.P., Durán, D.C., & Caballero, D. (2013). Chromatographic and mass spectrometric characterization of essential oils and extracts from *Lippia* (Verbenaceae) aromatic plants. Journal of Separation Science, 36, 192-202.
19. Castellanos, N.R., Castro, C.E., Stashenko, E.E., & Fuentes, J. *Lippia origanoides* supercritical fluid extract and its major constituent pinocembrin diminish ultraviolet radiation-induced DNA damage and modulate cell division in *Escherichia coli.* (In review)
20. Camperio, C., Armas, F., Biasibetti, E., Frassanito, P., Giovannelli, C., Spuria, L., et al. (2017). A mouse mastitis model to study the effects of the intramammary infusion of a food-grade Lactococcus lactis strain. PLOS ONE, 12(9), e0184218.
21. Xie, G., Chen, N., Soromou, L. W., Liu, F., Xiong, Y., Wu, Q., et al. (2012). p-Cymene protects mice against lipopolysaccharide-induced acute lung injury by inhibiting inflammatory cell activation. Molecules (Basel, Switzerland), 17(7), 8159–8173.
22. Lee, J.C., Kundu, J.K., Hwang, D.M., Na, H.K., & Surh, Y.J. (2007). Humulene inhibits phorbol ester-induced COX-2 expression in mouse skin by blocking activation of NF-kappaB and AP-1, IkappaB kinase and c-Jun-N-terminal kinase as respective potential upstream targets. Carcinogenesis, 28(7),1491-8.

23. Kim, C., Cho, S.K., Kim, K.D., Nam, D., Chung, W.S., Jang, H.J., et al. (2014). β-Caryophyllene oxide potentiates TNFα-induced apoptosis and inhibits invasion through down-modulation of NF-κB-regulated gene products. Apoptosis 19(4),708-18.
24. Nakshatri, H., Bhat-Nakshatri, P., Martin, D. A., Goulet, R. J., & Sledge, G. W. (1997). Constitutive activation of NF-kappaB during progression of breast cancer to hormone-independent growth. Molecular and Cellular Biology, 17(7), 3629–3639.
25. Sero, J. E., Sailem, H. Z., Ardy, R. C., Almuttaqi, H., Zhang, T., & Bakal, C. (2015). Cell shape and the microenvironment regulate nuclear translocation of NF-κB in breast epithelial and tumor cells. Molecular Systems Biology, 11(3), 790.
26. Vyas, S., Zaganjor, E., & Haigis, M. C. (2016). Mitochondria and Cancer. Cell, 166(3), 555-566.
27. Ashton, T. M., McKenna, W. G., Kunz-Schughart, L. A., & Higgins, G. S. (2018). Oxidative Phosphorylation as an Emerging Target in Cancer Therapy. Clinical Cancer Research: An Official Journal of the American Association for Cancer Research, 24(11), 2482–2490.
28. Rodríguez-Enríquez, S., Carreño-Fuentes, L., Gallardo-Pérez, J. C., Saavedra, E., Quezada, H., Vega, A., et al. (2010). Oxidative phosphorylation is impaired by prolonged hypoxia in breast and possibly in cervix carcinoma. The International Journal of Biochemistry & Cell Biology, 42(10), 1744–1751.

CHAPTER 5. CONCLUSIONS AND FUTURE DIRECTIONS

For thousands of years, human beings have used natural products in traditional medical remedies; for healing wounds, alleviating gastrointestinal diseases, fighting infections, and also as nociceptives, sedatives, and laxatives. Multiple modern cancer therapeutics have their bases in natural products; with taxanes, *Vinca* alkaloids, camptothecins, and epipodophyllotoxins the most well-known among them [1-4]. While most of these therapies are cytotoxic, often causing serious side-effects when used in aggressive combination regimens, by increasing our understanding of tumor-specific vulnerabilities, future naturally-sourced chemo-drugs could be screened for enhanced tumor-directed toxicity, thereby significantly reducing side-effects. Further, the tremendous diversity of natural compounds offers significant opportunities for the identification of entirely new classes of drugs, which can be further modified to specifically and more potently target cancer cells.

Modern technology and software tools have helped to profile the genome and transcriptome of tumors, and helped identify novel, exploitable characteristics. Treatments for triple-negative breast cancer (TNBC), an aggressive subtype with higher relapse and mortality rates, currently rely on combination chemotherapy regimens. However, an improved understanding of TNBC tumor characteristics through transcriptomics and metabolomics has identified several, previously unknown vulnerabilities, two of which will be discussed here [5, 6].

Firstly, TNBCs are often characterized by constitutive activation of NF-κB signaling, an inflammatory pathway normally utilized normal immune cells [7]. Activation of the pathway leads to the nuclear translocation of a transcription factor, p65/RelA, which induces transcription of genes involved in survival, EMT, and proliferation such as cIAP2, Cyclin D1, and MMP-9 [8-14]. Inhibiting NF-κB signaling can induce tumor cell death both *in vitro* and *in vivo*, and may thus be a potentially target for future chemotherapeutics.

Secondly, TNBCs are characterized by extensive metabolic reprogramming to fuel the massive ATP demands required for proliferation, growth, and migration. Unsurprisingly, TNBCs have been shown to have elevated levels of multiple amino acids, including aspartate, asparagine, glutamate, phenylalanine, methionine, and the branched-chain amino acids (BCAAs) leucine, isoleucine and valine [15]. These amino acids are subsequently converted into TCA cycle intermediates such as succinate, fumarate, and malate, with the by-products of the TCA cycle going on to fuel oxidative phosphorylation as well [16]. TNBCs also show increases in glycolysis, and a dependency on glutamine metabolism, a phenomenon known as 'glutamine addiction' [17-21]. As both the TCA cycle and oxidative phosphorylation are mitochondria-localized, the inhibition of mitochondrial metabolism may be another avenue to novel TNBC-specific therapies.

Our search for new natural sources of chemotherapeutics against TNBC lead to our current investigations of the South American plant *Lippia origanoides.* Extracts from this species have been used by the native people as topical analgesics and to alleviate gastrointestinal disorders, and have also been shown as anti-mutagenic and anti-microbial by Dr. Fuentes at the Universidad Industrial de Santander [22]. In the present studies, we used two extracts from *L. origanoides*, LOE and L42, prepared from different chemotypes of the plant, and studied their cytotoxic effects on TNBC cells *in vitro*, while also shedding light on their mechanisms of action, using conventional molecular biology tools as well as label-free quantitative (LFQ) proteomics. We also characterized the composition of L42 and finally, we studied its *in vivo* toxicity.

5.1 LOE inhibits NF-κB signaling and induces apoptosis in TNBC cells

Our studies initially identified LOE as capable of inducing a dose-dependent loss of viability in MDA-MB-231, CRL-2321, and MCF-10AH triple-negative breast cancer cells in the 0.15 – 0.2 mg/ml range (Chapter 2), with MDA-MB-231 cells showing a 50 % loss of viability upon 24 h treatment with 0.15 mg/ml LOE, and 95 % loss with 0.2 mg/ml LOE. In contrast, MCF-10A normal mammary epithelial cells showed only a 20 % loss of viability with 0.15 mg/ml, and 40 % loss with 0.2 mg/ml. This important

result indicated that LOE was targeting mechanisms specific to cancer cells, and our subsequent studies focused on defining a mechanism of action for the extract.

Differential staining analysis by flow cytometry revealed that LOE induced a loss in MDA-MB-231 cell viability by halting the cell cycle in the G_0/G_1 phase and promoted apoptosis without inducing necrotic cell death. We showed that these results were accompanied by a loss in protein levels of the proliferative and survival markers, Cyclin D1 and cIAP2, and the activation of caspase-8 and caspase-3. As mentioned previously, Cyclin D1 and cIAP2 are downstream products of NF-κB signaling, and inhibition of this pathway can activate caspase-8-induced cell death. In line with our observations, we hypothesized that upstream effectors of NF-κB signaling were inhibited by the extract and found that indeed, levels of RIP1, a scaffold protein required for downstream signaling, were significantly lost upon treatment with LOE (Chapter 2).

In summary, these results provided the first evidence that *L. origanoides* was a source of cytotoxic compounds that could be used to induce apoptosis in triple-negative breast cancer cells, with minimal effects on normal cells. The *L. origanoides* extract (LOE) was shown to inhibit NF-κB effector proteins, and based on previous studies identifying this pathway as important to TNBC proliferation and survival, we proposed that NF-κB inhibition could be involved in mediating the TNBC-specific loss of cell viability induced by the extract.

5.2 L42 induces extensive loss of mitochondrial proteins in TNBC cells

To ascertain that the effects of the *L. origanoides* extract (LOE) on TNBC vs. normal cell viability would be retained in other extracts from the plant, we tested L42, an extract prepared using an identical protocol but from a different chemotype (genetic variant) of *L. origanoides*. Treatment of MDA-MB-231 and MCF-10A cells with L42 confirmed that the extract retained the significant TNBC-specific cytotoxicity observed with LOE, and was also significantly more potent than LOE at the same concentration (See Figure 2.1, Chapter 2 and Figure 3.1, Chapter 3). For example, at 0.15 mg/ml for 24 h, LOE reduced viability by 50 %, compared to 80 % loss of viability with L42. In addition,

when treated for 24 h with up to 0.12 mg/ml L42, MCF-10A cells did not undergo any loss of viability, compared to a 50 % loss of viability in MDA-MB-231 cells.

Having established similar TNBC-specific cytotoxic effects of the extracts, we next studied the mechanism of action of L42. We confirmed that L42 induced caspase-8 activation and loss of Cyclin D1 (Figure 3.1, Chapter 3), and also induced a loss of RIP1 and cIAP2, while inducing the cleavage of PARP *(not shown)*. These results highlighted that both extracts could inhibit NF-κB signaling while activating the extrinsic pathway of apoptosis.

We acknowledged that multiple components could be responsible for the extracts' apoptotic effects, and multiple cellular pathways may be affected by treatment with *Lippia* extracts. We therefore utilized label-free quantitative proteomics to study the proteome-wide changes induced in MDA-MB-231 TNBC cells by treatment with L42. As described in Chapter 3, treatment with L42 lead to the significant loss of proteins involved in mitochondrial amino acid and lipid metabolism, the TCA cycle, and oxidative phosphorylation.

Using the freely-available STRING software and database, we observed that the down-regulated proteins were strongly-interacting, pointing to a loss of distinct protein complexes as occurring during treatment with L42 (Figure 3.4, Chapter 3). Further studies will be required to identify if these proteins do indeed function as part of large protein complex, and if disruption by L42 components leads to degradation of the entire complex.

In addition, L42 treatment lead to a significant loss of the rate-limiting enzyme of the TCA cycle, α-ketoglutarate dehydrogenase complex (KGDHC), a complex consisting of oxoglutarate dehydrogenase (OGDH), dihydrolipoamide S-succinyltransferase (DLST), and dihydrolipoamide dehydrogenase (DLD), which, in combination with its inhibitory effects on other TCA enzymes, would effectively halt the TCA cycle and starve the electron transport chain of the NADH and succinate required for Complex I and Complex II functioning (See Figure 3.5, Chapter 3, and Figure 5.1).

Treatment with L42 also lead to the loss of multiple matrix-localized Complex I subunits (Figure 3.6, Chapter 3). All the down-regulated Complex I subunits were nuclear-genome encoded; L42 components could therefore be disrupting the translocation of these proteins into the mitochondria or interfering with Complex I assembly, leading to subunit degradation. Further studies will be required to verify the mechanism of Complex I dysregulation by L42.

We also confirmed that the loss in TCA cycle and OXPHOS proteins was accompanied by reduction in mitochondrial membrane potential, which is a known trigger for apoptosis (Figure 3.7, Chapter 3) [23]. In combination with the inhibition of NF-κB signaling and loss of key enzymes involved in ATP and metabolite production, the depolarization of the mitochondrial membrane observed with L42 treatment could be an additional mechanism by which L42 induces rapid, irreversible apoptosis in TNBC cells (See Figure 5.1). Normal mammary epithelial cells (such as the MCF-10A cell line) may show resistance to one or more of these mechanisms, and proteomics analysis of the effects of L42 treatment on these cells is the subject of continuing studies.

Chapters 2 and 3 provided the mechanisms by which *Lippia* extracts exerted their cytotoxic effects on cancer cells. Future investigations will focus on identifying the bioactive components (BACs) of L42 and LOE, as well as their cellular protein binding partners, to validate *Lippia origanoides* as a source of the next generation of chemotherapeutics targeting triple-negative breast cancer.

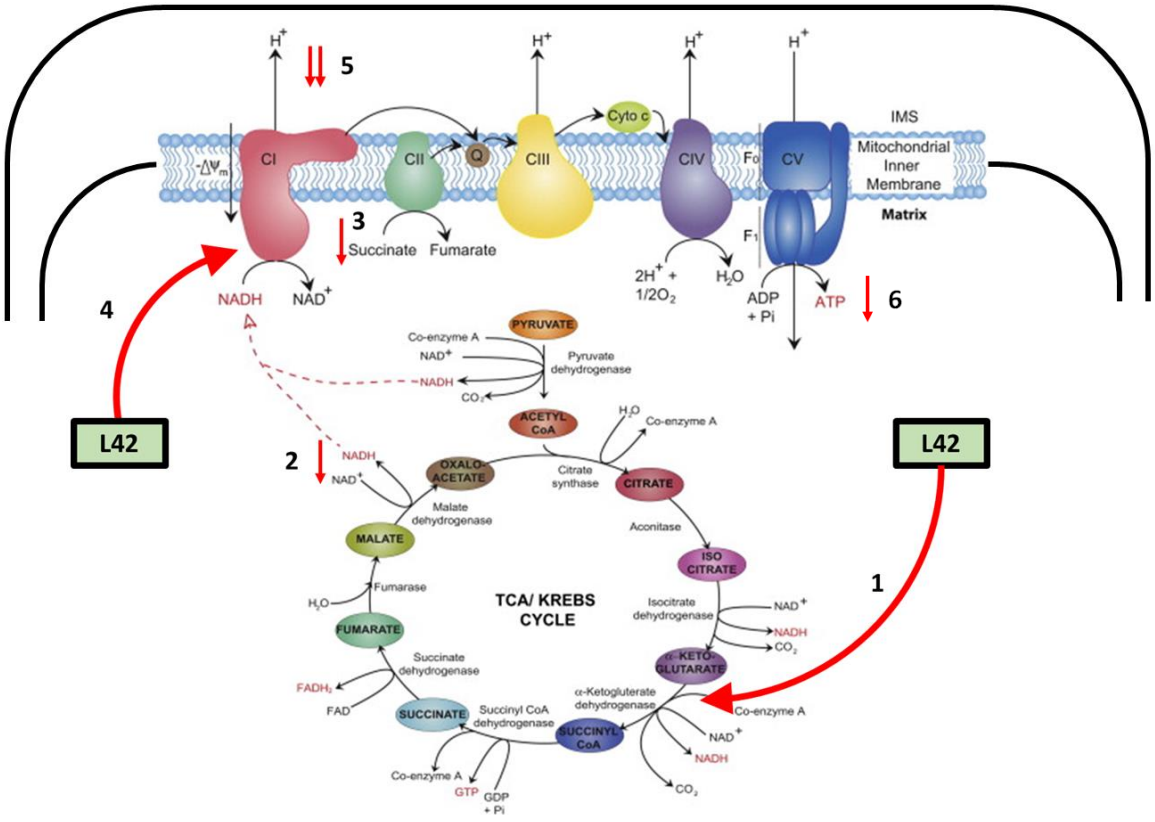

Figure 5.1 Mechanism of apoptosis induced in TNBC cells by L42. Treatment with *Lippia* leads to a significant reduction in the levels of several mitochondrial proteins involved in metabolism, including the rate-limiting enzyme of the TCA cycle, α-ketoglutarate dehydrogenase complex (KGDHC) **(1)**. Halting the TCA cycle would lead to a loss in NADH and succinate levels **(2, 3)**. This, in combination with the decrease in levels of multiple subunits of Complex I of the electron transport chain **(4)**, would result in reduced H^+ ions pumped into the intermembrane space **(5)**, preventing the synthesis of ATP by ATP Synthase (Complex V) **(6)**, and also depolarizing the mitochondrial membrane, activating cellular apoptosis.

Source: Modified from Osellame, L. D., Blacker, T. S., & Duchen, M. R. (2012). Clinical Endocrinology & Metabolism, 26(6), 711–723.

5.3 L42 treatment does not lead to *in vivo* toxicity

A major end goal of our lab's work on *Lippia* extracts are to investigate their ability to prevent tumor initiation and inhibit tumor growth *in vivo.* As a basis for this future work, we assessed the *in vivo* toxicity of L42 with IP injections of up to 100 mg/kg BW in C57BL/6 mice. The mice did not exhibit adverse effects during the two-week observation period, and had no significant changes in body weight. In addition, mammary glands excised from the L42-treated mice showed no pathological signs of inflammation, de-differentiation, or necrosis compared to control mice. We concluded that L42 could be used safely for future *in vivo* cancer studies. In preparation for these studies, we have also established an *in vivo* model of TNBC tumor establishment and growth, in female nude athymic mice (Figure 5.2), with the eventual goal of investigating if IP injections of L42 can prevent or delay tumor establishment, while diminishing tumor growth and overall size.

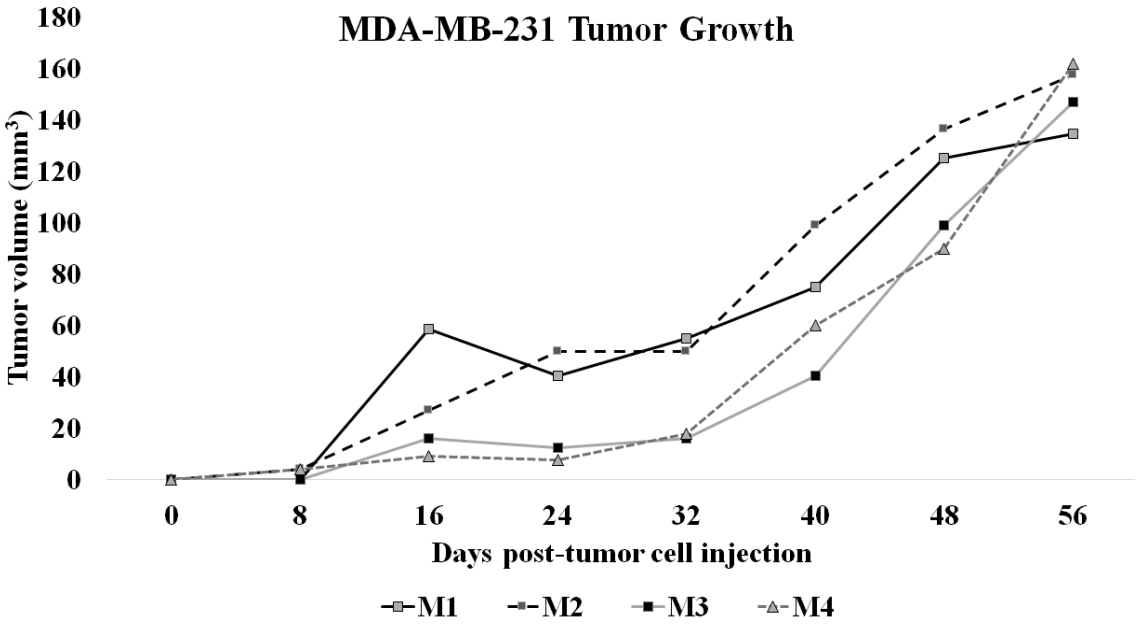

Figure 5.2 Establishment of *in vivo* model of TNBC. 2.5 x 10^6 MDA-MB-231 cells suspended in 200 µl of saline were injected into the inguinal fat pads of female athymic *nu/nu* mice (n = 6). Tumor dimensions were measured using calipers, and tumor volume was calculated as length x breadth x height. Following injections, 1 mouse was sacrificed due to loss of weight, and 1 mouse was sacrificed due to slow tumor growth. No adverse effects were observed in remaining mice.

5.4 Summary and Conclusions

Taken together, we have discovered that *Lippia origanoides* plant extracts can exert potent and specific cytotoxicity against triple-negative breast cancer cells. We have provided significant mechanistic insights into the extracts' effects, including the identification of inhibition of NF-κB signaling and mitochondrial metabolism as key to the induction of apoptosis upon treatment. Our results also confirm that the *Lippia* extract L42 is non-toxic *in vivo* and can be further investigated for its anti-cancer effects in future, using mouse models of TNBC. In line with this, our lab has established an MDA-MB-231 tumor growth model in *nu/nu* mice, which will be used to determine the inhibitory effects of L42 on tumor initiation and progression.

During the course of these studies, we showed for the first time that LC/MS-based quantitative proteomics could be used to identify the complex cellular changes induced in cancer cells by treatment with a combination of compounds. These results re-iterate that LC/MS-based technologies are powerful tools that can be used to rapidly screen extracts for novel compounds, investigate compounds individually or in combination for their proteome-wide effects, and perhaps even identify bioactive compounds (BACs) and their *in vivo* protein binding partners. In collaboration with the Purdue Proteomics and Metabolomics Facilities (PPF and MPF), our lab is in the process of developing an ambitious co-elution profiling-based scheme to simultaneously identify and quantify both the BACs and their protein binding partners from MDA-MB-231 cell lysates incubated with L42, with the ultimate aim of establishing this novel protocol as the gold standard for BAC identification; thereby replacing the expensive and time-consuming bioassay-driven fractionation methods in current use.

Finally, in addition to laying the foundation for future efforts attempting to identify the BACs of *Lippia* extracts, this report provides support for studies into the anti-cancer effects of <u>other</u> medicinal plants in order to better exploit the diversity of bioactive compounds found naturally.

5.5 References

1. Hartwell, J.L., & Shear, M.J. (1947). Chemotherapy of cancer: Classes of compounds under investigation, and active components of podophyllin. Cancer Research, 7, 716-717.
2. Noble, R. L., Beer, C. T., & Cutts, J. H. (1958). Role of chance observations in chemotherapy: *Vinca rosea*. Annals of the New York Academy of Sciences, 76(3), 882–894.
3. McAndrew, N., & DeMichele, A. (2018). Neoadjuvant Chemotherapy Considerations in Triple-Negative Breast Cancer. The Journal of Targeted Therapies in Cancer, 7(1), 52-69.
4. Wall, M. E., Wani, M. C., Cook, C. E., Palmer, K. H., McPhail, A. T., & Sim, G. A. (1966). Plant Antitumor Agents. I. The Isolation and Structure of Camptothecin, a Novel Alkaloidal Leukemia and Tumor Inhibitor from *Camptotheca acuminata*. Journal of the American Chemical Society, 88(16), 3888–3890
5. Liu, Y.-R., Jiang, Y.-Z., Xu, X.-E., Hu, X., Yu, K.-D., & Shao, Z.-M. (2016). Comprehensive Transcriptome Profiling Reveals Multigene Signatures in Triple-Negative Breast Cancer. Clinical Cancer Research: An Official Journal of the American Association for Cancer Research, 22(7), 1653–1662.
6. Lehmann, B. D., Bauer, J. A., Chen, X., Sanders, M. E., Chakravarthy, A. B., Shyr, Y., & Pietenpol, J. A. (2011). Identification of human triple-negative breast cancer subtypes and preclinical models for selection of targeted therapies. Journal of Clinical Investigation, 121(7), 2750–2767.
7. Nakshatri, H., Bhat-Nakshatri, P., Martin, D. A., Goulet, R. J., & Sledge, G. W. (1997). Constitutive activation of NF-kappaB during progression of breast cancer to hormone-independent growth. Molecular and Cellular Biology, 17(7), 3629–3639.
8. Khoshnan, A., Tindell, C., Laux, I., Bae, D., Bennett, B., & Nel, A. E. (2000). The NF- B Cascade Is Important in Bcl-xL Expression and for the Anti-Apoptotic Effects of the CD28 Receptor in Primary Human CD4+ Lymphocytes. The Journal of Immunology, 165(4), 1743–1754.

9. Hartman, Z. C., Poage, G. M., den Hollander, P., Tsimelzon, A., Hill, J., Panupinthu, N., et al. (2013). Growth of triple-negative breast cancer cells relies upon coordinate autocrine expression of the proinflammatory cytokines IL-6 and IL-8. Cancer Research, 73(11), 3470–3480.
10. Hinz, M., Krappmann, D., Eichten, A., Heder, A., Scheidereit, C., & Strauss, M. (1999). NF-kappaB function in growth control: regulation of cyclin D1 expression and G0/G1-to-S-phase transition. Molecular and Cellular Biology, 19(4), 2690–2698.
11. Huber, M. A., Azoitei, N., Baumann, B., Grünert, S., Sommer, A., Pehamberger, H., et al. (2004). NF-kappaB is essential for epithelial-mesenchymal transition and metastasis in a model of breast cancer progression. The Journal of Clinical Investigation, 114(4), 569–581.
12. Kagoya, Y., Yoshimi, A., Kataoka, K., Nakagawa, M., Kumano, K., Arai, S., … Kurokawa, M. (2014). Positive feedback between NF-κB and TNF-α promotes leukemia-initiating cell capacity. The Journal of Clinical Investigation, 124(2), 528–542.
13. Wang, C. Y., Mayo, M. W., Korneluk, R. G., Goeddel, D. V., & Baldwin, A. S. (1998). NF-kappaB antiapoptosis: induction of TRAF1 and TRAF2 and c-IAP1 and c-IAP2 to suppress caspase-8 activation. Science (New York, N.Y.), 281(5383), 1680–1683.
14. Yousef, E. M., Tahir, M. R., St-Pierre, Y., & Gaboury, L. A. (2014). MMP-9 expression varies according to molecular subtypes of breast cancer. BMC Cancer, 14(1), 609.
15. Kanaan, Y.M., Sampey, B.P., Beyene, D., Esnakula, A.K., Naab, T.J., Ricks-Santi, L.J. et al. (2014). Metabolic Profile of Triple-Negative Breast Cancer in African-American Women Reveals Potential Biomarkers of Aggressive Disease. Cancer Genomics and Proteomics, 11, 279-294.
16. Berg, J. M., Tymoczko, J. L., & Stryer, L. (2002). Carbon Atoms of Degraded Amino Acids Emerge as Major Metabolic Intermediates. Biochemistry. 5th Edition.
17. Kung, H.-N., Marks, J. R., & Chi, J.-T. (2011). Glutamine Synthetase Is a Genetic Determinant of Cell Type–Specific Glutamine Independence in Breast Epithelia. PLOS Genetics, 7(8), e1002229.

18. Lim, S.O., Li, C.W., Xia, W.Y., Lee, H.H., Chang, S.S., Shen, J. et al. (2016). EGFR Signaling Enhances Aerobic Glycolysis in Triple-Negative Breast Cancer Cells to Promote Tumor Growth and Immune Escape, Cancer Research, 76, 1284-1296.
19. Lampa, M., Arlt, H., He, T., Ospina, B., Reeves, J., Zhang, B.L. et al. (2017). Glutaminase Is Essential for the Growth of Triple-Negative Breast Cancer Cells with a Deregulated Glutamine Metabolism Pathway and Its Suppression Synergizes with Mtor Inhibition. PLoS One, 12, e0185092.
20. Goode, G., Gunda, V., Chaika, N.V., Purohit, V., Yu, F., Singh, P.K. (2017). Muc1 Facilitates Metabolomic Reprogramming in Triple-Negative Breast Cancer. PLoS One, 12, e0176820.
21. Van Geldermalsen, M., Wang, Q., Nagarajah, R., Marshall, A.D., Thoeng, A., Gao, D. et al. (2016). ASCT2/SLC1A5 Controls Glutamine Uptake and Tumor Growth in Triple-Negative Basal-Like Breast Cancer. Oncogene, 35, 3201-3208.
22. Castellanos, N.R., Castro, C.E., Stashenko, E.E., & Fuentes, J. *Lippia origanoides* supercritical fluid extract and its major constituent pinocembrin diminish ultraviolet radiation-induced DNA damage and modulate cell division in *Escherichia coli.* (In review)
23. Ly, J.D., Grubb, D.R., Lawen, A. The Mitochondrial Membrane Potential (Delta Psi M) in Apoptosis, an Update. Apoptosis. 2003, 8, 115-

VITA

VISHAK RAMAN

(812) 391-4038 • vishak.ramaniml@gmail.com

SUMMARY

Highly-motivated Cell and Molecular Biologist possessing strong presentation and communication skills, with a core interest in disease marker identification, immunotherapy, and drug discovery.

RESEARCH EXPERIENCE

Purdue University, Department of Biological Sciences Indiana, USA
Ph. D Student, *Camarillo Lab, Purdue Center for Cancer Research (PCCR)* 2013 – Present

- Identified the targeted apoptotic effects of a *Lippia origanoides* extract (L42) on triple-negative breast cancer (TNBC) using plate-based viability assays
- Demonstrated L42 induced cell cycle arrest in TNBC cells using flow cytometry and fluorescence microscopy
- Utilized label-free quantitative proteomics to show L42 induced metabolic arrest in TNBC cells by inhibiting the TCA cycle and OXPHOS
- Mastered several data analysis and visualization tools (InfernoRDN, Cytoscape, DAVID 6.8, GOrilla) to process large datasets from proteomics experiments

SRM University, Department of Biotechnology Chennai, India
Undergraduate Research Intern, *Integrative Medicine Lab* 2011 – 2012

- Received extensive F344 rat-handling experience including basic maintenance, oral gavage treatment, anesthetic injection, sacrifice, and lymphatic tissue isolation
- Studied the immuno-modulatory anti-ageing effects of *Morinda citrifolia* extracts on the immune system of old F344 male rats
- Performed plate-based bioassays (ELISA and enzyme activity assays) to measure cytokine levels and antioxidant enzyme activity in draining lymph nodes during ageing

PRESENTATIONS AND PUBLICATIONS

Talks:

- **Vishak Raman**. "A *Lippia origanoides* extract induces apoptosis and suppresses NF-κB signalling in MDA-MB-231 triple-negative breast cancer cells." Graduate Student Retreat, Burton D. Morgan Center, West Lafayette, IN. (2016) **[1st Place Winner]**

Posters:

- **Vishak Raman**. "Proteomic analysis reveals that an extract of the *plant Lippia origanoides* suppresses mitochondrial metabolism in triple-negative breast cancer cells." Eight International Breast Cancer Prevention Symposium, Dauch Alumni Center, Purdue University, West Lafayette, IN, 2018.
- **Vishak Raman**. "Proteomic analysis reveals *L. origanoides* extract targets mitochondrial metabolism and function to induce rapid apoptosis in triple-negative breast cancer cells." Amelia Project, Alumni Hall, Indiana University, Kokomo, IN. (July 14, 2018)
- **Vishak Raman**. "A novel mass spectrometry-based approach to discover anti-cancer bioactive compounds and their protein binding partners." Dept. of Biol. Sci. Retreat, Fourwinds Lakeside Inn, Bloomington, IN. (2017)

- **Vishak Raman**. "A *Lippia origanoides* extract induces cell cycle arrest and apoptosis and suppresses NF-κBsignaling in MDA-MB-231 triple-negative breast cancer cells." Purdue Sigma Xi Chapter Poster Competition, Stewart Center, Purdue University, IN. (2017)

Publications:

- **Raman V**, Aryal UK, Hedrick V, Fuentes Lorenzo JL, Stashenko EE, Levy M, Levy MM, Mohallem R, and Camarillo IG. "Proteomic analysis reveals an extract of the plant *Lippia origanoides* suppresses mitochondrial metabolism in triple-negative breast cancer cells." J Proteome Res. 2018 [Epub ahead of print]
- **Raman V**, Fuentes Lorenzo JL, Stashenko EE, Levy M, Levy MM, Camarillo IG. "*Lippia origanoide*s extract induces cell cycle arrest and apoptosis and suppresses NF-κB signaling in triple-negative breast cancer cells." Int J Oncol. 51(6): 1801-1808, 2017.
- Pratap UP, Priyanka HP, Ramanathan KR, **Raman V**, Hima L, Thyagarajan S. "Noni (*Morinda citrifolia L.)* fruit juice delays immunosenescence in lymph nodes of old F344 male rats. J Integr Med. 16(3):199-207, 2018.
- Mittal L, **Raman V**, Camarillo IG, and Sundararajan R. "Ultra-microsecond pulsed curcumin for effective treatment of triple negative breast cancers." Biochem Biophys Res Commun. 2017 Sep 30;491(4):1015-1020 2.

EDUCATION

Purdue University Indiana, USA
Ph. D, Biological Sciences 2013 – Present
Characterizing the apoptotic effects of *L. origanoides* extract on triple-negative breast cancer using quantitative proteomics and metabolomics

SRM University Chennai, India
B. Tech, Biotechnology 2009 – 2013
Modulation of cytokine production and antioxidant enzyme activities in draining lymph nodes of old F344 male rats treated with *M. citrifolia* extract.

SCIENTIFIC LEADERSHIP EXPERIENCE

Purdue Center for Cancer Research Indiana, USA
Sr. Research Mentor, Camarillo Lab 2016 – 2019

- Established standard laboratory protocols for several cell and molecular biology techniques including:
  - Quantitative Real-time PCR (qPCR)
  - Western Blotting
  - Immunofluorescence staining
  - Sample preparation for LC-MS/MS
- Spear-headed new collaborations with Purdue Proteomics Facility and Flow Cytometry and Cell Sorting Facility
  - Lead directly to 2 first-author manuscripts
- Mentored 5 non-thesis,1 thesis-undergraduate student, and 3 Ph. D students
- Designed and directed individual and group research projects for all students mentioned above

Dept. of Biological Sciences, Purdue University Indiana, USA
Teaching Assistant Sep. 2013 – Present

- Lectured for over 400 students in the Anatomy and Physiology Lab (BIOL 203/204) over 4 years
- Oversaw lab experiments, graded quizzes and worksheets, and held office hours for students every week
- Frequently substituted for senior instructors for recitation lectures

Dept. of Biotechnology, SRM University Chennai, India

Conference Host, *NCFB 2012*

- Selected to host the Animal Biotechnology Conference as part of the National Conference on Frontiers in Biotechnology (NCFB) 2012

AWARDS

Purdue University, Department of Biological Sciences Indiana, USA

- Graduate School Summer Research Grant 2016
- Best Presentation at Annual Graduate Student Retreat, Burton D.Morgan Center, 2016

SRM University, Department of Biotechnology Chennai, India

- 50% tuition-waiver scholarship for academic year 2010-2011
- 50% tuition-waiver scholarship for academic year 2009-2010

RELEVANT TECHNICAL SKILLS

Cell and Molecular Biology Techniques:

- Mammalian Cell Culture
- Western Blotting
- qRT-PCR
- ELISA
- Differential-staining analysis via Flow Cytometry
- Sample preparation for quantitative proteomics via LC-MS/MS

Software and Omics Tools:

- ImageJ (Densitometry for Western Blotting/IF Imaging)
- InfernoRDN (Proteomic data analysis and visualization)
- STRING (Protein interaction analysis)
- Cytoscape (Pathway visualization)
- DAVID 6.8 (Gene enrichment analysis)
- GOrilla (Gene Ontology Enrichment Analysis and Visualization tool)